Increasing Renewable Energy System Value Through Storage

by

Joshua Michael Mueller

B.S., United States Naval Academy (2004)
B.A., University of Oxford (2006)

Submitted to the Engineering Systems Division
in partial fulfillment of the requirements for the degree of

Masters of Science in Technology and Policy

at the

MASSACHUSETTS INSTITUTE OF TECHNOLOGY

June 2015

© Massachusetts Institute of Technology 2015. All rights reserved.

Author .....
Engineering Systems Division
May 8, 2015

Certified by .....
Jessika E. Trancik
Atlantic Richfield Career Development Assistant Professor in Energy Studies
Thesis Supervisor

Accepted by .....
Dava J. Newman
Professor of Aeronautics and Astronautics and Engineering Systems
Director, Technology and Policy Program

Increasing Renewable Energy System Value Through Storage

by

Joshua Michael Mueller

Submitted to the Engineering Systems Division
on May 8, 2015, in partial fulfillment of the
requirements for the degree of
Masters of Science in Technology and Policy

Abstract

Intermittent renewable energy sources do not always provide power at times of greatest electricity demand or highest prices. To do so reliably, energy storage is likely required. However, no single energy storage technology is dominant when comparing cost intensities of the energy capacity and power capacity of storage. Past research on energy storage technologies has debated the value of storage technologies for different applications, and has compared the cost structures of different storage technologies without finding generalizable results across both locations and technologies. Here, a single performance metric, the benefit / cost ratio (χ) of storage value added is analyzed across six locations globally to show that the relative value of storage technologies is largely location invariant. Electricity price dynamics, specifically the frequency and height of price spikes determine the value of storage, while the duration of price spikes determines the relative value of one technology versus another. We find that cost targets can be set for different technologies with ranging energy and power costs of storage.

Thesis Supervisor: Jessika E. Trancik
Title: Atlantic Richfield Career Development Assistant Professor in Energy Studies

Acknowledgments

I would like to use this page to say a short thank you to my advisor, Jessika, who has been incredibly supportive and giving of her time and resources over these two years. Also, thank you to my friends and family for their support and camaraderie.

Thanks lastly to the Fannie and John Hertz Foundation whose funding has made my graduate education possible. The support of that organization and their flexibility with both my naval service and course of study has made the transition to graduate research painless. Their funding supported this research.

Contents

List of Figures

List of Tables

Chapter 1

Introduction

Energy storage technologies vary widely in their performance, function, and design. One metric of performance that is of great importance to those investing in power plants, and especially in renewables, is the cost. For renewables in particular, the cost of the storage that is likely required to transform intermittent renewables into power plants providing energy on demand is an additional concern. This thesis examines how storage can increase the value of renewables despite also increasing the cost [1, 2]. In this chapter, the motivation for increasing the value of renewables is explained, and a variety storage technologies are described according to their method of converting and storing energy. The different functions that storage can provide to support the electric grid are defined next, followed by the many different metrics that can be used for comparing the technologies. Lastly, the literature on techno-economic modeling of storage to determine its benefit is discussed in order to show how this research contributes to the literature.

1.1 Motivation

In order to meet the climate change mitigation goal of limiting global temperature rise to 2 °C, global electricity generation portfolios will have to shift substantially to carbon-free energy sources [3]. Renewable energy sources, such as wind and solar power, do not follow the electrical load, instead they produce electricity when the

resource is available, regardless of whether there is demand [4]. Other carbon-free energy sources, such as nuclear fusion, provide base-load energy demand but are unable to provide peaking power due to ramp rate or other thermal limitations [5]. For these reasons, increasing the proportion of the electricity generation portfolio provided by carbon-free sources creates a number of challenges for the stability of the electric grid.

One possible solution to these challenges is the addition of grid-scale energy storage systems (ESS) to the energy portfolio. Improved energy storage technologies will be a requirement for the transportation sector, if it is to move away from fossil fuel dependence in internal combustion engines [6], but also bring important benefits to the electricity transmission and distribution system. Intermittent renewables generation combined with energy storage is capable of providing energy on demand. As increased renewable penetration in the energy grid likely requires that renewables be able to provide energy on demand, ESS's will support by storing electricity when demand is low and providing it when demand is high.

1.2 Energy storage technologies

Energy storage technologies can be classified in four broad categories: mechanical, electrical, chemical, and thermal [7, 8]. In this review, only technologies which use electricity as part of the charging process and produce electricity during discharge operations are considered. Thermal energy storage systems are discussed for completeness, as they may be used for electrical-to-electrical energy storage. However, it is more likely that they will be used for storage of waste heat for later reuse by other systems, for example in industrial processes [9].

This thesis focuses primarily on a comparison of mechanical storage technologies, such as pumped hydro storage and compressed air energy storage, and chemical storage technologies, including many kinds of sealed batteries and flow batteries. This restriction is due to the nature of these technologies as being primarily beneficial in performing arbitrage as bulk energy storage devices. Flywheels and electrical storage,

such as supercapacitors, may one day develop to a point where they can effectively perform bulk services, so they are described here as well. However, their current costs are not included in the analysis of chapter 3. The remainder of this section describes in detail the variety of energy storage technologies that may be employed to enable increased renewables penetration.

1.2.1 Mechanical

Mechanical ESS's either use the potential energy difference of fluids at a pressure gradient or the kinetic energy of a rotating mass to store energy. All three mechanical ESS's are relatively mature technologies that have been in commercial operation for decades.

Pumped hydro storage

Pumped hydro storage (PHS) stores energy in the gravitational potential energy difference between two reservoirs at different elevations [10]. Energy is stored when water is pumped from the lower reservoir to the higher reservoir. When the water is released, the driving head of the elevation difference causes the water flow to spin turbines, thereby generating electricity. Total storage capacity for PHS is a function of both the height difference between reservoirs and the volume of the upper reservoir. Schoenung and Hassenzahl (2003), provide a rule of thumb which equates the volume of the upper reservoir to the height differential between the two reservoirs and the energy stored in the system, equation (1.1) [11]. The volume of the upper reservoir and the height differential are also the two largest constraints on siting PHS stations as there are a limited number of adequate locations. Additionally, deregulation of the electricity markets and mounting environmental concerns with the loss of animal habitats due to dam construction and reservoir flooding have led to a decline in popularity for PHS [7].

$$V = 400\frac{E}{h} \tag{1.1}$$

Power capacity is a function of the flow rate and the head, or elevation difference between the reservoir and the turbine. The charging and discharging power capacities can be completely separate if using separate pumps and turbines or combined if using reversible pumping turbines. When charging and discharging are combined in a single pump-turbine, the design is known as a single-penstock system. Separate units for charging and discharging are referred to as a double penstock design. In either situation, the choice of turbine is dependent upon the expected head and flow rate for the location and desired power [12].

PHS has been used as large scale energy storage in the United States since 1929, when the first station was built in Connecticut [11]. The development of PHS in the United States accelerated in the 1960s with the advent of nuclear fission generation facilities, which when coupled with PHS provided both base and peaking power [13]. Since the 1980s construction of PHS has stalled, mostly due to environmental concerns. Despite this, it is the most widely used technology for bulk energy storage [14]. Alternative designs for PHS include using the sea for the lower reservoir in coastal locations or using underground reservoirs, such as an abandoned mine, for the lower reservoir [15]. Using the sea as a lower reservoir is beneficial due to the decreased construction costs of building only one dam rather than two [12]. However, it should be noted that this is not always a possibility, especially for small islands, due to the Ghyben-Herzberg lens effect on the freshwater table.

Compressed air energy storage

Compressed air energy storage (CAES) is considered a mature technology despite only being used in three power plants worldwide. In a CAES ESS electricity is stored in pressurized air and generated by the subsequent expansion of that air [7]. The first two CAES plants in the world, in Huntorf, Germany and McIntosh, Alabama are diabatic CAES facilities. Diabatic CAES is not a pure energy storage technology, but rather a combined cycle natural gas turbine in which the compression of air is temporally separated from the production of electricity [16]. A small plant in Gaines, TX is the first advanced adiabatic CAES (AA-CAES) plant, in which no external fuel

source is required during the expansion phase.

In CAES systems, compressed air can be stored in caverns in the ground, known as geological CAES, or in aboveground tanks, referred to as aboveground CAES [17]. There are three primary types of storage cavern proposed for geological CAES: solution mined salt caverns, aquifers, and conventionally mined hard rock caverns [18]. It is estimated that 75% of the United States has geologies favorable to CAES with one of these three features [18, 19]. All three CAES plants currently in operation use solution mined salt domes [20, 21, 19]. CAES in either a salt dome or conventionally mined cavern operates at a single pressure throughout the cavern. In porous media, such as underground aquifers, the air displaces water along a pressure gradient which may respond dynamically to repeated cycling [22]. This raises concerns about the feasibility of CAES using aquifers, limiting the area in which this is a viable storage technology.

The two diabatic CAES plants in operation both use natural gas as a fuel source, though significant advancements in design have been made between the Huntorf plant in 1978 and the McIntosh plant in 1992 [21, 20]. In the 290 MW Huntorf plant, compressed air is stored in two underground caverns and then this air is used to combust natural gas increasing the energy released by the combustion of natural gas three-fold [21]. The 110 MW McIntosh plant uses the natural gas to heat the air released from the cavern as it powers the turbine through expansion [20].

Advanced adiabatic CAES removes the need for natural gas combustion during the expansion phase by combining CAES with a thermal energy storage (TES) medium. Heat generated by the compression of air is removed and stored in the TES to later reheat the air for expansion [23]. In AA-CAES intercoolers are used between each stage of compression and recuperators between each expansion turbine. Higher efficiencies are achieved through varying the operation of a group of compressors from series to parallel in multiple configurations depending on the final pressure required. A similar manipulation of expanders is used during the expansion phase [23].

Flywheels

Flywheels store energy in the kinetic energy of a rotating mass. In the charging state, electricity powers a motor which speeds up the rotating mass. The process is reversed for discharging, where the rotating mass is used to power the motor, now operating as a generator to provide electricity back to the grid [24]. This highly reversible and scalable system finds many applications beyond grid-scale energy storage, including use in vehicles and satellites [25].

The two main categories of flywheels in use today are distinguished by their rotor material, which in turn specifies their limitations and uses. Low-speed flywheels use massive steel rotors, while newer high-speed flywheels use light weight composites or carbon fiber materials for the rotor [7]. The kinetic energy stored in a flywheel is a function of the mass, rotor design, and angular velocity; equation (1.2) accounts for the mass and rotor design in the term I, the moment of inertia. For a solid disk of radius r, $I = 1/2mr^2$. As can be seen in equation (1.2), high-speed flywheels are capable of higher energy densities as the energy increases as a function of the square of angular velocity, but only linearly in mass [26]. The moment of inertia for composite materials is more difficult to calculate, as carbon fibers are anisotropic, and therefore, design, loading, and details of the fabrication process must be accounted for in calculating the moment of inertia [27]. Equation (1.2) also demonstrates one of the major advantages of flywheels for energy storage, that it is relatively simple to accurately determine the state of charge simply by accurately measuring the angular velocity [25].

$$E_{\text{kinetic}} = {}^{1}/_{2} I\omega^2 \tag{1.2}$$

Composite materials are also more desirable than large steel rotors because they tend not to catastrophically explode when design speeds are exceeded [27]. Heavy projectiles resulting from flywheel failure are one of the major safety design considerations, and one of the engineering design limits on the energy that can be stored in the flywheel. These safety considerations generally require large containment vessels

to house the flywheel [28]. These containment vessels serve a dual purpose. They also maintain vacuum in order to reduce air drag losses; however, the reduction of drag losses through magnetic bearings and vacuum systems does increase the number of parasitic loads on the flywheel, thereby reducing overall system efficiency [26].

1.2.2 Electrical

Electrical ESS's store energy in either the electric field created between two charged plates or in the magnetic field induced by a current in a coil of wire. No transformation of energy is required for these ESS's, resulting in systems primarily designed for high power operations. The two technologies described below are commonly considered useful for provision of ancillary services which require a high power capacity but lower energy capacity. For this reason, their costs are not included in the analysis of chapter 3.

Superconducting magnetic energy storage

In a superconducting magnetic energy storage (SMES) system, energy is stored in the magnetic field created by a current in a toroid [29]. SMES systems use direct current in a material that has been supercooled to the point of superconductivity. The energy stored in the magnetic field and is proportional to the square of the current. There is a critical current, beyond which the current cannot be increased, at which point the material no longer behaves as a superconductor [29].

Because of the high capital costs for energy storage in SMES, the technology is used mainly as a source of power quality management, frequency regulation, and voltage support [30]. The system is usually sized to only provide a few seconds at rated power [31]. Because the current is not dissipated through ohmic resistance due to the superconductivity of the storage medium, SMES systems only suffer the efficiency loss of the power conversion system for converting AC to DC power but don't suffer from efficiency losses in the superconducting material itself [31]. Instead, SMES systems suffer from high parasitic losses and expenses in maintaining the low

temperatures needed for superconductivity.

Capacitors and supercapacitors

Capacitors and supercapacitors, also referred to as ultracapacitors, operate on the same principle. Electrical energy is stored in the electric field between two charged plates. Supercapacitors store significantly more energy than capacitors due to their use of a liquid dielectric and their geometry [29]. As opposed to the metal plates of a traditional capacitor, a supercapicitor uses a porous carbon structure which enables a greater surface area in contact with the dielectric [7]. As with SMES and batteries, supercapacitors operate on direct current, and therefore require a power conversion system for operation in the AC electric grid.

Supercapacitors do not suffer from charge rate limitations but are expensive means of storing large amounts of energy. For these reasons they are most often promoted for power factor correction and voltage support rather than energy storage [31]. The primary advantage of supercapacitors over capacitors, such as the original Leyden jars, is the increased energy density. Finally, supercapacitors last for more than 100,000 cycles, making replacement costs low [10].

1.2.3 Chemical

Chemical, or electrochemical, energy storage comprises both batteries and fuel cells. Fuel cell technology is a technology capable of both generation and energy storage. It is outside the scope of this paper.

Batteries consist of multiple electrochemical cells in which a potential exists between the materials comprising the two electrodes. The anode is the positive electrode, while the negative electrode is known as the cathode, and positive ions are conducted between them via the electrolyte. Electrons are conducted via the connected circuitry to provide power. For bulk energy storage purposes, only secondary batteries are of concern, as their ability to be recharged is a required feature [8].

Lead-acid batteries

First developed by Gaston Plante in 1860, lead-acid batteries are the oldest and most mature chemical bulk energy storage technology, having been used for over a century for electricity storage [32]. Lead-acid batteries comprise over 90% of the market for electrochemical storage devices [33] by virtue of being the preferred technology for automotive batteries before the recent development of advanced batteries for use in hybrid and battery electric vehicles [34]. Despite the maturity of the technology, lead-acid batteries continue to be the subject of much research and improvement, with the most recent change being the development of valve regulated lead-acid batteries, which reduce the operations and maintenance requirement of frequently adding water to the cells [35].

In a lead-acid battery the anode is made of a spongy lead substrate while the cathode is lead dioxide. The acid is diluted sulfuric acid, which is generally a 25% solution when the battery is fully charged [34]. Lead-acid batteries are highly recyclable, but only the spongy lead anode can be made easily made of recycled lead as the cathode has high purity requirements for the lead dioxide [36]. As the battery discharges, the sulfate ions bond with the lead from the anode reducing the concentration of acid and raising the pH of the electrolyte. The efficiency of the battery is dependent on the state of charge, with the battery being less efficient at higher states of charge [37]. However, the relationship between state of charge and efficiency is non-linear and dependent on whether the battery is being charged or discharged and at what rate. Additional challenges with lead-acid batteries are their loss of capacity at both high and low temperatures, and the nonlinearity in their amp-hours capacity as a function of discharge [33, 38]. Due to this nonlinearity, as the discharge rate increases, the total capacity of the battery decreases.

Sodium-sulfur batteries

Sodium-sulfur (NaS) batteries are high temperature batteries which use molten sulfur as the anode and molten sodium as the cathode [39]. The temperature must be

maintained between 280 °C and 390 °C during use in order to keep the electrodes in their molten state for the transfer of the Na ion during charging and discharging operations [40, 41]. The electrolyte is a solid ceramic substrate of β" alumina which conducts the Na ion between electrodes. Cell voltage for NaS batteries is 2.08 volts, and a typical 25kW module requires 320 cells connected in a combination of series and parallel units. An electric heating unit provides for temperature control, mostly during the endothermic charging process, while special high-temperature dissipating casing is needed to ensure the battery does not overheat during discharge.

The electric heating unit accounts for most of the inefficiency during operation, especially during diurnal peak-shaving operation during weekdays, and no operation on weekends. A commercially deployed system at Meisei University in Japan has demonstrably operated in this mode with 77.9% efficiency over a two and half year period, during which the battery provided 1 MW of the 3 MW peak demand [41]. Current focus on NaS batteries focuses on establishing appropriate operating conditions to enable the battery to provide for peak-shaving, power quality management, and uninterrupted power supply (UPS) services. This focus is especially important to understand the impact of pulse operations, when the battery is operated at up to 5 times rated power for 30 seconds to several minutes, on battery temperature and lifetime.

NaS batteries began commercial development in 1984 through a partnership of NGK Insulators, Ltd. and the Tokyo Electric Power Company [42]. Over 100 MW of NaS battery have been deployed in Japan as of 2006 for distributed and grid-scale operations. NaS batteries are well suited to a multi-function deployment as they can respond to both short and long demand signals, and they suffer no self-discharge. While the technology is considered technically mature, research into better packaging materials for temperature control have the highest potential for improving battery efficiency.

Li-ion batteries

Lithium ion batteries use lithium as the main reactive species at both the graphite anode and Li metal oxide cathode [8]. Originally developed by Sony in 1991 [43], Li-ion batteries have gained widespread usage in high-end distributed home energy storage, consumer electronics, and electric vehicles and are being proposed for use in grid-scale energy storage systems [44]. Research and advancements in Li-ion technologies focus on three major components of the technology. The carbon anode into which Li ions intercalate during charging can be made of graphite, hard carbon, or nanospheres, and the electrolyte can be an organic based compound, lithium salts in ionic liquids, or a polymer compound for the transport of Li ions during both charge and discharge. Multiple Li metal oxide anodes are under development [45, 46].

Major advances in Li-ion batteries require significant changes in battery design and chemistry. Cobalt, manganese, and nickel have been explored as metal oxide transition metals for the cathode, and new advances also focus on blending different intercalating metal oxides in fabricating the cathode [47]. However, each of these metals has issues with either scalability or toxicity and environmental concerns [48]. Current designs, in which Li ions are transferred between a graphite matrix and a Li metal oxide have approached theoretical limits of efficiency and energy density [49]. New chemistries, such as using tin or silicon alloys for the anode rather than carbon structures may provide the answer for continuing to improve Li-ion performance factors. Other advances involve shifting to LiS conversion chemistry, as opposed to the current intercalation chemistry, and the use of organic proteins and polymers for faster ion transport [43, 49].

Concerns with Li-ion batteries include the scalability of the technology for use in applications as diverse as grid-scale storage, electric vehicles, and portable consumer electronics [46]. If all the vehicles in the world were replaced with battery electric vehicles powered by Li Ion cells as produced today, this would consume 30% of the known reserves of mineable Li [43]. This does not include Li that can be extracted from sea water. Similarly, the use of Co as the primary metal oxide in the cathode

raises both environmental concerns and scalability concerns due to the scarcity of cobalt [43].

Nickel-cadmium and nickel-metal hydride batteries

Nickel-cadmium (Ni-Cd) and its successor nickel-metal hydride (Ni-MH) are mature battery technologies first developed in the 1970s [43]. A nickel oxyhydroxide cathode and potassium hydroxide electrolyte are common components between Ni-Cd and Ni-MH with the difference being the anode material [7]. Ni-MH provide performance improvements over Ni-Cd batteries and also do not have the human toxicity concerns that arise from the use of cadmium as the anode material [9].

Despite their improved performance over lead-acid batteries, nickel based batteries have not enjoyed the same levels of commercial success. Partially this is due to their higher costs and the toxicity of the cadmium before invention of the metal hydride alternatives. In Europe, recycling requirements for Ni-Cd batteries have contributed to higher lifecycle costs as well [9]. There are concerns however, that recycling cadmium is not a solution to the problem of disposal if large Ni-Cd batteries are recycled to produce smaller batteries for consumer electronics, which are difficult to recollect [50]. In response, Europe has banned the use of Ni-Cd in consumer appliances [15]. Lastly, the memory effect of Ni-Cd raises distinct challenges, in which improper cycling of the battery leads rapidly to reductions in performance and battery life [7].

Flow batteries

In a flow battery, the anode and cathode are stationary units with a separating membrane comprising a reactor area. Two electrolytes are pumped into the reactor area for the generation of electric current [51]. As a result of this system, the power capacity and energy capacity of flow batteries are completely modular; changing one has no effect on the size of the other [52]. This is not the case for any of the sealed batteries, in which the design and spacing of the electrodes determines both the power capacity of the cell as well as the energy capacity. In general, the design specifications

for sealed batteries are such that either battery life or energy constraints limit the minimum size of the electrode reaction area [53]. Thus, energy capacity is the more binding constraint for sealed batteries.

Flow batteries can be designed to meet grid-scale energy storage requirements, but need large tanks to store enough electrolyte to meet hours of demand. They also require additional balance of plant components, such as pumps for each electrolyte [51]. Multiple chemistries have been proposed for flow batteries, with the two most extensively researched and installed being zinc bromine (Zn/Br) and vanadium redox (VRB) [15, 8]. Although VRB and Zn/Br are the two flow cell chemistries available on the market, other promising chemistries include polysulphide bromine, vanadium bromine, iron chromium, zinc cerium, and potentially a soluble lead acid flow battery [52].

Flow batteries are often described as a cross between stationary batteries and fuel cells, in that they operate as a small chemical plant with a reactor area [53]. Each chemistry requires separate electrolytic solutions for the anode and cathode with separation of reactive species by an ion exchange membrane, such as Nafion, that allows for transport of water and non-reactive species to maintain electrical balance [52]. The use of Nafion as the ion exchange membrane is a further similarity between flow batteries and fuel cells [54, 55].

1.2.4 Thermal

Thermal energy storage technologies are not explored deeply in this thesis. Most TES are not used primarily for electrical to electrical energy storage, instead being used in combined heat and power applications. TES can be either high temperature or low temperature with 200 °C serving as the conventional boundary [9]. Within each of these temperature regimes, TES can be further subdivided into sensible or latent heat storage systems. As this distinction cross-cuts the temperature regimes, the features of each will be discussed below.

Sensible heat storage

Sensible heat ESS's store energy in a medium which does not change phase during the heating process. The charging process involves either heating or cooling the medium, with most systems storing energy through a heating process. The system is reversed during discharge with the medium using the temperature differential to drive a heat pump to generate electricity [15]. More commonly, TES are used in conjunction with other ESS's, such as AA-CAES, to store waste heat during system charging, which can then be reused during discharge to vastly improve overall system efficiency. The storage medium need not be a fluid, although water is often used as it is has a high specific heat capacity and is readily available. When the storage medium is a fluid stored in either separate hot or cold tanks or in a single tank system with a thermocline, the sensible heat TES is known as an active system [56]. Passive sensible heat TES use a fluid as the heat transfer mechanism, but use gravel beds as the storage medium or they store the heat in rocks below the surface of the Earth mimicking renewable geothermal electricity generation systems [5]. High temperature sensible heat TES commercially available use molten salts for the storage medium, and are often used in combination with concentrating solar power generation [9, 56].

Latent heat storage

Latent heat TES store energy in the phase change, either latent heat of fusion or vaporization, or crystalline restructuring of a medium undergoing a temperature change. One example, though not necessarily one that provides electricity-to-electricity storage, is the freezing of water to make ice when electricity demand is low, and the subsequent using of that ice for cooling purposes during day time peak electricity hours in order to avoid running an air conditioning system.

Latent heat TES have several advantages and challenges in relation to sensible heat TES. Significantly more energy can be stored per volume in a latent heat system due to the energy required for phase change. This means that for equivalent capacity systems, sensible heat TES must be larger [9]. However, the phase change process

usually results in property changes such as expansions and density variations as well as non-uniformities that may impact the cycle life of the latent heat TES. Expansions and contractions during phase change provide unique challenges for latent heat containment systems, as does destabilization of the phase change material, especially when byproducts can lead to corrosion of the containment system [57]. Additionally, finding materials with high heat transfer coefficients and high specific heats that are also inexpensive and readily available is a challenge for both sensible and latent heat TES.

Current phase change materials for use in latent heat TES, are categorized as organics, inorganics, or eutectics, which are mixtures of two phase change materials that melt at one well-defined temperature [9]. Common organic materials for latent heat TES are paraffin waxes, which are non-corrosive but suffer from low thermal conductivity. Inorganic materials,primarily hydrated salts, correct for the low thermal conductivity, but are more corrosive, making containment difficult [57]. Lastly, eutectic materials can be either inorganic-inorganic, organic-organic, or inorganic-organic combinations of phase change materials, but are expensive to manufacture.

1.3 Energy storage functions

The technologies described above provide a number of benefits for the electrical grid beyond merely enabling renewables to provide energy on demand. EPRI lists fifteen functions of energy storage which it classifies in five broad categories: bulk energy, ancillary, transmission infrastructure, distribution infrastructure, and customer energy management services [58]. Each of these functions will be described below, particularly focusing on how specific technologies can perform these functions. While all of these features are benefits that can be provided by an ESS, the remainder of this thesis will explore the ways in which energy storage can provide value when performing arbitrage.

1.3.1 Bulk energy services

Bulk energy services comprise three different functions of energy storage [58]. The first two, price arbitrage and electric energy time-shifting, are essentially the same function used to meet different goals. In price arbitrage the goal is defined by the price signal and the function of the ESS is to take advantage of lower electricity prices during one time of day for the purchase of electricity to charge the storage device and then resell that electricity during another time of day when the prices are higher. Electric energy time-shifting is the same process but based on the goal of meeting demand. For this function, the energy storage device charges when demand is low and discharges to meet periods of higher demand.

Energy storage can also be used to help meet capacity requirements or to defer investment in new generation capacity. Total generation capacity is only used on a few days a year, but is expensive to install. Seasonal energy storage can be used to meet electricity demand when it is at its highest in the year by saving electricity from earlier in the year when demand is lower [31]. Storage allows for flexibility in system design by deferring investment in new generation units until demand has grown so that decisions can be made on actual demand rather than forecasted demand. This minimizes the risk associated with capacity planning; this flexibility will be discussed further in section 1.3.3 where storage serves a similar role in deferring transmission upgrades to minimize investment risk.

Bulk energy storage, and in particular energy arbitrage and time-shifting, is the primary role of energy storage at the level of grid operations. This thesis focuses on this role of storage to time-shift energy generated by a renewable resource in one period to a different period so as to maximize revenue. Other models may use a similar function of energy storage to shift production to meet demand. Figures 2-3, 2-4, A-1, A-2, and A-3 discussed in section 1.4 demonstrate a model in which electricity generated by solar power is time-shifted to meet demand. The more positively correlated electricity prices and demand, the more that arbitrage and demand based time-shifting produce the same outcome.

1.3.2 Ancillary services

Energy storage is also highly suited to provide ancillary services to the grid because of the fast ramping and cycling of many storage technologies [58]. These services are important for the incorporation of variable renewable generation int the electricity generation supply mix [31, 59]. Ancillary services affect the quality of power provided by generators, an aspect of electricity generation that is highly important for sensitive machinery, for example rotating equipment dependent on a steady 60 Hz power source and electronics.

Frequency regulation corrects for short duration mismatch of demand and generation. Over-generation manifests itself as a higher frequency, while demand higher than generation depresses the frequency [60]. Without storage, this service is provided by generation units operating at partial loading so that they have capacity to either increase or decrease generation to match demand. This is problematic for thermal generation units which have very specific loading requirements for operation at maximum efficiency and equipment life. Fast-ramping energy storage can provide this service without the damage to equipment or the high losses associated with the current techniques. Additionally, use with variable renewables generation helps to smooth power fluctuations which may occur when clouds pass over photovoltaic arrays or when the wind exceeds cut-in or furl-out speeds [59]. This service is primarily suited to high-power and low-energy capacity systems, with long cycle-lifetimes.

One of the primary benefits of energy storage is its capability to provide reserve power. This can be power in the case of a system blackout, or power to restart generators, known as black start capability. Electricity systems maintain three different levels of reserve capability, dependent on the time required to bring the reserve generator online in case of the failure of a different generation unit. Spinning reserves are those generators that are operating unloaded and ready for immediate loading to meet demand in case of a failure in the system. Non-spinning reserves and supplemental reserves can be brought on in longer time periods but provide similar services [58]. Storage can provide reserve capability without the wasted fuel and

emissions generated through the unit commitment of unloaded spinning reserves [31]. Charged storage systems with a low self-discharge can meet reserve requirements until additional generation can be brought online to replace the failed unit.

Just as the frequency of alternating current must be maintained within specified limits, the voltage provided must also meet certain criteria. Rotating and other equipment which exhibit inductance and capacitance effects on the grid introduce reactive power which must be controlled through other equipment which readjusts the system power factor, or phase angle between voltage and current. The power conversion equipment of most ESS's can meet this criteria without drawing upon the real power in the storage system [58]. Similarly, the generators employed in PHS or CAES may also be used to adjust system power factor to help restore voltage and reduce the effects of reactive power [12].

1.3.3 Transmission infrastructure services

Storage can also be used to reduce stresses on the transmission system by relieving congestion during periods of high usage, sometimes referred to as peak shaving [59]. It can also be used to defer upgrades in the transmission system to reduce the risk associated with predicted demand expansion. Transmission lines are limited in the amount of power they can carry. As demand grows, more transmission capacity may be required to meet new demand. However, as with generation capacity described in section 1.3.1, the maximum transmission capability is only needed briefly throughout the year. Congestion relief can help meet demand at this time without overloading the transmission network but requires appropriate placement of an ESS at the ends of transmission lines that would have exceeded capacity without the aid of storage [58]. A containerized ESS that can be moved to other locations as needed may be the most appropriate way to match functional need with ESS life.

Transmission upgrade deferral allows for flexibility in the planning of the transmission network by deferring upgrade costs that might be incurred by upgrading congested transmission lines to meet periods of peak demand. Deferring the upgrade increases its net present value since the future cost is discounted to the present. An-

other benefit of deferring transmission infrastructure upgrades is to minimize the risk of upgrading transmission to meet projected demand which never materializes. In this situation, the additional cost of storage now provides flexibility to the system which increases the average net present value of the transmission system under a variety of scenarios [61]. It reduces the losses in the worst case scenarios while only minimally increasing the costs for all other scenarios.

1.3.4 Distribution infrastructure services

Storage can also provide benefits on a smaller, distributed scale relative to the full grid. These services, and those discussed in section 1.3.5, are not the primary focus for this study and cannot be practically accomplished by many of the technologies described in section 1.2. For example, PHS and CAES are primarily grid-level bulk energy storage technologies, and their geographical constraints prevent them from providing localized, distributed services. Distribution infrastructure services are similar to the grid-level services described above, but are more precisely tuned to the needs of a few customers rather than to all customers.

The two distribution infrastructure services that can be provided by ESS's are distribution upgrade deferral and voltage support. Distribution upgrade deferral is analogous to transmission upgrade deferral but focused on the smaller distribution lines which may be similarly capacity limited. In the same way, distribution voltage support focuses on voltage excursions that may occur at the neighborhood level, perhaps due to single large loads or household photovoltaic arrays [58], rather than voltage spikes at the grid level. For both these functions, smaller local ESS's can help defer costs and provide reliable service.

1.3.5 Customer energy management services

Customer energy management services use ESS's at the household or industry level to provide services that are analogous to those that ESS's can provide at the grid level. Services in this functional category are even more limited in the technologies

that can be considered, since they must be of a small enough system size to be used by individual customers. Specific functions of an ESS for use by individual customers, with their grid level analogue in parentheses are: power quality (frequency regulation and voltage support), retail time-shift (arbitrage), power reliability (spinning reserves and black start), and demand charge management (arbitrage).

Demand charge management and retail time-shift are both analogous two different forms of arbitrage that customers can perform to reduce their electricity bill by minimizing either the price of electricity purchased from the grid or the additional charges that are applied when power is drawn from the grid. These two functions focus on the retail price of electricity as opposed to the wholesale or locational marginal price which is the focus of the arbitrage function of storage. Power reliability refers to storage used to provide continuous power in the place of a household gas generator, and power quality is using storage to minimize frequency and voltage excursions that may be caused by large loads in a home or more likely a factory or industrial setting.

1.4 Energy storage technology performance criteria

The storage technologies described in section 1.2 can be evaluated in terms of many different criteria, all contributing to how well they perform the functions listed in section 1.3. This section details many of these metrics: some related to the technology performance and some related to the scalability of the technology. One pair of performance factors, the cost intensity of energy capacity and the cost intensity of power capacity, will be examined closely in this thesis as the primary performance intensity metrics of interest.

1.4.1 Performance metrics

Energy storage technologies may be constrained in their ability to perform the functions of section 1.3 by physical limits of the technology or by their design. Design variables of consideration for storage include the power capacity and energy capacity, or the size of the system. Physical limits of the technology are often measured

as intensive variables, a ratio of one variable to another. A specific subset of intensive variables that are used to measure a technology's performance are performance intensity metrics [62]. Design variables, performance intensity metrics, and other intensive factors which influence the performance intensity metrics all limit the ability of storage to perform a function. Performance intensity metrics and the other factors which enable them both serve as ways of comparing technologies and might be improved through research and development (R&D) or increased production and experience [63, 3].

Specific energy and energy density are two metrics that are intensive measures of the energy potential of a technology [7, 10, 63]. Specific energy is the energy capacity per unit of mass, while energy density is the energy capacity per unit of volume. Similarly specific power is the available power capacity per unit of mass and power density is the power capacity per unit of volume. All four of these metrics are extremely important for small scale energy storage systems, and especially for vehicular systems, as they limit the amount of power and energy available in a constrained environment.

Efficiency is a measurement of the losses that occur during charging and discharging and is an example of a factor which influences other performance intensity metrics. In addition to the efficiency of the storage medium, the efficiency of the power conversion system must be considered for energy storage systems such as batteries, supercapacitors, and SMES which require conversion of alternating current (AC) to direct current (DC) prior to storage. Specific technology intensity metrics for charging are generally reported in terms of AC-AC efficiency, combining both charging and discharging into a single term. However, a more detailed analysis accounting for differences in charging and discharging efficiency is valuable if these two values are not the same. For example, in a double penstock PHS design, pumping water from the lower to upper reservoir may occur at a different power loss than the generation of electricity as the falling water turns a turbine.

Self-discharge is the loss of energy from a storage medium over time, and like efficiency is a metric which influences other performance metrics. While efficiency is

a metric for the power components of storage, self-discharge is the analogous metric for the energy components. Energy can be lost from the storage system in a variety of ways. Flywheels suffer from high self-discharge due to the friction of spinning masses [24], PHS might suffer self-discharge due to evaporation of water from the upper reservoir, and many batteries suffer from self-discharge through secondary chemical interactions occurring in the cell [35]. Self-discharge can also be thought of as a scalability metric, in the sense that high self-discharge would limit a technology's use in systems which require long duration of storage, such as seasonal storage. Such systems would only be valuable for storing large amounts of energy.

Ramping time is the amount of time it takes for a storage (or generation) facility to achieve a desired level of output, and is a third metric which influences performance. It measures the phenomenon that a storage or generation facility cannot instantly begin producing at maximum capacity, but must instead be brought up to rated speed. The rate in terms of kW/min that a facility can increase its output is known as the ramp rate. Ramp rate is an important feature of energy storage and for renewable integration, as existing thermal and nuclear facilities can be highly constrained by their ramp rate [64]. One of the primary concerns caused by the increased penetration of renewables, especially solar power, is the need for facilities with high ramp rates to meet demand as it peaks at the same time solar resources decrease due to sunset [65]. This is shown graphically in figure 1-1 in which future increased renewable penetration necessitates higher ramp rates to meet evening demand. ESS's can help mitigate this sharp ramp rate by smoothing renewables production over the course of a day.

Depth of discharge is a limitation applied to the available energy capacity of a storage system. It is a requirement that some stored energy remain in the system for proper functioning. Primarily, depth of discharge is associated with sealed batteries and is a design feature of battery cycling, violations of which result in shortened battery life. Maintaining energy levels within the rated depth of discharge also improves efficiency in systems in which efficiency is a function of storage level. In addition to batteries, depth of discharge can also be a feature of compressed air energy storage, where a certain positive pressure must be maintained in a cavern, perhaps to prevent

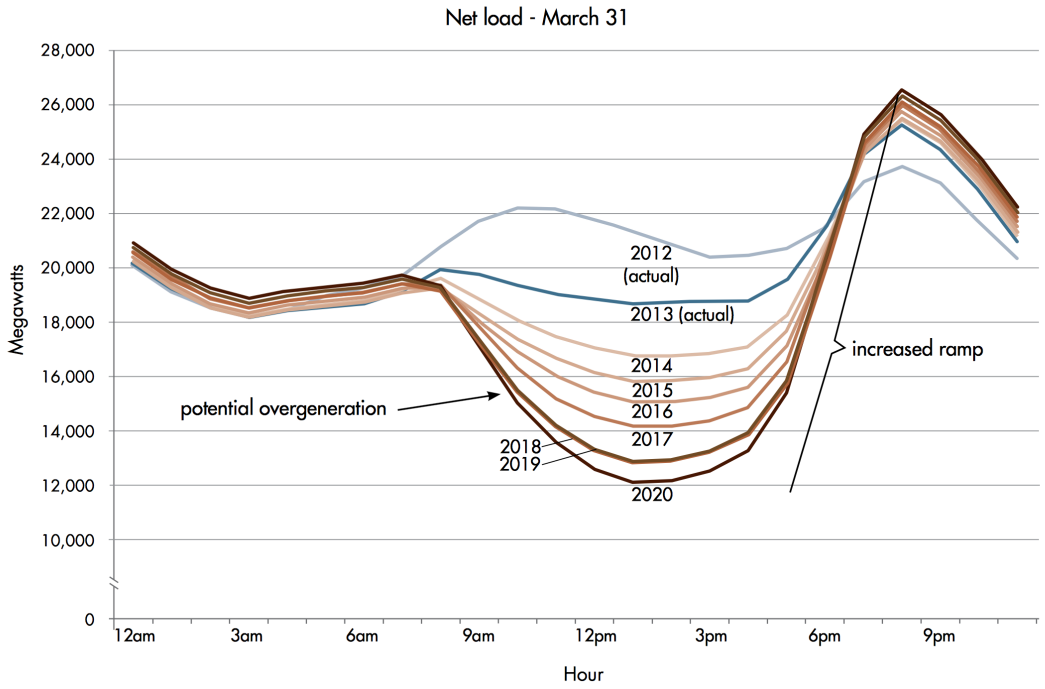

Figure 1-1: The California ISO "duck" curve highlights the importance of both ramp rate and the need for energy storage as renewable penetration increases [65]. As future energy portfolio mixes rely more heavily on solar power, the ramp rate required of thermal generation units, in order to meet late afternoon demand, increases.

the introduction of water or corrosive materials. Flywheels may also suffer depth of discharge limitations if they must maintain some rotational velocity. When exploring the value and optimal sizing of storage facilities, depth of discharge limits necessitate a higher energy capacity to be installed to achieve the same desired output.

Safety is performance metric of storage which is not necessarily always an intensive variable and therefore a performance intensity metric. It can be either an intensive variable if dependent on the quantity of storage or it can be a factor independent of system size, but it is a concern of many different ESS's. Li-ion and lead-acid batteries have both experienced fires and other catastrophic failures [46]. Li-ion batteries require extra controllers to maintain safety, as the cell charging rate is not self-regulated [8]. Flywheels also present a particular safety concern due the high amounts of energy released in the form of flying projectiles in the case of catastrophic failure [26, 27]. A NaS battery system suffered a serious fire in September of 2011 resulting in suspension of production by NGK Insulators, LTD. the sole producer of

this technology [66, 67].

Carbon emissions per unit power provided or energy stored are performance intensity metrics which enable comparison of technologies in terms of environmental performance. CAES is the one ESS that requires a fuel source, and therefore the only technology with direct emissions during operation. This is not true for AA-CAES, which relies on the storage and recovery of thermal energy generated during charging and used during the expansion phase. Diabatic CAES plants, such as those in Huntorf, Germany and McIntosh, AL burn natural gas during the discharge phase of energy storage [21, 20]. Carbon emissions as a performance intensity metric for diabatic CAES require detailed information about both CO_2 and methane emissions in particular, as well as consensus on the proper equivalency tools for all other greenhouse gasses that might be emitted [68]. In addition to direct emissions, overall life cycle emissions can be determined for each technology, and these can also serve as an environmental performance intensity metric.

Power and energy capital cost intensities represent the overnight capital costs contributed by different components of an energy storage system, usually reported in units \$/kW and \$/kWh (or other currencies as applicable) [69, 70, 7, 15, 30, 9, 71, 72]. Cost intensities serve as the primary performance intensity metric of interest for this thesis. Cost intensities assume that a technology is modular in the sense that each additional kW of power will cost the same amount as will each additional kWh or energy capacity. This assumption is stronger for some technologies such as flow batteries where the size of both the reactor and the storage tanks can be designed to any scale. Other technologies, such as underground CAES are less modular in the energy capacity since the size of a cavern is dependent on many other variables.

Cost intensities of power and energy also present a second modularity in terms of costs because they split a system into its power components and its energy components. For some technologies, such as PHS or CAES, the cost modularity in terms of power and energy is prima facie evident. There are costs that are associated with pumps, turbines, compressors, and expanders - the power related components - and costs associated with the energy storage components, such as the cost of building

reservoirs or underground storage chambers. Flow batteries similarly have separable costs of power and costs of energy [53, 52]. However, stationary sealed batteries, flywheels, and SMES are not clearly separable into power components and energy components. For example, in a sealed battery such as a lead-acid battery, the power and the energy capacities are both a function of the geometry of the electrodes, their spacing, and the volume of electrolyte. Changes to any of these components necessarily changes both the power capacity and the energy capacity, which in turn changes the $/kW and$/kWh costs of the battery. One common method of maintaining power and energy cost modularity in these ESS's is to ascribe the power related costs solely to the power conversion system and using the battery costs in total as the energy related costs [11]. One reason this is a reasonable solution is that batteries are often designed with energy capacity as the limiting feature [53]. Section 2.2 provides more detail on the range of estimates for power and energy capital costs as presented in the literature.

1.4.2 Scalability and other metrics

Scalability metrics measure the achievable scale of a technology. This scale may be for a specific project installation or the scale of meeting the needs of all energy storage projects globally Given the conditions of the scenario, these metrics assess whether it is reasonable to expect that a given technology may be capable of meeting a set need. Many of these metrics have to do with resource constraints that might limit their ability to provide a service at the grid level on a global scale. Absent a defined scenario, these metrics in general describe limitations that might apply to the technology when developed for commercialization purposes. Scalability metrics also provide constraints upon the design variables of installed power and energy capacity for a specific project, thus limiting the ability of storage to perform a specific function.

Resource constraints are the most general types of scalability metrics. These may take the form of space or location constraints, geographic constraints, or material constraints. In section 1.2.1 the types of geological features required for underground storage of compressed air were described. The geographic dispersal of the types of

bedrock and aquifers required for building storage caverns is an example of a geographic limitation on the scalability of CAES [19]. Similarly, PHS requires two reservoirs with a height difference between them for the storage of energy. Locations that cannot provide this are prevented from using PHS as an ESS, unless new techniques such as the use of underground reservoirs can be commercialized [13].

Location constraints may limit which storage technologies can perform transmission and distribution deferral services as described in section 1.3. These deferral functions require that technologies be located in specific places in the grid. Additionally, technologies which can be moved are more beneficial since they can be reused over time as the grid needs change. Technologies such as PHS and CAES are unlikely to be able to fulfill this function as they are both immobile and also highly restricted in where they can be located. Aboveground CAES using storage cylinders may mitigate these concerns, but this technology has yet to be proven commercially viable.

Material needs are a primary scalability constraint for some battery chemistries. These constraints also include the environmental damage that might occur through mining. Lead, zinc, lithium, and cobalt are all examples of metals which might constrain the production of either lead acid, Zn/Br, or Li-ion batteries [31]. Alternatives to these resource constraints include recycling of used batteries to recover rare materials, research into alternative chemistries requiring only abundant materials, and possible new sources for minerals other than mining [43]. As an example of this last alternative, lithium can be extracted from seawater through adsorbents and the application of electricity [73]. Material needs may also manifest themselves as limitations through the application of disposal and recycling costs which will raise the life cycle costs of a technology [50]. Lastly, water requirements for PHS can also qualify as a material need if this limits the use of this ESS.

Parasitic load requirements place a different type of limitation on the scalability of an ESS. Parasitic loads are a concern for technologies such as NaS batteries which require heating sources to maintain the temperature between 280 °C and 390 °C and SMES which requires additional equipment to cool the superconductor [40, 29]. The

ability to maintain temperature control in very large or very small systems presents a scalability metric for these technologies. When parasitic load requirements increase more than linearly with system size, they provide a constraint on the size of a system which can perform one of the specific function from section 1.3. The additional costs applied by parasitic loads apply a scaling requirement to these technologies, as they must be sized so that they can meet demand while also supplying their own loading requirements.

1.5 Techno-economic modeling

Comparing the technologies of section 1.2 according to the different criteria of section 1.4 generally requires that the technologies be modeled according to how they would best perform the functions of section 1.3. Techno-economic modeling uses the technical features and limitations of the different technologies as constraints limiting their ability to be remunerated for providing a service. This section provides an overview of the different types of techno-economic models that have previously been published to highlight the need for the research presented in this thesis. Most models study only one technology or one location, as opposed to comparing multiple technologies across locations according to their cost intensities. This thesis contributes to the techno-economic modeling literature by examining the value of multiple technologies when performing arbitrage at different locations.

Benitez et al. (2008) use a non-linear optimization model to study the use of storage to facilitate the growth in wind power in Alberta, Canada [74]. They model PHS of a constrained size to study the effect the ESS has on reducing the needs for peak generation capacity as wind penetration is increased. They find that storage can reduce the need for maintaining peaking generators by providing reserve capacity for the increased wind penetration. Connolly et al. (2012) similarly research the effect PHS has in Ireland on increasing wind capacity for a national grid [75]. They investigate both single penstock designs, in which the pumps and turbines are a single unit and only one function can operate at a time, and double penstock designs, in

which pumps and turbines are separate and so the storage can be both storing and generating at the same time. They find that double penstock designs significantly increase the penetration of wind power and reduce costs by eliminating the need for redundant peaking plants, but that storage is not feasible because it is too costly.

Studies using storage combined with intermittent renewables to provide baseload power frequently model storage with wind power and will be discussed next. Wind generation has a non-zero probability of providing energy at any given time. This is different than solar power, where providing baseload generation necessitates planning for the diurnal cycle and days of less irradiance. Denholm et al. (2005) explore the possibility of using CAES in the midwest U.S. to enable wind power to provide baseload energy [76]. They find that this is possible, but the use of diabatic CAES reduces the environmental performance of wind, due to the burning of natural gas as part of the energy recovery process. They also find a tradeoff between the capacity factor energy storage enables wind to achieve and the amount of spilled or curtailed wind energy. In a similar study, Greenblatt et al. (2007) show that wind and CAES operating as baseload power greatly expands the penetration potential for wind energy [77]. They find that this is only economically feasible with the inclusion of greenhouse gas emission prices in the market along with natural gas prices higher than current values.

Birnie (2014) optimizes the size of a battery for a given solar array size to meet demand in three case study locations in the U.S. [78]. The locations, Newark, NJ, Boulder, CO, and Tucson, AZ, span a range of solar availability. The study focuses on meeting as much demand as possible with either the size of the array, which limits the total energy that can be generated, or the capacity of the battery serving as the limiting factors. In a different demand based model, Leadbetter and Swan (2012) study battery ESS's for residential neighborhoods for use in peak shaving applications [79]. This study uses the battery storage to provide peak shaving services while meeting demand, and demonstrates a method for determining the optimal size of the battery and the resulting battery lifetime given light cycling and few deep discharges.

Kaabeche and Ibtiouen (2014) focus on hybrid systems of PV, wind, a diesel generator, and a battery ESS [80]. In their model they combine both an energy deficit model, for meeting overall system demand, with a cost model to find the optimal sizing and operation of the hybrid system for use by small islanding networks of approximately 10 houses. Kaldellis and Zafirakis (2007) similarly use a minimum cost optimization model to study hybrid renewable and storage configurations on two Aegean islands [81]. They find that ESS viability is dependent on input energy pricing, which can contribute up to 70% of total production costs. Hittinger et al. (2010) take a different approach to the question of integrating renewables by focusing instead on the ability of storage and natural gas to facilitate the integration of wind by accounting for short duration, 10 seconds, fluctuations in power [82]. They find that when analyzing the frequency regulation stresses that renewables penetration places on the grid, storage is required to facilitate wind penetration levels about 12%.

Sioshansi (2010) studies how energy storage can be used to perform price arbitrage in conjunction with wind power to increase the value of wind energy systems [83]. Using a supply function equilibrium model as an economic model and a simple energy balance without power capacity constraints for the technical aspects, he shows that the addition of storage helps a wind generator gain some market power which it can then use to increase its value. However, a side effect of the increased value is reduced consumer surplus, and in practicality he finds that no existing storage technologies have sufficiently low enough capital costs to justify installing energy storage for this purpose.

Sealed batteries have been installed in many locations in the U.S. to provide ancillary services such as frequency regulation and spinning reserves [84]. Alt et al. (1997) optimize the size of a battery ESS to produce the most savings when providing either frequency regulation, reserves, or load leveling functions [85]. Using a unit commitment model, they find that the most savings are provided when battery ESS's are remunerated for providing reserves services. Similarly, Oudalov et al. (2007) optimize the size of a battery for providing frequency regulation based on historical frequency data [86]. An optimally sized battery ESS will also include emergency

resistors to take care of higher energy events, so that meeting these events through battery sizing doesn't require additional capacity that is infrequently used. Lead acid batteries may be profitable for this service at current price estimates.

Connolly et al. (2011) ask if it is possible to profit from PHS facility in an existing market, and how would one operate such a system to maximize revenue [87]. In studying the Irish electricity market, they compare operation based on perfect foresight of electricity prices to three different operation heuristics which preset the times in which the system charges and discharges. They find that profits are feasible, and that up to 97% of the perfect foresight profit can be captured through use of the appropriate realistic operating strategy. Both Fares and Meyers (2013) and Ippolito et al. (2014) investigate the appropriate use of batteries for providing frequency regulation, load shifting, or voltage regulation services in existing markets [60, 88]. Fares demonstrates how a VRB used in the ERCOT market of Texas can be optimally operated to provide a profit by offering frequency regulation services. Ippolito studies different distributions of batteries within the existing grid of an Italian Island would be distributed and operated to provide different functions. They find that when optimally offering one service, the ESS provides minimal benefit when analyzed in terms of other functions it could provide.

Maximizing the profit from a hybrid wind and storage facility is likely to provide additional benefits such as emissions reductions and reductions in the amount of renewable energy that is curtailed. Castronuovo and Lopes (2004) optimize the operation of a PHS system with wind power in Portugal [89]. In addition to finding that storage shifts production of electricity to times of high prices, they also find a substantial reduction in wind power. In another study of wind and PHS, Jaramillo et al. (2004) compare the economic performance of the hybrid plant with other technologies in Oaxaca, Mexico [90]. Not only can wind power be combined with storage to provide energy on demand, but the levelized production cost per kWh is comparable to other technologies. Mason et al. (2008) study solar power used in conjunction with CAES plants in the southwest U.S. [91]. CAES combined with solar power can be used to replace either peaking natural gas plants or baseload power. However,

they find that only operation as a peaking plant is likely to be cost competitive by 2020 because of the higher prices paid to peaking plants.

One last techno-economic model investigates a specific location and determines which features of existing storage make certain technologies more suitable than other technologies. Feng et al. (2014) use the EnergyPLAN model, which was also used in Connolly et al. (2012) [75] to determined the amount of excess energy production that could be conserved between various combinations of Li Ion and NaS batteries [92]. Similarly, Kaldellis et al. (2009) study technology neutral hybrid renewable storage systems for various sized islands [93]. They find that sizes of islands and the markets influence which technology is an appropriate choice. Sioshanshi et al. (2011) use an energy balance cost minimization model with perfect foresight to compare diabatic CAES with pure storage technologies for the PJM interconnection [94]. They find that for arbitrage purposes pure storage out performs CAES because the extra cost of natural gas prevents CAES from taking full advantage of low off-peak prices. Finally, Walawalkar et al. (2007) study the NYISO and compare NaS batteries providing arbitrage services and flywheels providing frequency regulation services [95]. Both technologies can provide positive net present value in NY city, but only frequency regulation provided by flywheels is likely to be profitable in the NY east and west regions. They also find that trading efficiency for reduced capital costs is likely to not be cost effective in the long run.

While these studies have explored the challenges and benefits of incorporating ESS's into the electric grid and operating them in combination with renewables, they do not quantify how the value of storage depends on cost features of the storage technology, across diverse technologies and installation locations. This study fills this gap, exploring the value of storage for both wind and solar power plants.

Chapter 2

Methodology

This thesis reports a technology cost evaluation of energy storage systems using a linear optimization model. The analysis focuses on the use of a small energy storage and renewables hybrid facility operating the ESS in arbitrage mode. The hybrid facility is modeled as a price-taker, a reasonable simplification given the low levels of renewable generation in the United States and globally. Using two years worth of hourly electricity spot-market price data and renewables generation data, the optimal operation of the ESS to provide maximum revenue is determined. This optimal behavior provides increased revenue to the hybrid facility. This increase in revenue is compared with the increased cost from adding energy storage to determine the value of added storage.

Solar and wind data from three sites in the United States are compared with similar wind generation data from Eastern Denmark, Western Denmark, and Portugal. European price data was converted to U.S. dollars using the average currency conversion for the two year period in question as provided by XE Currency Conversion [96]. Locations were chosen for data availability and as representative locations for performance as a wind site, a solar site, or neither. European locations were chosen as examples where high levels of penetration by wind power have been achieved.

2.1 Solar and wind generation and electricity price data

Three sites from the United States were examined: McCamey, TX; Palm Springs, CA; and Plymouth, MA along with Eastern Denmark, Western Denmark, and Portugal. McCamey, TX was chosen for the relatively high capacity factor for wind power over the time period observed, 32%. Palm Springs, CA was chosen as a high performing site for solar power, as exemplified by the average capacity factor of 23% over the two year period. Plymouth, MA had a lower capacity factor in both wind and solar power and was chosen as representing areas with neither high performance for wind or solar generation facilities. Denmark was chosen as an example of a country which has over 20% penetration by wind generation [97]. Portugal was chosen as a location representative of regulated electricity markets.

For the locations in the United States, hourly zonal real-time prices for 2004 and 2005 were collected from ERCOT [98], CAISO [99], and ISONE [100]. The renewables generation facility was simulated based on local windspeed and solar insolation data from the Eastern and Western National Wind Integration Datasets and the National Solar Radiation Database [101]. Power output per installed MW for the solar system was based on a photovoltaic array producing rated power at an insolation of 1 kW m^{-2} while wind output was modeled from published performance data for a Vestas V90 3 MW wind turbine [102].

Eastern and Western Denmark real-time hourly price and wind generation were taken from Energinet.dk [103]. During the period of this study, the Danish electricity grid was run as two separate systems unconnected by transmission lines, with Eltra in the west and Elkraft in the east as the two independent systems operators [104]. The majority of wind generation was in the west, which had nearly double the generation capacity of the eastern region, and it is expected to maintain this lead through at least 2020 [105]. Wind power in the west accounted for nearly half of the total demand, making Denmark a unique location for the analysis of the value of energy storage. The separation between the eastern and western systems provides for relative comparisons

within the nation and also for comparisons with the data from locations in the United States.

Danish price and wind generation data was taken from January 2008 through December 2009, which is four years later than the data analyzed for the U.S. locations, since Danish data was not available for the 2004-2005 period. 2008-2009 was chosen in order to use the same experimental setup which accounts for the leap year in 2004 (2008). Similarly, the Danish Climate and Energy Ministry did not have data on solar generation for either time period. As opposed to the U.S. locations where resource availability was used to simulate the renewable generation, actual generation data was used for the analysis of both Eastern and Western Denmark. Electricity prices were converted to US$ based on the average exchange rate with the € for that time period [96].

Portuguese electricity price data and wind generation data were obtained from OMIP, the Iberian Energy Derivatives Exchange [106]. The time period for the Portuguese data used is the same as for the Danish data. As the time periods were the same, the same exchange rate was used to convert electricity prices in € to prices in US$ for comparison to the cost intensities of power and energy of storage.

2.2 Energy storage capital cost intensity data

Extracting real world relevance from the storage model used in this study requires knowledge of the cost intensities for a specific technology. This way, the technology can be evaluated for the value it provides in a given location, and how much it must improve to provide a given value or to reach profitability. Power capacity and energy capacity cost intensities are reported from six different sources [11, 69, 70, 9, 7, 72]. Figures 2-1 and 2-2 and tables 2.1 and 2.2 demonstrate the large range in energy storage cost estimates. With the exception of [11], the references are meta-analyses of other studies. Several of these studies share sources and therefore some of the underlying data may be repeated. The cost estimates presented here are meant to represent approximate ranges of costs presented in the literature.

The large range of reported values for storage cost intensities highlights an important gap in the literature. The large range may merely be an indicator of a lack of information exchange between industry and academia. It may also represent a larger gap in the publication of detailed component-based cost analyses of ESS's. Lastly, as previously mentioned many of these studies are meta-analyses; as a result it is unclear which sources for the initial values for the reported costs of storage are used. It should be noted that many of the papers used for the construction of tables 2.1 and 2.2 also cite one another, in particular references [70, 7, 9, 72] all cite Chen et al. (2009) [69]. While there are differences in the values they report for the cost of energy storage, there are enough similarities between the papers to suggest that the Chen et al. values are a strong influence on the costs reported elsewhere. Chen et al. cites Kondoh et. al (2000) in their reporting of cost intensities of storage [69, 30]. Further attempts to find the initial sources for this data were unsuccessful.

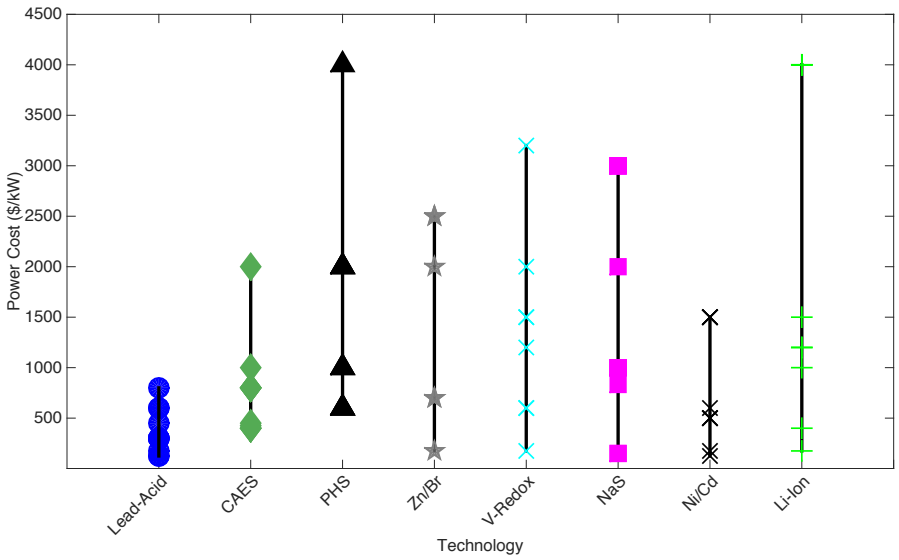

Figure 2-1: Power capacity capital costs presented in the energy storage literature demonstrating the wide range in reported cost estimates[11, 69, 70, 9, 7, 72].

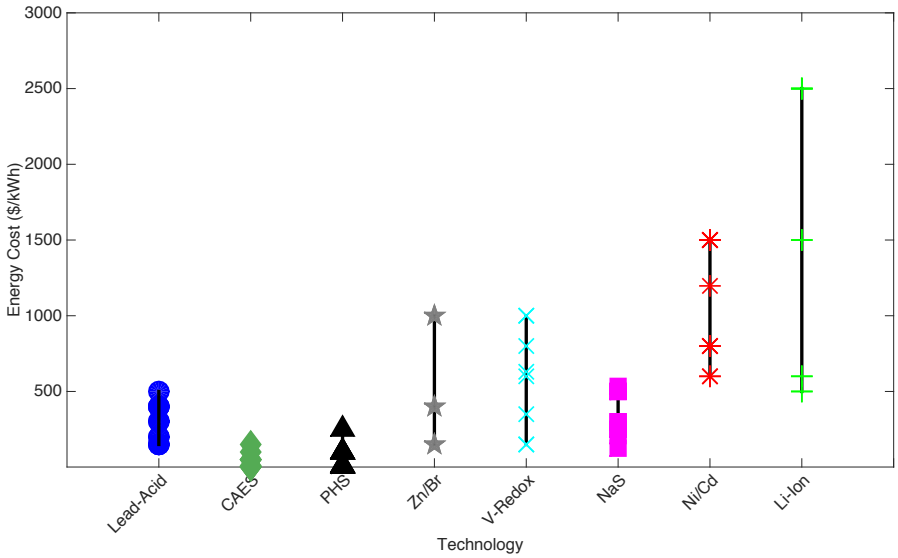

Figure 2-2: Energy capacity capital costs presented in the energy storage literature demonstrating the wide range in reported cost estimates[11, 69, 70, 9, 7, 72].

Table 2.1: Power capacity capital costs shown in $/kW as presented in the literature.

Power Costs	$/kW										
Technology	Schoenung Bulk[11]	Schoenung Distributed[11]	Evans [7]	Sundarara-gavan[72]	Chen Low[69]	Chen High[69]	Castillo Low[70]	Castillo High[70]	Kousksou Low[9]	Kousksou [9]	Kousksou High[9]
Lead-acid	125	175	300	450	300	600	300	800		300	
Ni/Cd	125	175	1500	600	500	1500			500		1500
Na/S	150	150	3000	3000	1000	3000	1000	2000	1000		3000
CAES	425	550	800	450	400	800	800	1000	400		2000
PHS	1000		600	2000	600	2000	1000	4000	600		2000
Zn/Br		175		2000		700	2500				
Li-Ion		175	4000	1500	1200	4000	400	1000		4000	
V-redox		175		3200	600	1500	1200	2000			

Table 2.2: Energy capacity capital costs shown in $/kWh as presented in the literature.

Energy Costs	$/kWh										
Technology	Schoenung Bulk[11]	Schoenung Distributed[11]	Evans [7]	Sundarara-gavan[72]	Chen Low[69]	Chen High[69]	Castillo Low[70]	Castillo High[70]	Kousksou Low[9]	Kousksou [9]	Kousksou High[9]
Lead-acid	150	150	400	300	200	400	150	500		400	
Ni/Cd	600	600	1500	1197	800	1500			800		1500
Na/S	250	250	500	534	300	500	125	250	300		500
CAES	3	120	50	10	2	50	50	150	2		100
PHS	10		100	12	5	100	100	250	5		100
Zn/Br		400		400		150	1000				
Li-Ion		500	2500	1500	600	2500	500	1500		2500	
V-redox		600		630	150	1000	350	800			

2.3 Optimizing charging and discharging behavior

An optimization, as described in (2.1), was performed for each location using hourly electricity price data and generation data. The optimization is designed to provide maximum revenue for the operator of the hybrid renewables and energy storage facility through control of the charge and discharge rate of energy from the ESS. Efficiency losses in an AC-AC ESS will occur in both the charging and discharging phases while self-discharge losses occur as a function of time in the storage medium. For the purposes of this analysis, the roundtrip efficiency is applied as a single term during system charging as seen in (2.1b) and (2.1c). Self discharge effects are not analyzed.

The optimization is performed in three week intervals using a week of overlap between each interval to maintain continuity. The shorter time period is used to reduce the computational intensity of the optimization, while the overlap ensures that the storage system is not fully discharged at the end of each two week block. Sioshansi (2010) used a similar method of overlapping periods to reduce computational time [83]. It is assumed that the operator has perfect foresight of electricity prices and resource availability or generation profile for each three week period. Connolly et al. (2011) show that the losses in revenue from operating according to a heuristic rather than through perfect foresight might be as low as 3%, making this a reasonable assumption [87]. A linear optimization is performed on the price and generation data for each period, treating charging and discharging separately, and an energy offset is included in the energy constraint to account for energy in the storage unit carried over from the previous period.

$$R_{\text{total}} = \max(\sum_{t=0}^{N} P(t)(x_{generation}(t) + x_{discharge}(t) - x_{charge}(t)/\eta))$$

$$0 \leq x_{discharge}(t) \leq \dot{E}_{\max} \tag{2.1a}$$

$$0 \leq x_{charge}(t) \leq \min(\eta x_{generation}(t), \eta \dot{E}_{\max}) \tag{2.1b}$$

$$0 \leq \sum_{t} i = 0^{N} \left(x_{charge}(t) - x_{discharge}(t)\right) \leq h\dot{E}_{\max} \tag{2.1c}$$

The power capacity, $\dot{E}_{\max}$, and storage duration, h, serve as constraints to the rate at which energy can be added to the system ($\dot{E}_{\max}$) and the total amount of energy that can be stored in the ESS ($\dot{E}_{\max}h$). These values define the system size given in units of $\text{MW}/\text{MW}_{\text{gen}}$ and hours. For this analysis, the size of the storage facility both in terms of power capacity and total energy capacity, $\dot{E}_{\max}h$, are defined relative to the size of the generation facility. To reduce the computational time, these values range in increments of .25 $\text{MW}/\text{MW}_{\text{gen}}$ and .25 hours spanning the ranges provided in (2.2a) and (2.2b).

$$0 \leq \dot{E}_{\max} \leq 5 \tag{2.2a}$$

$$0 \leq h \leq 4 \tag{2.2b}$$

Discharging is constrained by the power capacity of the storage unit as seen in (2.1a). Charging is constrained by the smaller of either the power capacity of the ESS or by the amount of electricity generated by the renewables, shown in (2.1b). This prevents the storage unit from providing pure arbitrage on the grid in which it would purchase electricity when prices are low and sell back when prices are higher. Thus, the hybrid system is operating as a generation facility which provides non-negative levels of electricity to the grid (either positive or no electricity). Lastly, the amount of energy in the storage unit is limited by the energy capacity of the unit, equal to the power capacity multiplied by the duration of storage. In (2.1c) the lower bound serves to prevent the storage unit from operating at a deficit. It can only discharge electricity that has been previously stored, and cannot borrow against future storage.

Power and energy capacity, or $\dot{E}_{\max}$ and $\dot{E}_{\max}h$, serve as independent variables in the model which are manipulated within the constraints of (2.2a) and (2.2b). As choices that can be made for each specific energy storage project they impact the ability of storage to achieve a desired goal. This is different than limitations impacted the physical limits of the technology, such as efficiency and self-discharge, though separating the impacts of the design variables from the physical limits can be

challenging. This research optimizes a storage system in terms of these design metrics in order to determine the best value added of storage so that storage technologies can be compared according to their cost intensities. In this way, both design variables and performance intensity metrics contribute to determining the final performance of a system. The remainder of this section describes the demonstrates the difference in impact on storage from the design variables of power and energy capacity and the physical limits of efficiency and self-discharge.

Figures 2-3, 2-4, A-1, A-2, and A-3 demonstrate the effects of system size constraints and the enabling metrics of efficiency and self-discharge on the ability of a hybrid solar and storage facility to meet demand. Figure 2-3 demonstrates in isolation the effect of an 8 MW charging power capacity limit of storage on the amount of energy in storage and the subsequent ability to use stored energy to meet demand. Of interest is the shallower slope of energy in storage leading to a lower total quantity of energy in the bottom figure, and a shorter period in which demand is met in the limited case compared to the non-limited case in the middle figure. A similar analysis is shown in figure 2-4 where a 45 MWh energy capacity limits the total amount of energy in storage.

2.4 Dimensionless performance metric - χ

By shifting generation output to periods of higher prices, the addition of storage increases the revenue of the wind or solar generation facility. This increased revenue comes at increased capital cost for both the energy capacity component and the power capacity component that define the total cost of storage. To determine the value added by the addition and optimal use of storage a unitless benefit / cost ratio, annual revenue over annual cost, is used. This performance metric, χ, as defined in (2.3), is evaluated for each pair of the independent variables: energy capacity cost, $C_{\text{storage}}^{\text{energy}}$, and power capacity cost, $C_{\text{storage}}^{\text{power}}$. Also included in the total system cost is the cost of generation, C_{gen}, and the capital recovery factor, CRF, which amortizes the capital costs for comparison to the yearly revenue.

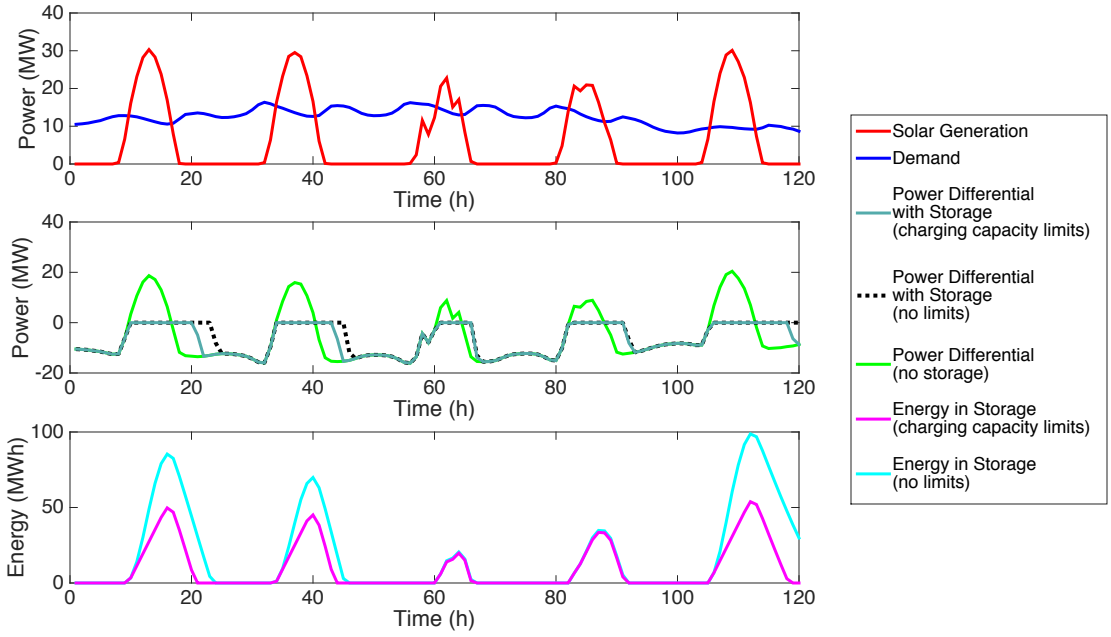

Figure 2-3: These figures demonstrate the effect of charging power capacity on the amount of energy in storage, and the ability of that energy to meet demand. In the top figure, hourly demand and solar generation data are presented for January 1, 2008 through January 5, 2008 for the north central region of ERCOT [98]. The middle figure shows unmet demand, demand minus solar generation, for the case without storage, with storage with no limitations, and with storage with a limitation of 8 MW charging power capacity. The bottom figure shows the amount of energy in storage for both the limited and non-limited case.

$$\chi = \frac{R_{\text{total}}}{CRF\left(C_{\text{gen}} + \dot{E}_{\text{max}}(C_{\text{storage}}^{\text{power}} + hC_{\text{storage}}^{\text{energy}})\right)} \tag{2.3}$$

For constant C_{gen} and CRF, the cost intensities of storage are varied in \$2 increments spanning the ranges given in (2.4a) and (2.4b). The C_{gen} is calculated for \$.5/Watt, \$1/Watt, \$2/Watt, \$3/Watt, and \$4/Watt. A single CRF is used in this analysis based on a 20 year period with a 5% interest rate [59]. For each pair of cost intensities, the highest value of χ is determined based on the optimal charge and discharge operation of storage for the range of power capacities and duration of storage.

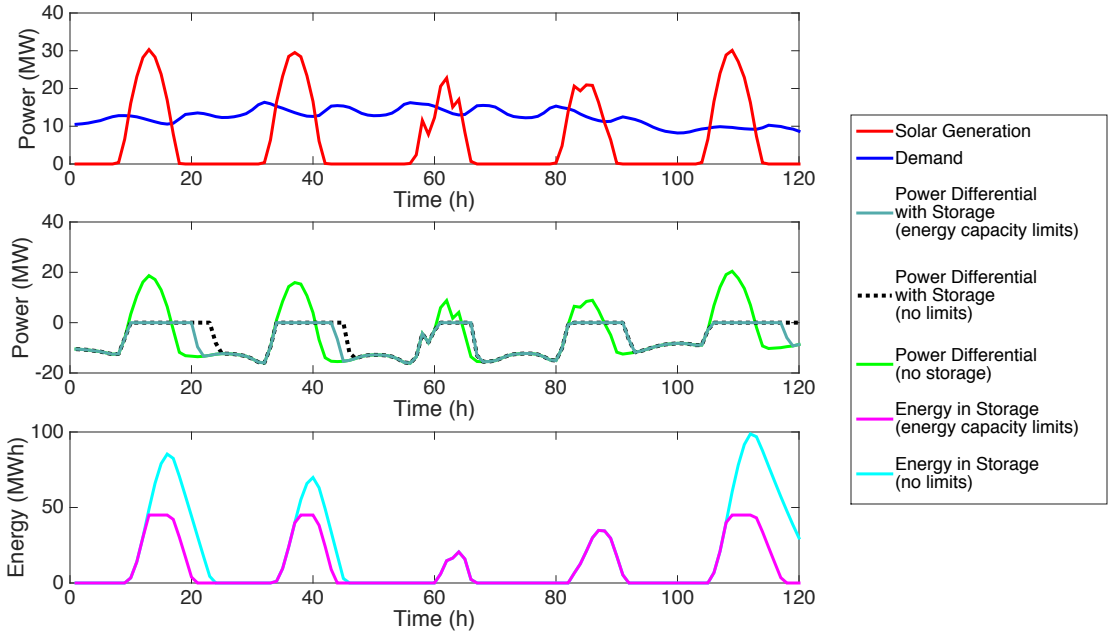

Figure 2-4: These figures demonstrate the effect of energy capacity on the amount of energy in storage, and the ability of that energy to meet demand. In the top figure, hourly demand and solar generation data are presented for January 1, 2008 through January 5, 2008 for the north central region of ERCOT [98]. The middle figure shows unmet demand, demand minus solar generation, for the case without storage, with storage with no limitations, and with storage with a limitation of 45 MWh energy capacity. The bottom figure shows the amount of energy in storage for both the limited and non-limited case.

$$2 \leq C_{\text{storage}}^{\text{energy}} \leq 700 \tag{2.4a}$$

$$2 \leq C_{\text{storage}}^{\text{power}} \leq 400 \tag{2.4b}$$

The total cost of storage is a function of both the cost intensities and the power capacity and energy capacity of storage as seen in the dominator of (2.3). The highest value of χ for each $C_{\text{storage}}^{\text{energy}}$ and $C_{\text{storage}}^{\text{power}}$ is defined for a unique power capacity and duration of storage. Thus, the total output of the model is a matrix of χ, optimal power capacity, and optimal storage duration for each pair of cost intensities.

2.5 Artificial price time series

To understand the way emergent features of the hourly electricity prices affect the optimal sizing and value of storage a series of artificial hourly electricity prices were developed and used in the optimization model. The artificial price series is composed of a sinusoidal base price overlaid with price spikes of a set frequency, height, and duration. The sinusoidal base varies with an amplitude of $10 centered at $110. Price spikes are added to the sinusoidal base at varying in frequency of occurrence, duration, and $ value, hereafter referred to as height.

The frequency ranged from less than diurnal to more than once a day, or specifically from 100 times per year to 500 times per year in 50 spike increments. Duration was varied in one hour increments from one to four hours. Four additionally scenarios were modeled building on this initial case: duration of two hours every third and every other, and three hour long price spikes every third and every other spike. Lastly, the height for any given series was a constant value ranging in $50 increments from $150 to $500. The height was set as a constant $ value, and not an increase above the value of the sinusoid, so that the spike was always of the same height regardless of where it occurred in the base oscillation.

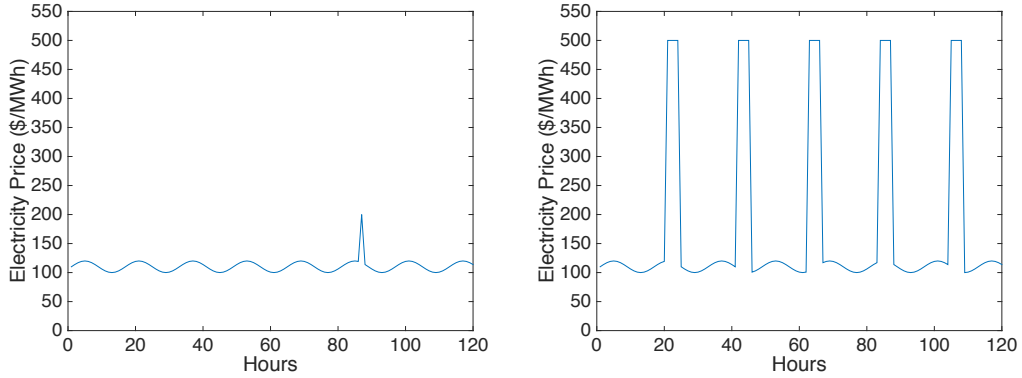

(a) Artificial price series of frequency 100 spikes/year, height $200/MWh, duration 1 hour

(b) Artificial Price Series of Frequency 400 spikes/year, Height $500/MWh, Duration 3 hour

Figure 2-5: Comparison of two example electricity price artificial time series

In figure 2-5 a comparison is shown between two extreme examples of artificial

electricity price series generated to explore the impact of changing price spike frequency, height, and duration. Figure 2-5a shows price spikes that occur 100 times per year to a height of $200/MWh and last 1 hour in duration. This can be compared to figure 2-5b which has 400 price spikes per year of $500/MWh for three hours each time. Neither figure 2-5a nor 2-5b are realistic price dynamics for a real market place; their importance lies in the discrete manipulation of the price spike features for exploring the effect of these features on the model output.

In addition to varying the duration of every price spike, artificial price series were also developed with price spikes of longer duration ever other and every third spike. Figure 2-6 shows an example price series in which the duration of price spikes is two hours every other price spike, figure 2-6a, opposite an artificial price series where the duration is two hours every third price spike, figure 2-6b. For both artificial price series in figure 2-6 the frequency and height of price spikes are identical, the only change is the frequency of longer price spikes.

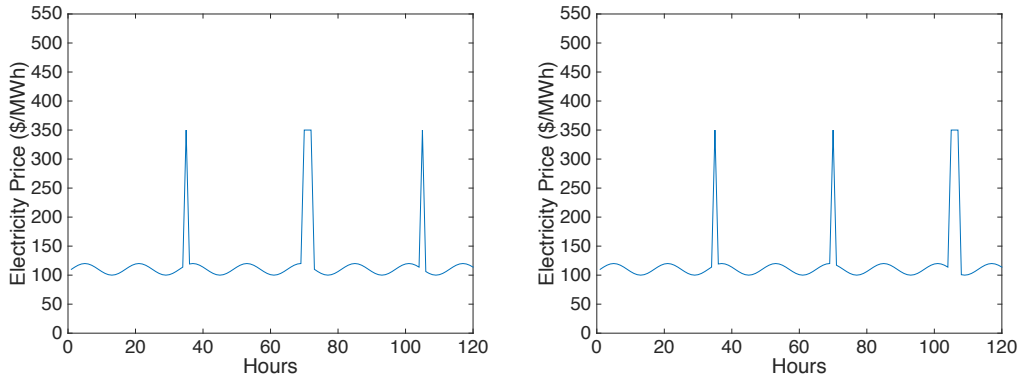

(a) Artificial price series of frequency 250 spikes/year, height $350/MWh, duration 2 hours every other spike

(b) Artificial Price Series of Frequency 250 spikes/year, Height $350/MWh, Duration 2 hours every third price spike

Figure 2-6: Comparison of two example electricity price artificial time series in which the price spikes vary in duration within the time series.

Chapter 3

Results

This chapter presents the main results of the analysis of χ and the electricity price dynamics which are responsible for the variation in χ across locations. After demonstrating the model output and using the model to compare storage technologies, an analysis of the slopes of lines of constant χ is performed. It will be shown that the frequency and height of price spikes are important for determining the value of χ while duration of price spikes is primarily responsible for the slope of the iso-χ lines, and therefore for the relative value of storage technologies across locations. This relative tradeoff in the value of storage is largely location invariant. Lastly, an analysis of the electricity price dynamics is conducted for the locations studied to show how the features seen in the hourly electricity prices across locations explain the similarity in the slopes of the iso-χ lines.

3.1 χ, optimal storage duration, and optimal power capacity

The final output of the linear optimization model used to analyze the value of storage is a set of three matrices which provide the optimal χ value and the optimal storage duration and power capacity used to obtain that χ for each pair of cost intensities and each generation cost. For a given generation cost, the value of χ is plotted as a

function of the cost intensity of energy energy storage on the horizontal axis and the cost intensity of power storage on the vertical axis. Figure 3-1 is an example of the increased value which storage provides to a wind plant in Texas when the generation cost is \$2/W. The constant value of χ in the upper right corner of figure 3-1 is the benefit / cost ratio when storage is prohibitively expensive. This lower χ value is the value of the renewables facility without any storage included.

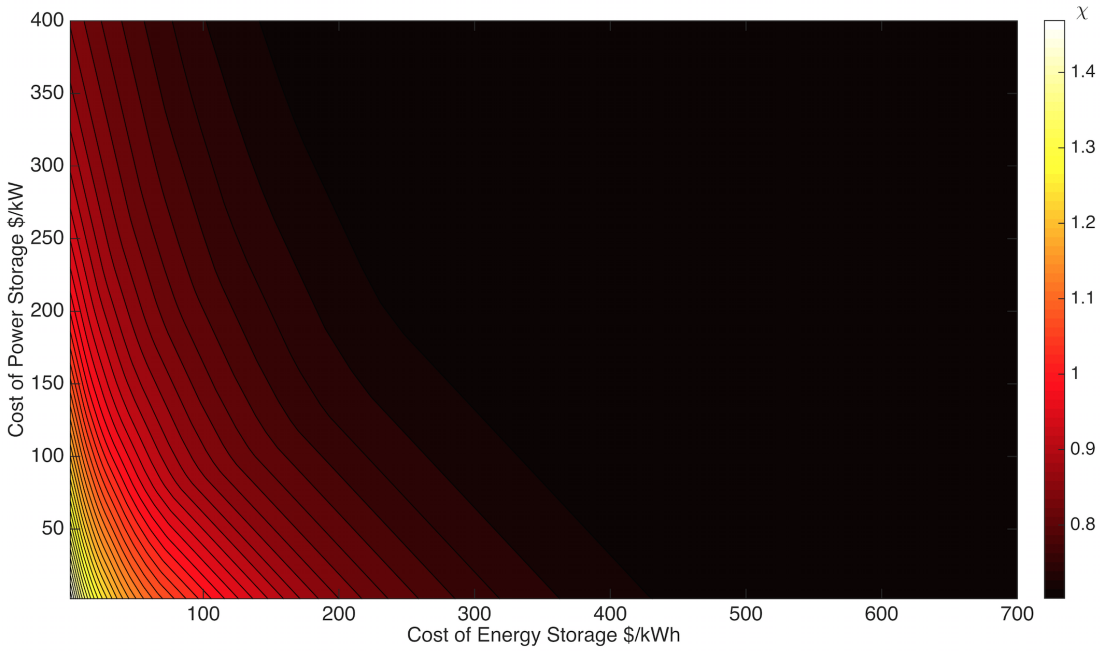

Figure 3-1: Example benefit / cost ratio χ for Texas wind farm with \$2/W generation cost

Figures 3-2 and 3-3 are examples of the optimal storage duration and power capacities which correspond to the χ values in figure 3-1. It should be noted that the boundary at which storage becomes valuable can be clearly seen in figures 3-2 and 3-3 as the limit at which storage duration and power capacity go to zero. The figures presented here are stylized renditions of the optimal model output that have reduced some of the system noise which results from the discrete values of storage duration and power capacity that serve as inputs to the model.

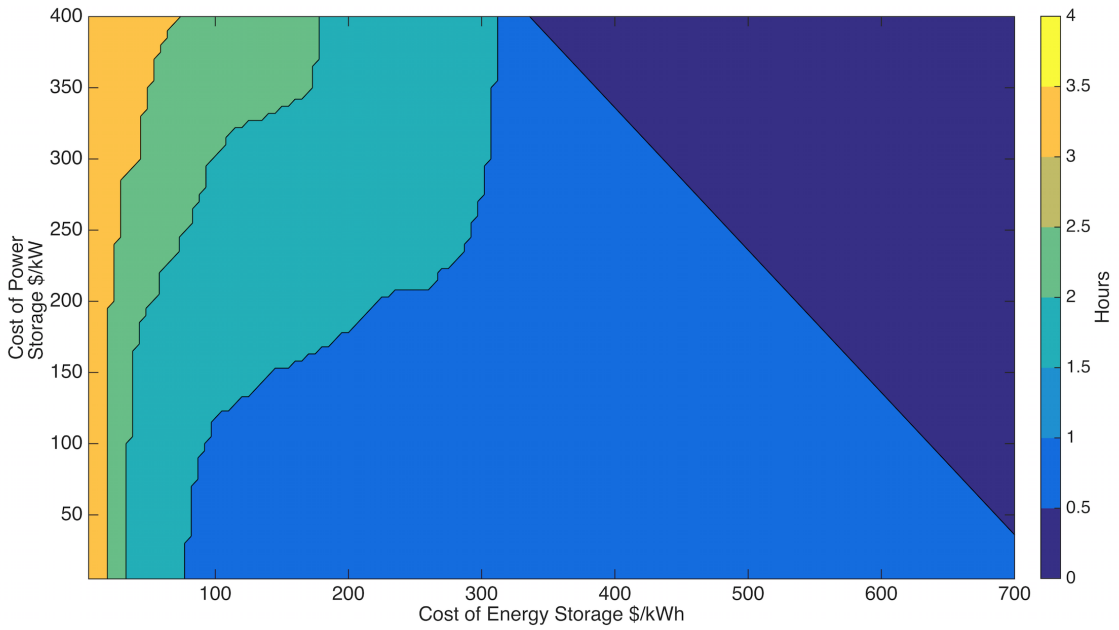

Figure 3-2: Example optimal energy storage duration for the χ values in figure 3-1

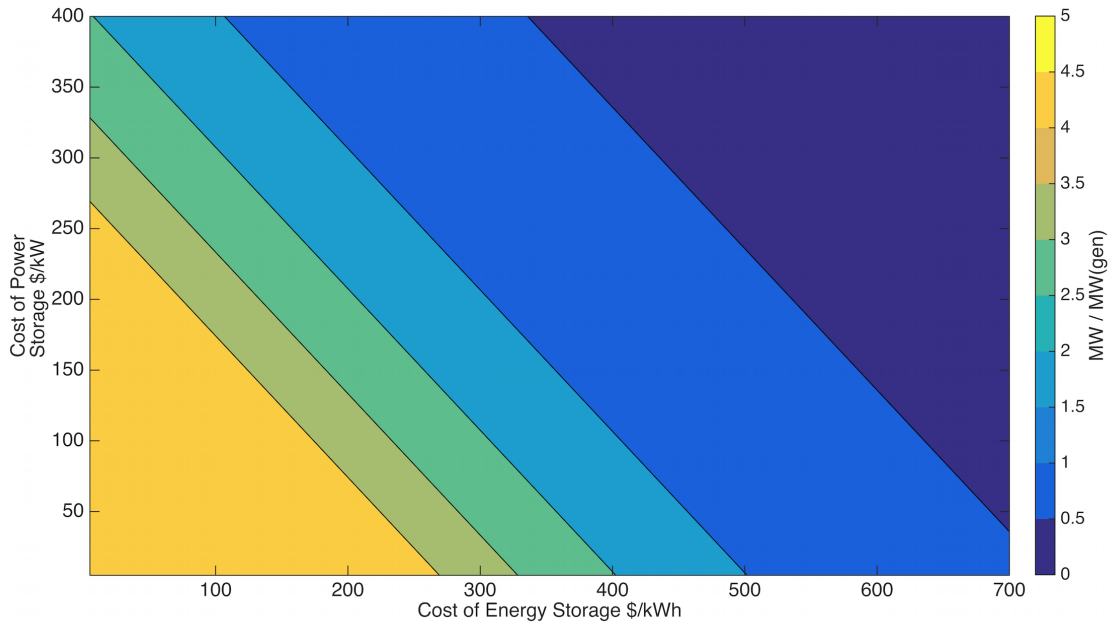

Figure 3-3: Example optimal power capacities for the χ values in figure 3-1

3.2 Energy storage technology comparisons

Overlaying the cost intensities of a specific technology onto the plot of χ allows for comparison of technologies based on the value they add to a renewables generation

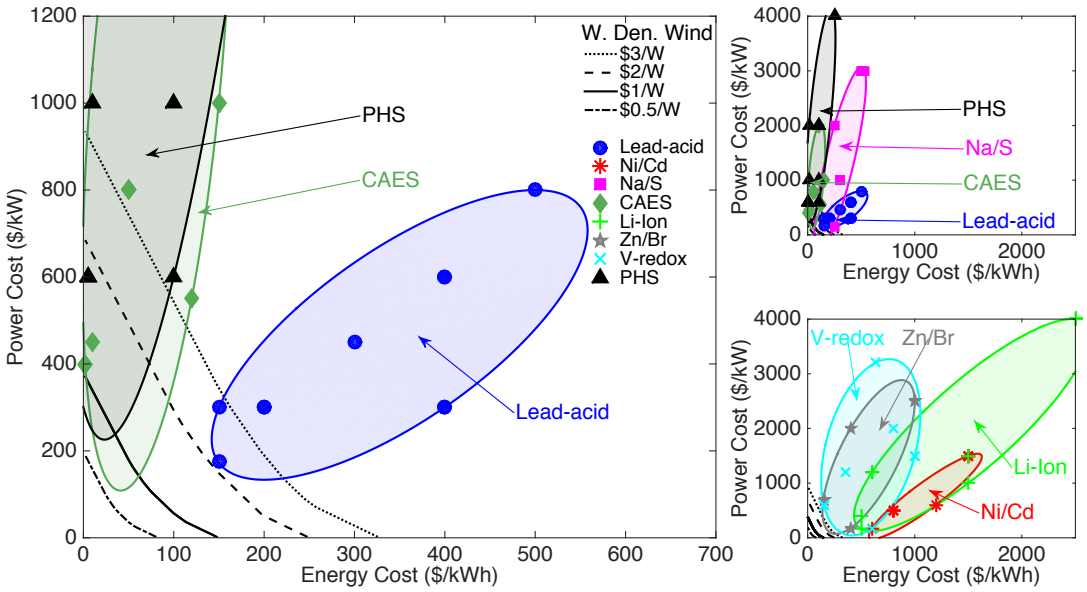

Figure 3-4: Cost intensities of a range of energy storage technologies [69, 70, 7, 9, 11, 72] overlaid with lines, for a given generation cost, which show the threshold storage cost intensities at which it becomes valuable to incorporate storage into an West Denmark wind farm. The ellipses are plotted for each storage technology to highlight the uncertainty of energy and power costs of storage. Figures B-1, B-2, B-3, B-4, B-5, B-6, B-7, and B-8 present similar results for the other locations studied [1].

facility with a given C_{gen}. Using the technological cost intensity data presented in 2.2, the published costs for each technology is plotted in the cost plane. The downward sloping lines in figure 3-4 depict the boundary at which storage becomes valuable for each given C_{gen} of renewables.

The large range in the reported cost intensities is shown in figure 3-4 represented as ovals overlaid on the energy and power cost space. As can be seen, when compared against the iso-χ lines which denote when storage becomes valuable for different generation costs, a technology's individual cost intensities are an important determinant as to whether or not it will provide value to a hybrid renewables and storage system. The distance from a technology's initial cost intensities to the iso-χ line of value determines the cost target for the technology.

The ranges of some technologies are much larger than the area on the cost plane where storage is valuable. This complicates the determination of technological cost targets and the comparison of different technologies. Rather than choose values from

a particular reference, the rest of this analysis will utilize a hypothetical pair of cost intensities designed to be representative of the differences technologies can have in their cost of energy storage and cost of power storage.

3.3 Slope of iso-χ lines

The lines in figure 3-4 which depict the boundary for the cost space for a given C_{gen} are also lines with the same χ value, iso-χ lines. Iso-χ lines for the regions of study have the same general shape; they are downward sloping when plotted on a plane defined on the vertical axis by the variable $C_{\text{storage}}^{\text{power}}$ and by $C_{\text{storage}}^{\text{energy}}$ on the horizontal axis.

An analysis of the units of $C_{\text{storage}}^{\text{power}}$ and by $C_{\text{storage}}^{\text{energy}}$ shows that the slope of the iso-χ line is in units of hours: $\frac{\$/\text{kW}}{\$/\text{kWh}}$ = hours. The derivative of an iso-χ line with respect to $C_{\text{storage}}^{\text{power}}$ and $C_{\text{storage}}^{\text{energy}}$, $\frac{dC_{\text{storage}}^{\text{power}}}{dC_{\text{storage}}^{\text{energy}}}$ can be determined for all points by taking the partial derivative $\frac{\partial \chi}{\partial C_{\text{storage}}^{\text{energy}}}$ and dividing it by $\frac{\partial \chi}{\partial C_{\text{storage}}^{\text{power}}}$. So,

$$\frac{dC_{\text{storage}}^{\text{power}}}{dC_{\text{storage}}^{\text{energy}}}|_{\chi} = \frac{\partial \chi / \partial C_{\text{storage}}^{\text{energy}}}{\partial \chi / \partial C_{\text{storage}}^{\text{power}}} \tag{3.1}$$

By making the simplifying assumption that $\dot{E}_{\text{max}}$ and h are independent of the $C_{\text{storage}}^{\text{power}}$ and $C_{\text{storage}}^{\text{energy}}$ the partial derivatives of χ become relatively simple to calculate. Note that the capital recovery factor, CRF, will be written as γ for the following derivation.

$$\frac{\partial \chi}{\partial C_{\text{storage}}^{\text{energy}}} = \frac{-R_{\text{total}} \gamma \dot{E}_{\text{max}} h}{\left(\gamma \left\{ C_{\text{gen}} + \dot{E}_{\text{max}} (C_{\text{storage}}^{\text{power}} + h C_{\text{storage}}^{\text{energy}}) \right\} \right)^2} \tag{3.2}$$

$$\frac{\partial \chi}{\partial C_{\text{storage}}^{\text{power}}} = \frac{-R_{\text{total}} \gamma \dot{E}_{\text{max}}}{\left(\gamma \left\{ C_{\text{gen}} + \dot{E}_{\text{max}} (C_{\text{storage}}^{\text{power}} + h C_{\text{storage}}^{\text{energy}}) \right\} \right)^2} \tag{3.3}$$

It can therefore be seen that the ratio of these two terms leaves only the energy

storage duration, h. Along a constant χ the marginal decrease in the power capacity cost for a marginal increase in energy capacity cost is equal to the optimum number of hours of energy storage capacity. An inspection of equation (2.3) for χ shows that this is indeed the case, with the key term being $C^{\text{power}}_{\text{storage}} + hC^{\text{energy}}_{\text{storage}}$ which appears in the denominator.

A full derivation or χ must account for the fact that $R_{\text{total}}, \dot{E}_{\max}$, and h are themselves functions of $C^{\text{power}}_{\text{storage}}$ and $C^{\text{energy}}_{\text{storage}}$ and can more accurately be expressed as:

$$R_{\text{total}} = f(\dot{E}_{\max}, h) \tag{3.4a}$$

$$\dot{E}_{\max} = f(C^{\text{energy}}_{\text{storage}}, C^{\text{power}}_{\text{storage}}) \tag{3.4b}$$

$$h = f(C^{\text{energy}}_{\text{storage}}, C^{\text{power}}_{\text{storage}}) \tag{3.4c}$$

This leads to partial derivatives:

$$\frac{\partial \chi}{\partial C^{\text{energy}}_{\text{storage}}} = \frac{\dfrac{\partial R_{\text{total}}}{\partial \dot{E}_{\max}}\dfrac{\partial \dot{E}_{\max}}{\partial C^{\text{energy}}_{\text{storage}}} + \dfrac{\partial R_{\text{total}}}{\partial h}\dfrac{\partial h}{\partial C^{\text{energy}}_{\text{storage}}}}{\gamma\Big(C_{\text{gen}} + \dot{E}_{\max}(C^{\text{power}}_{\text{storage}} + hC^{\text{energy}}_{\text{storage}})\Big)} - \frac{R_{\text{total}}\left(\gamma\big\{\dfrac{\partial \dot{E}_{\max}}{\partial C^{\text{energy}}_{\text{storage}}}C^{\text{power}}_{\text{storage}} + (\dfrac{\partial \dot{E}_{\max}}{\partial C^{\text{energy}}_{\text{storage}}}h + \dfrac{\partial h}{\partial C^{\text{energy}}_{\text{storage}}}\dot{E}_{\max})C^{\text{energy}}_{\text{storage}} + \dot{E}_{\max}h\big\}\right)}{\left(\gamma\big\{C_{\text{gen}} + \dot{E}_{\max}(C^{\text{power}}_{\text{storage}} + hC^{\text{energy}}_{\text{storage}})\big\}\right)^2} \tag{3.5}$$

$$\frac{\partial \chi}{\partial C_{\text{storage}}^{\text{power}}} = \frac{\frac{\partial R_{\text{total}}}{\partial \dot{E}_{\max}} \frac{\partial \dot{E}_{\max}}{\partial C_{\text{storage}}^{\text{power}}} + \frac{\partial R_{\text{total}}}{\partial h} \frac{\partial h}{\partial C_{\text{storage}}^{\text{power}}}}{\gamma\Big(C_{\text{gen}} + \dot{E}_{\max}(C_{\text{storage}}^{\text{power}} + hC_{\text{storage}}^{\text{energy}})\Big)}$$
$$- \frac{R_{\text{total}}\left(\gamma\big\{\frac{\partial \dot{E}_{\max}}{\partial C_{\text{storage}}^{\text{power}}} C_{\text{storage}}^{\text{power}} + (\frac{\partial \dot{E}_{\max}}{\partial C_{\text{storage}}^{\text{power}}} h + \frac{\partial h}{\partial C_{\text{storage}}^{\text{power}}} \dot{E}_{\max}) C_{\text{storage}}^{\text{energy}} + \dot{E}_{\max}\big\}\right)}{\left(\gamma\big\{C_{\text{gen}} + \dot{E}_{\max}(C_{\text{storage}}^{\text{power}} + hC_{\text{storage}}^{\text{energy}})\big\}\right)^2} \tag{3.6}$$

Equations (3.5) and (3.6) simplify to equations (3.2) and (3.3) respectively when the following conditions are met:

$$\frac{\partial h}{\partial C_{\text{storage}}^{\text{power}}} = 0 \qquad \frac{\partial h}{\partial C_{\text{storage}}^{\text{energy}}} = 0 \tag{3.7a}$$

$$\frac{\partial \dot{E}_{\max}}{\partial C_{\text{storage}}^{\text{power}}} = 0 \qquad \frac{\partial \dot{E}_{\max}}{\partial C_{\text{storage}}^{\text{energy}}} = 0 \tag{3.7b}$$

There are two reasons (3.7a) and (3.7b) are reasonable simplifications for this study. The first is that as the choice of power capacity and energy storage capacity become more continuous, the magnitude of the marginal change in the number of hours of storage, h, and the power capacity, $\dot{E}_{\max}$ each as a function of either $C_{\text{storage}}^{\text{power}}$ or of $C_{\text{storage}}^{\text{energy}}$ gets smaller. The small change in h and $\dot{E}_{\max}$ that is currently modeled as a discrete step will now be spread over the entire region of storage choices. This can be seen in the large space between contours in figures 3-2 and 3-3.

The second reason the simplified equations, (3.2) and (3.3), are appropriate in understanding the relationship between the χ value and the cost inputs is that many technologies are not fully modular in the size of their power capacity and energy capacity. For example, many battery manufacturers only produce cells of a certain size. Similarly, the companies which produce pumps and turbines for PHS and CAES are also discrete in the sizes of these pieces of equipment. Because there will be some granularity of h in terms of $C_{\text{storage}}^{\text{power}}$ and $C_{\text{storage}}^{\text{energy}}$, the approximation that the slope of

the iso-χ line in the $C^{\text{energy}}_{\text{storage}}$ / $C^{\text{power}}_{\text{storage}}$ plane is equal to the hours of storage capacity holds.

This relationship can be seen graphically by overlaying a plot of the optimal energy capacity with the plot of the iso-χ lines. The inflection points in the iso-χ lines overlap with the transition from one discrete energy storage capacity to the next. Another illustration of this can be performed by allowing the energy capacities to be evaluated in quarter hour increments as opposed to only half hour increments. When this is performed, the iso-χ lines are noticeably smoother, since there are more inflection points with smaller changes in slope at each point.

A direct comparison of the ratio of partial derivatives of χ, $\frac{\partial \chi}{\partial C^{\text{energy}}_{\text{storage}}}$ and $\frac{\partial \chi}{\partial C^{\text{power}}_{\text{storage}}}$ and the optimal storage duration for each pair of cost intensities confirms the results of this section. The ratio of these two terms are within 1% of the optimal energy storage capacity in hours when operating in the space where (3.7a) and (3.7b) hold. The percent error is higher at the points at which either the h or $\dot{E}_{\max}$ increase to the next discretized value.

3.4 Detailed exploration of iso-χ lines

Comparing ESS's based on cost intensities is complicated by the two dimensions of costs, $C^{\text{energy}}_{\text{storage}}$ and $C^{\text{power}}_{\text{storage}}$. No current technology is strictly dominant in both; rather, most technologies have either lower energy costs but higher power costs - for example, CAES and PHS, or they have lower power costs but higher energy costs - batteries, flow batteries, flywheels, and others are examples of this ratio of cost intensities. The importance of χ is that it provides a single metric for valuing storage, and the iso-χ lines map to storage technologies that provide the same value. This section explores the relationship of the slope of the iso-χ lines across locations, showing that they are roughly location invariant.

Iso-χ lines also represent cost targets for ESS's. The minimum cost reduction to reach an iso-χ line, is a cost improvement target. Particularly important targets are the iso-χ lines which demarcate the value threshold for a given generation cost. These

lines denote the improvement required to make storage valuable in a given market place. Several key items of interest arise in the exploration of the value of storage. The first is the similarities across locations in the direction of optimal improvement in storage costs for a given technology. Second, a storage technology will have nearly the same relative value as another ESS independent of location. This is because the slopes of the iso-χ contour lines are roughly the same. Storage provides different value in different locations, but the relative comparison across technologies is largely location invariant.

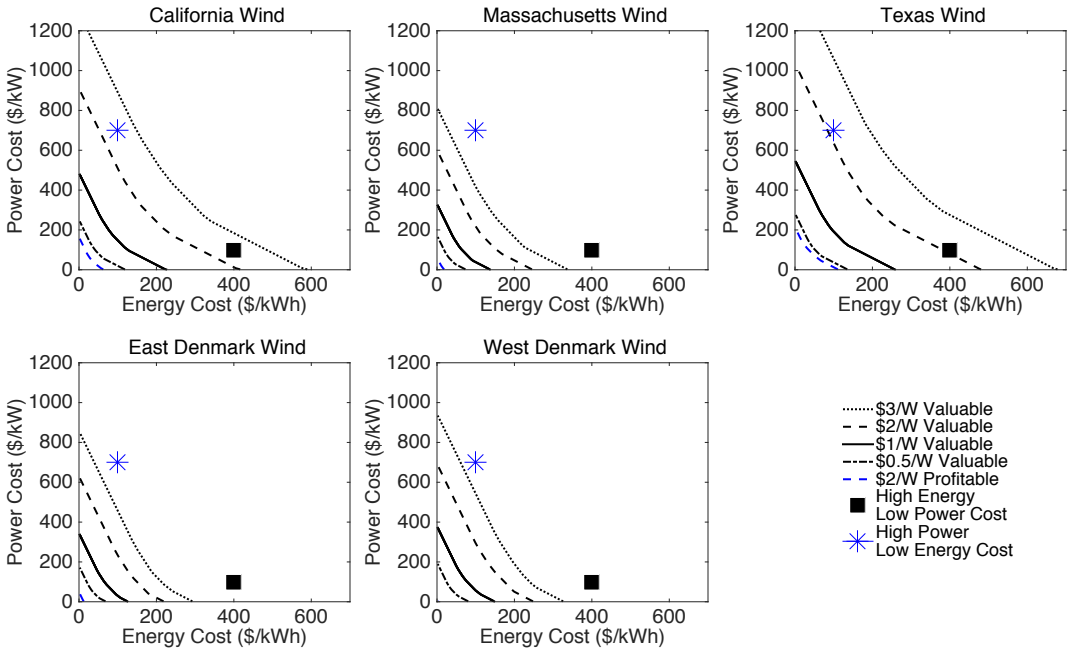

Figure 3-5: Thresholds of value for storage with renewables are shown for different generation capital cost intensities for wind and solar. The blue lines show profitability thresholds, $\chi = 1$. For wind power in all locations \$1/W is always profitable even without storage, but sufficiently in expensive storage can still provide additional value. Figure B-9 show similar results for wind in Portugal, and solar in California, Massachusetts, and Texas.

The location invariance of the relative value of storage can be seen in figure 3-5. A hypothetical low energy / high power cost technology (\$100/kWh and \$700/kWh) is compared with a high energy / low power cost technology (\$400/kWh and \$100/kW) across locations and it is evident that in general these two technologies fall on roughly

Location	Technology	Required Improvement to Meet Generation Cost	Energy Cost Reduction	Power Cost Reduction	Energy Cost Reduction Percent	Power Cost Reduction Percent
California	Solar	\$2/W	\$20/kWh	\$22/kW	5%	22%
California	Wind	\$2/W	\$44/kWh	\$43/kW	11%	43%
Massachusetts	Wind	\$3/W	\$80/kWh	\$81/kW	20%	81%
Texas	Solar	\$2/W	\$25/kWh	\$26/kW	6.5%	26%
Texas	Wind	\$2/W	\$10/kWh	\$9/kW	2.5%	9%
W. Denmark	Wind	\$3/W	\$86/kWh	\$86/kW	22%	86%

Table 3.1: Required cost improvements for a high energy (\$400/kWh) and low power cost (\$100/kW) technology to reach the nearest generation threshold. This table only shows those improvements that are not corner solutions - where the optimal solution is to reduce power costs to \$2/kW. Improvements that require reducing power costs to \$2/kW are presented in table B.1 and improvements to meet one of the profitability thresholds depicted in figures 3-5 and B-9 can be found in table B.3. All improvements to meet the profitability thresholds are corner solutions.

the same iso-χ line for each location. There are some subtle differences between locations in the United States and those in Europe that a deeper exploration of χ demonstrates is related to differences in the electricity price dynamics of those locations. This difference is the slightly higher slopes seen in West and East Denmark relative to the U.S. locations.

Actual cost reductions for the hypothetical higher energy and lower power cost technology and lower energy and higher power cost technology shown in figure 3-5 are shown in tables 3.1 and 3.2. The results show that the best way to improve χ for a given technology is to focus on cost reductions of whichever is already less expensive between the cost of energy storage and cost of power storage. This may not be a feasible solution for improvements in ESS cost intensities as the potential for large gains in cost reductions may be unachievable when the target cost intensity is already the lower cost. Tables 3.1 and 3.2 also demonstrate a feature of the best direction of improvement for ESS cost intensities which will be further explained below. For high energy / low power cost technologies, the ratio of required improvements in cost of

Location	Technology	Required Improvement to Meet Generation Cost	Energy Cost Reduction	Power Cost Reduction	Energy Cost Reduction Percent	Power Cost Reduction Percent
California	Solar	\$2/W	\$13/kWh	\$4/kW	13%	0.5%
California	Wind	\$2/W	\$45/kWh	\$12/kW	45%	1.7%
Massachusetts	Wind	\$3/W	\$67/kWh	\$16/kW	67%	2.3%
Texas	Solar	\$2/W	\$37/kWh	\$10/kW	37%	1.4%
Texas	Wind	\$2/W	\$15/kWh	\$4/kW	15%	0.6%
E. Denmark	Wind	\$3/W	\$57/kWh	\$14/kW	57%	2%
W. Denmark	Wind	\$2/W	\$96/kWh	\$24/kW	96%	3.4%
W. Denmark	Wind	\$3/W	\$37/kWh	\$10/kW	37%	1.4%

Table 3.2: Required cost improvements for a low energy (\$100/kWh) and high power cost (\$700/kW) technology to reach the nearest generation threshold. This table only shows those improvements that are not corner solutions - where the optimal solution is to reduce energy costs to \$2/kW. Improvements that require reducing energy costs to \$2/kWh are presented in table B.2 and improvements to meet one of the profitability thresholds depicted in figures 3-5 and B-9 can be found in table B.4. All improvements to meet the profitability thresholds are corner solutions.

energy storage to cost of power storage is approximately equal, while for low energy cost / high power cost technologies, a 4:1 ratio of improvement is needed. These ratios are the same across the locations studied.

Figures 3-5 and B-9 show multiple value thresholds and profitability thresholds that may provide cost targets for improvements in ESS cost intensities. Only those improvements which don't require either the minimum cost of energy storage or cost of power storage are shown. More extreme improvement targets will tend to intercept the nearer of the two axes before intercepting the iso-*chi* line. These boundary condition cases require minimizing one of the cost intensities, as the best way to meet an improvement target. Tables B.1 and B.2 show the required improvements to meet the closest value threshold which constitute one of the boundary conditions for improvement. These results do not follow the same ratios of cost of energy storage to cost of power storage as seen in tables 3.1 and 3.2 but rather can be explained as following that ratio until one of the cost intensities reaches its minimum and then further reducing the remaining intensity until the threshold is achieved. Similar results are found for the required improvements to reach a profitability threshold, all of which also require a boundary condition improvement, which can be seen in tables B.3 and B.4.

In section 3.3 a derivation of the formula for χ was performed to show that the slopes of the iso-χ lines in areas where the optimal power capacity and optimal storage duration are constant are equal to the values for the optimal storage duration. For this reason it is informative to look at the optimal storage duration as a way to more easily perceive the actual values for the slopes of the iso-χ lines. This makes it easier to compare the shapes of the curves across locations as presented in figures 3-5 and B-9.

Figure 3-6 shows the optimal storage duration for each of the locations with renewables generation being provided by wind power. For California and Texas a generation cost of \$2/W was used, while for Massachusetts and both East and West Denmark, a \$3/W generation cost was used. These different generation costs were compared in order to use figures which had a threshold of value at roughly the same costs of

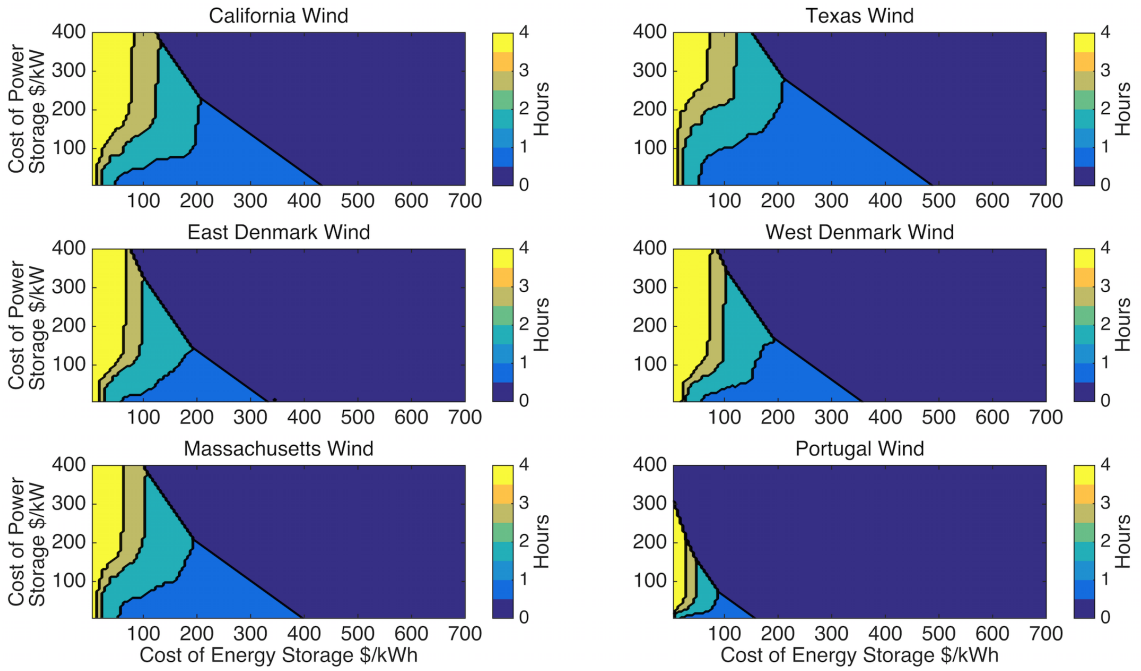

Figure 3-6: Hours of storage duration for wind power for various generation costs such that the threshold of value across location are roughly similar. Of importance is that for a given cost of energy storage and power storage, the duration of storage in Denmark and Portugal is equal to or higher than in the U.S. locations. Thus the slopes of the iso-χ lines are steeper. Figure B-10 shows similar results for solar power and storage hybrid.

energy storage and costs of power storage. For Portugal, the highest generation cost studied of \$4/W was used to make the largest area in which storage adds value, in the cost of energy storage and cost of power storage, for ease of comparison.

Important similarities across locations can be seen in figure 3-6. For the U.S. locations, the optimal storage durations for any given cost of energy storage and cost of power storage are roughly the same for wind generation in California, Massachusetts, and Texas. This can be seen in figure 3-6 in the similar locations of colors across the cost of energy storage and power storage plane. This same color distribution is found in figure B-10 for solar generation, providing an indication that this feature is less dependent on the properties of the renewables generation dynamics. West and East Denmark similarly have distributions of optimal storage duration that are roughly the same, though different than those seen for California, Massachusetts, and Texas. While difficult to show as clearly as the difference between optimal storage

duration, and therefore iso-χ slopes, in Denmark and the U.S., Portugal data appears to be more similar to the Denmark data, with a much larger region of longer storage duration in the cost of energy storage and power storage plane for which storage is valuable.

The important feature that is different between the slopes of the iso-χ lines in Europe and those in the U.S., as seen in figure 3-6 as the value of optimal storage duration, is that for any given cost of energy storage and cost of power storage the slope of the iso-χ line in Europe is as high or higher than the slope for U.S. locations. This is clearly seen in figure 3-6 where Denmark has a comparatively smaller region where the optimal storage duration is one hour in length and a much larger region where the optimal duration is 4 hours in length. Storage in Portugal appears to follow a similar pattern as storage in Denmark.

The optimal storage duration for European locations are as high or higher than in the US at any point in the cost of energy storage and power storage plane in which storage is valuable. Section 3.6 will explore causes for these differences that arise from the properties of the input price time series. After exploring how the different features of price spikes change the value of χ and the slope of the iso-χ lines in section 3.6, the actual electricity prices for each location will be analyzed for these features in section 3.7. This analysis will be used to explain the observed differences in the slopes of iso-χ lines between U.S. and European locations. First, however, one additional result of the analysis of χ will be discussed.

3.5 Direction of optimal improvement in χ

The derivation results of (3.5) and (3.6) will be primarily used in this study to analyze the slope of the iso-χ lines in order to understand the relative value of different storage technologies and how this relative value is location invariant. The derivation results are also inputs into a $\bigtriangledown\chi$ analysis which enables determination of the change in $C_{\text{storage}}^{\text{energy}}$ and $C_{\text{storage}}^{\text{power}}$ which lead to the greatest increase in χ. Equation (3.8) details this calculation of the gradient of χ in which the terms $\hat{C}_{\text{storage}}^{\text{energy}}$ and $\hat{C}_{\text{storage}}^{\text{power}}$ provide

the unit vectors in the direction of the respective axis.

$$\nabla\chi = \frac{\partial\chi}{\partial C^{\text{energy}}_{\text{storage}}}\hat{C}^{\text{energy}}_{\text{storage}} + \frac{\partial\chi}{\partial C^{\text{power}}_{\text{storage}}}\hat{C}^{\text{power}}_{\text{storage}} \tag{3.8}$$

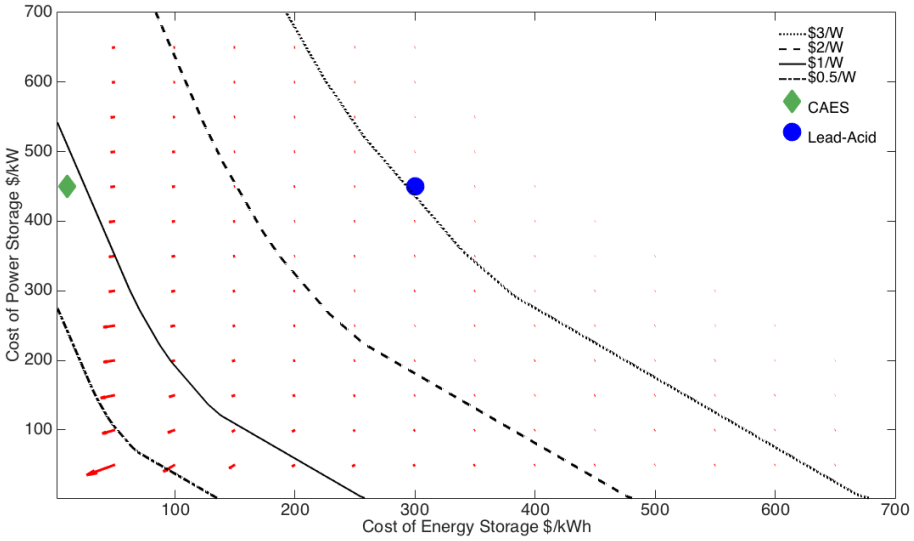

Figure 3-7: Gradients for Texas wind. $\nabla\chi$ shows the direction of greatest improvement in χ. It is greater for lower costs because the same absolute improvement in cost of energy storage or cost of power storage is a relatively greater improvement in cost for lower cost technologies. For reference, the cost estimates as provided by [72] are shown for CAES and lead-acid batteries. Figures B-11 and B-12 show similar results for the other locations and generation technologies studied.

The red arrows in figure 3-7 show the direction and relative magnitude of greatest improvement in χ; fully described in equation (3.8). The gradient vectors of χ show a relative invariance across location and technology, which is expected since the direction of the gradient is orthogonal to the iso-χ line. The gradient vectors show the relative magnitudes of improvement for different costs of energy storage and costs of power storage. Figure 3-7 shows the gradient vectors for wind generation in Texas, where each vector is given in multiples of \$50/kW and \$50/kWh for reference. Also shown are cost estimates for CAES and lead-acid from Sundararagavan and Baker (2012) [72]. These cost estimates are provided to highlight where in the $C^{\text{energy}}_{\text{storage}}$ and $C^{\text{power}}_{\text{storage}}$ plane actual technology estimates fall and their relative $\nabla\chi$.

The improvement in χ is largest for cost reductions when costs of energy storage

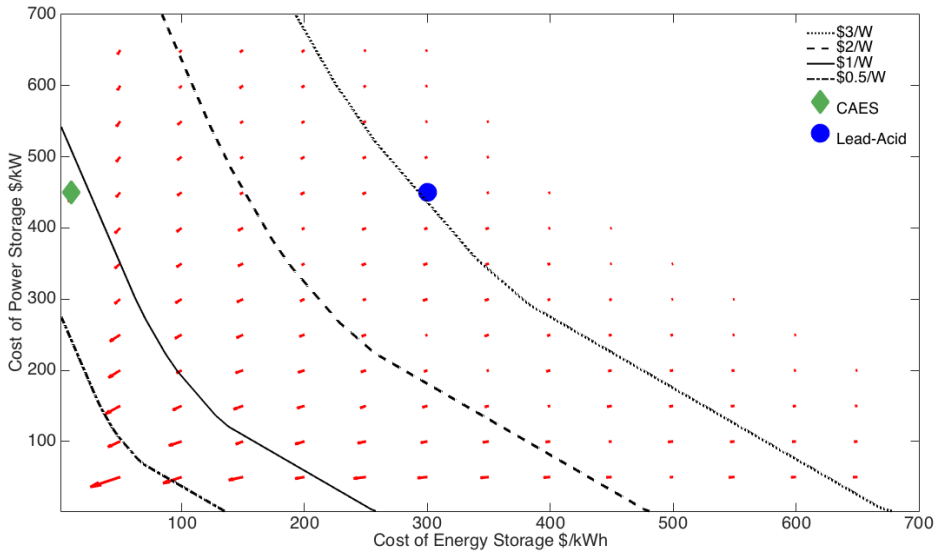

Figure 3-8: Gradients for Texas wind. $\bigtriangledown\chi$ shows the direction of greatest improvement in χ given a 10% decrease in cost of energy storage or cost of power storage. Proportional changes in cost show a generally consistent relative improvement in χ as compared with figure 3-7. For reference, the cost estimates as provided by [72] are shown for CAES and lead-acid batteries. Figures B-13 and B-14 show similar results for the other locations and generation technologies studied.

and power storage are already low. This is due to the fact that χ is based on an absolute change in costs and therefore a larger proportional change in cost occurs for the same cost reduction when the starting costs are lower. This difference can be seen in figure 3-8 which uses the same generation data for wind in Texas but instead looks at when costs have reduced by 10% for either the cost of energy storage or the cost of power storage. In this case, in which the absolute cost reductions are higher for higher initial costs, the relative magnitudes for changes in χ can be seen to be more consistent across the cost of energy storage and cost of power storage plane. Similar results are seen for other generation technologies and locations as shown in figures B-11, B-12, B-13, and B-14.

3.6 Artificial price series and the effects of price spikes

Using the artificial price time series described in section 2.5, examples of which were shown in figure 2-5, the effect of changing frequency, height, and duration of price

spikes on chi and on the optimal storage duration was explored. While all three features of price spikes have an influence on the shape of the iso-χ lines and on the value of storage, the duration of price spikes goes the furthest in explaining the similarities seen across the locations studied. This section shows the effect on χ when each of these features is varied independently. For the following figures, a generation cost of \$3/W along with the solar generation data for Texas was used to help exaggerate the effects of frequency, height, and duration of price spikes by making them easier to see in the $C_{\text{storage}}^{\text{energy}}$ and $C_{\text{storage}}^{\text{power}}$ plane.

3.6.1 Price spike frequency

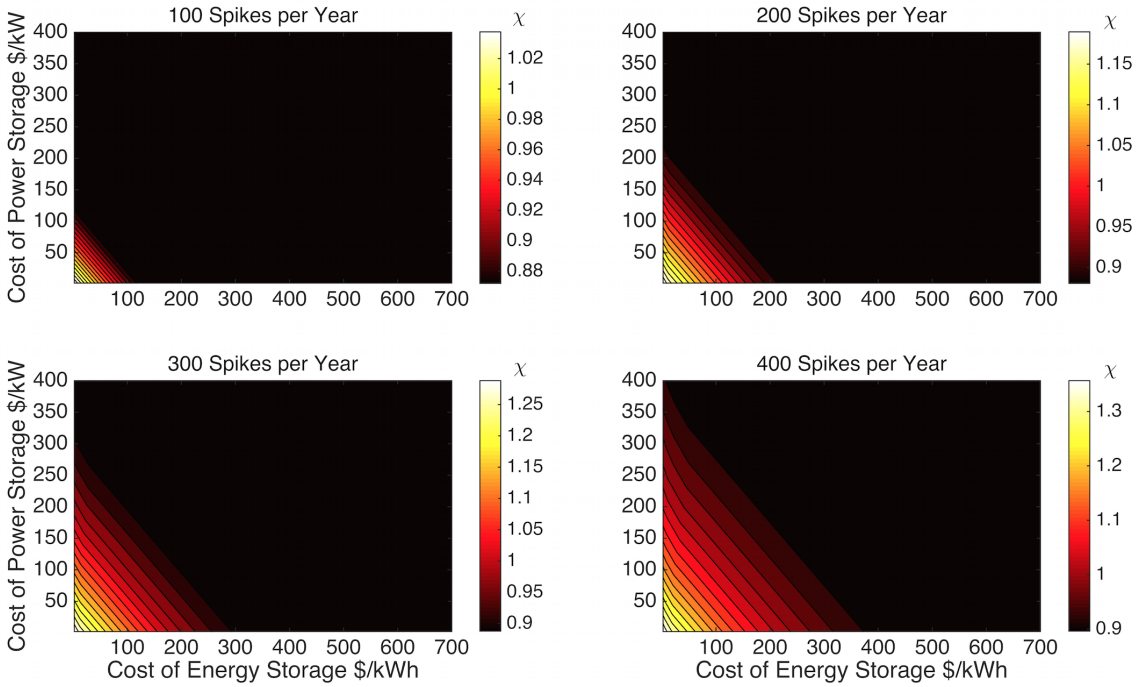

Figure 3-9: Using generation data for solar power in Texas, the effect of the frequency of price spikes of constant height \$200 and duration 1 hour on the benefit/cost ratio χ is shown. Figure 3-10 shows the optimal duration of storage resulting in the χ values shown in this figure, and therefore, as was shown in section 3.3, the values for the slope of the iso-χ lines. Figures B-15 and B-16 show similar results for higher price spikes.

Increasing the frequency of price spikes has two effects on the value of storage. The first is that for a given pair of cost intensities, storage becomes slightly more

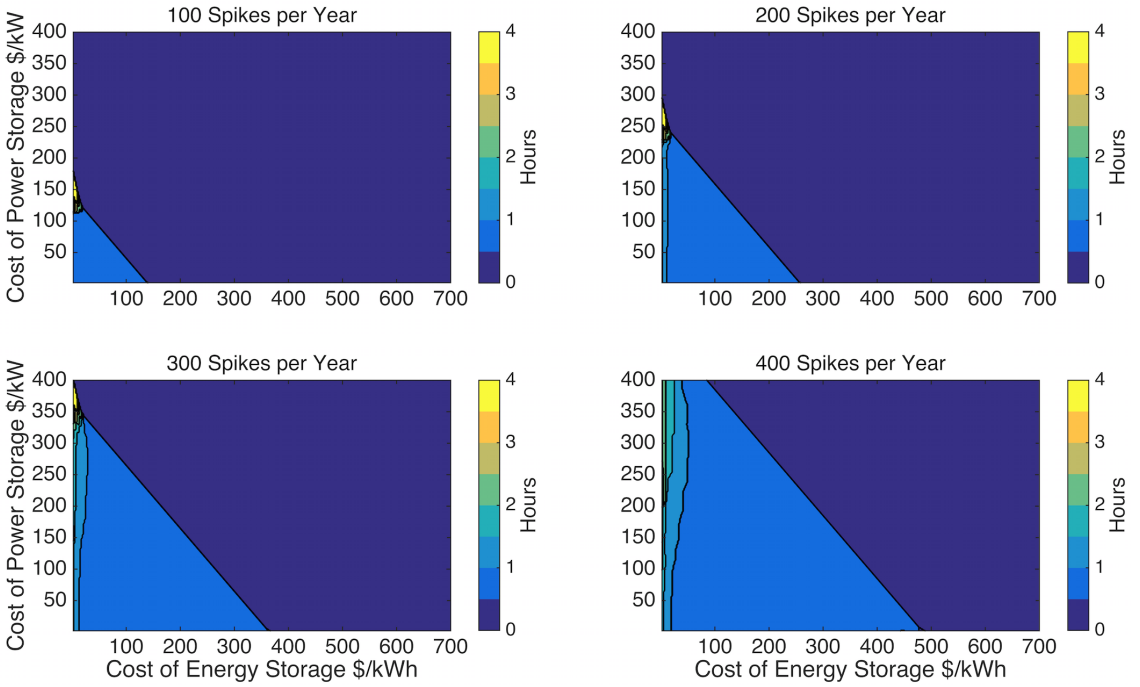

Figure 3-10: Using generation data for solar power in Texas, the effect of the frequency of price spikes of constant height $200 and duration 1 hour on the optimal duration of storage is shown. Figure 3-9 shows the optimal χ resulting from the optimal storage duration shown in this figure; as was shown in section 3.3, the values for the slope of the iso-χ lines in figure 3-9 are equal to the duration values shown here. Figures B-15 and B-16 show similar results for higher price spikes.

valuable and the second is that more expensive storage technologies can also provide benefit to the system despite their cost. The first effect is seen in the colorbar scales in figure 3-9. For the second effect, the threshold of value at which storage becomes valuable occurs at a higher $C_{\text{storage}}^{\text{energy}}$ and $C_{\text{storage}}^{\text{power}}$. Locations with more price spikes will find storage to be more valuable and will find that even more expensive ESS's may still provide value. Changing the frequency has little to no effect on the slope of the iso-χ lines as it does not change the optimal storage duration as seen in figure 3-10. The small variations in duration of storage at low $C_{\text{storage}}^{\text{energy}}$ seen in figure 3-10 are a feature of the generation data, but are not strong enough to explain the kinds of variation seen in the slopes of the iso-χ lines across costs of energy storage and power storage for the locations studied.

3.6.2 Price spike height

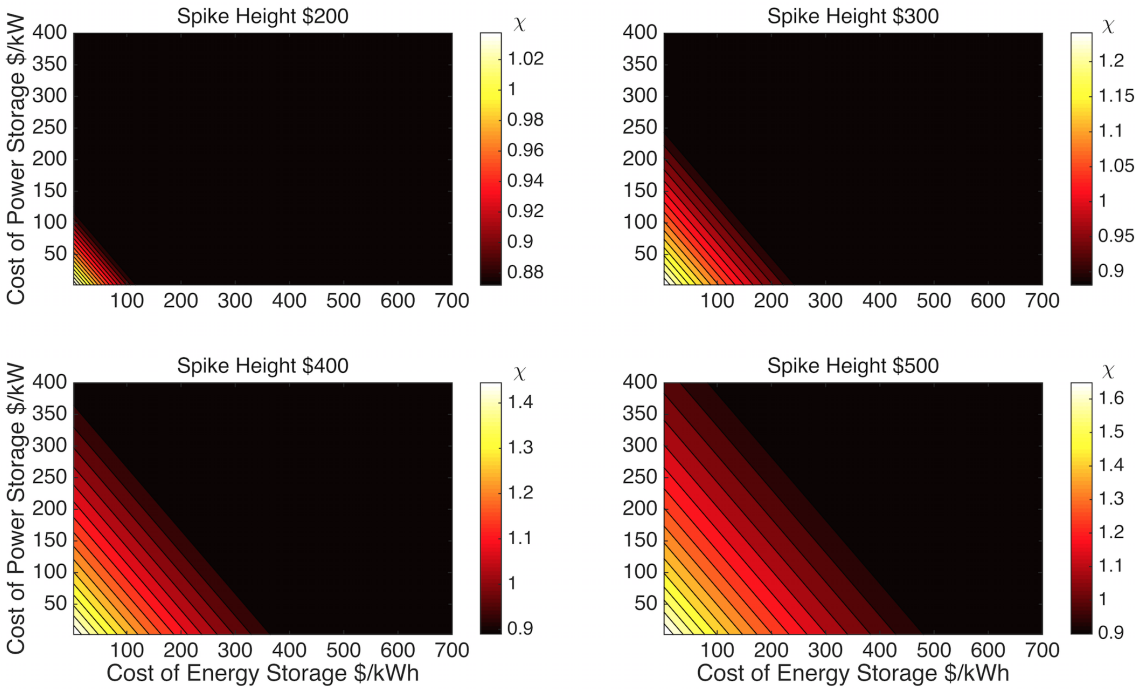

Figure 3-11: Using generation data for solar power in Texas, the effect of the height of price spikes of constant frequency 100 spikes per year of duration 1 hour on the benefit/cost ratio χ is shown. Figure 3-12 shows the optimal duration of storage resulting in the χ values shown in this figure, and therefore, as was shown in section 3.3, the values for the slope of the iso-χ lines. Figures B-17 and B-18 show similar results for more frequent price spikes.

Changing the height of the price spikes has similar effects as changing the frequency of the price spikes and also provides only a small part of the explanation for the value of storage of different cost intensities seen across the locations studied. As shown in figure 3-11 increasing the height of price spikes has a larger effect on the value of χ than increasing the frequency of price spikes when comparing the χ values in the colorbars between figures 3-9 and 3-11. The differences in value added of storage across locations might be partially explained by the different heights of price spikes in each location. Higher price spikes also increase the area in the $C_{\text{storage}}^{\text{energy}}$ and $C_{\text{storage}}^{\text{power}}$ plane in which storage is valuable. Height of price spikes has no effect on changing the slopes of the iso-χ lines as can be seen in figure 3-12, where even the noise caused by the generation data that was seen in figure 3-10 is absent.

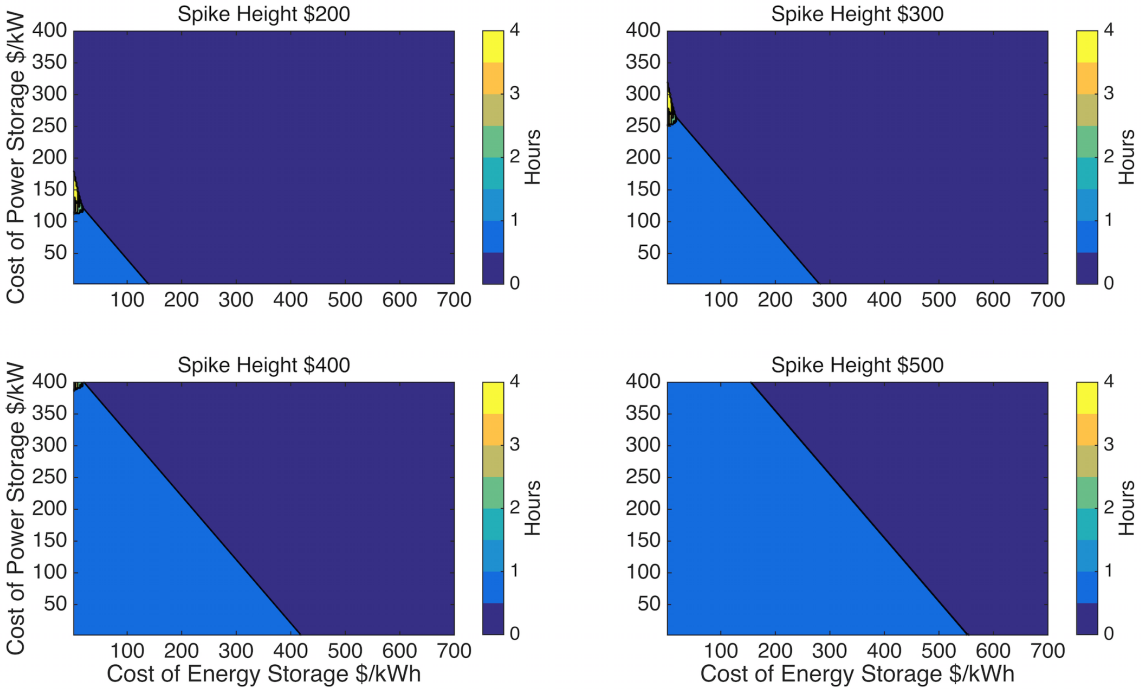

Figure 3-12: Using generation data for solar power in Texas, the effect of the height of price spikes of constant frequency 100 spikes per year of duration 1 hour on the optimal duration of storage. Figure 3-11 shows the optimal χ resulting from the optimal storage duration shown in this figure; as was shown in section 3.3, the values for the slope of the iso-χ lines in figure 3-11 are equal to the duration values shown here. Figures B-17 and B-18 show similar results for more frequent price spikes.

3.6.3 Price spike duration

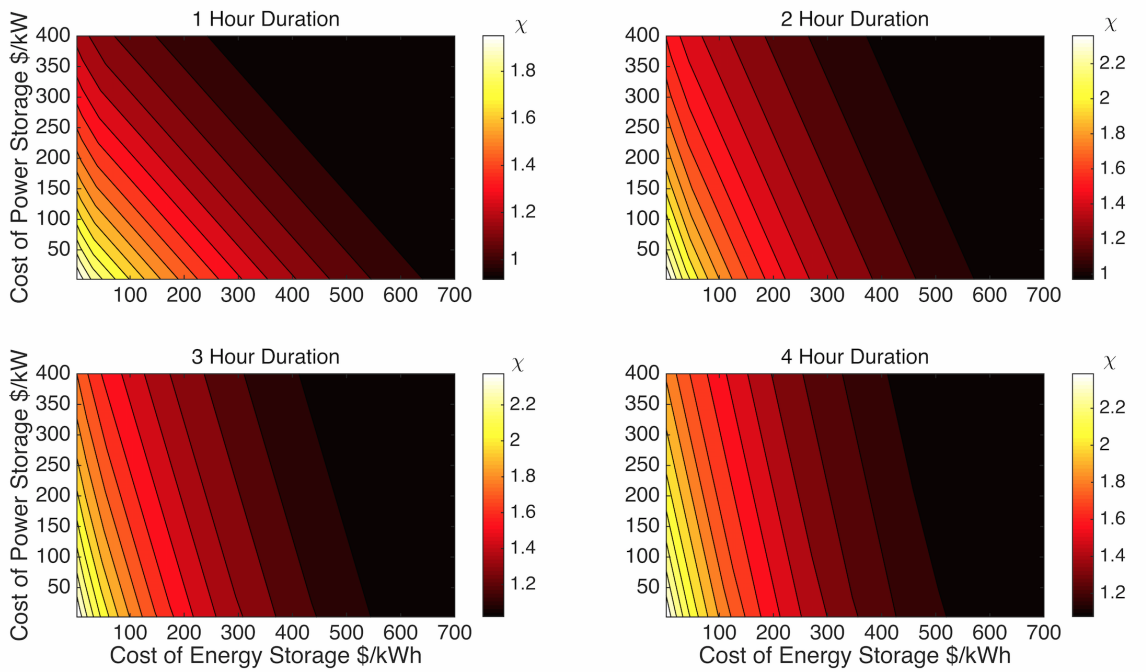

Figure 3-13: Using generation data for solar power in Texas, the effect of the duration of price spikes of constant frequency 250 spikes per year of height $350 on the benefit/cost ratio χ is shown. Figure 3-14 shows the optimal duration of storage resulting in the χ values shown in this figure, and therefore, as was shown in section 3.3, the values for the slope of the iso-χ lines. Figures B-19, B-20, B-21, and B-22 show similar results for price spikes of other frequencies and heights.

Duration of price spikes explains most of the features of the iso-χ lines for the real price data for each location studied. Unlike frequency and height of price spikes, the duration of the price spike has no effect on the value of χ, as seen in figure 3-13. Duration does have the effect of making storage of higher power cost valuable, and it does this because it changes the slope of the iso-χ lines. This can be more clearly seen in figure 3-14 where the optimal storage duration is shown, a value which equals the slope of the iso-χ lines seen in figure 3-13. This effect can also be clearly seen in figures B-19, B-20, B-21, and B-22 which show similar results for price spikes of other frequencies and heights.

The sawtooth pattern at low $C^{\text{power}}_{\text{storage}}$ seen most clearly in the optimal storage duration at 4 hours in figure 3-14 is a result of the granularity of the changing power

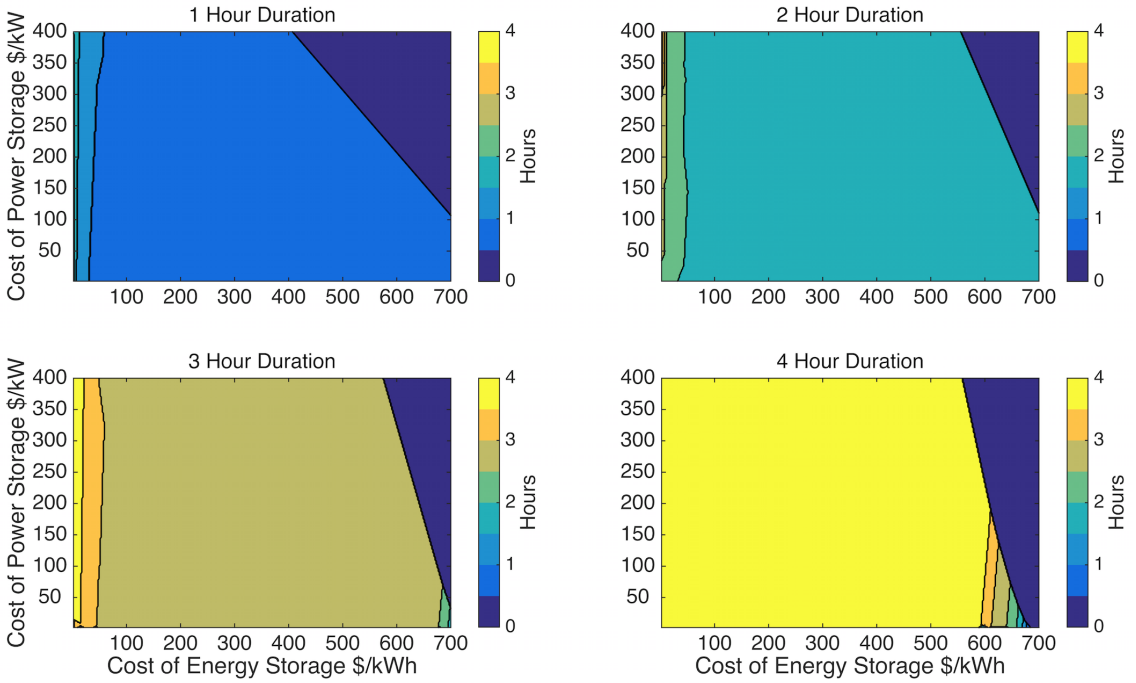

Figure 3-14: Using generation data for solar power in Texas, the effect of the duration of price spikes of constant frequency 250 spikes per year of height $350 on the optimal duration of storage. Figure 3-13 shows the optimal χ resulting from the optimal storage duration shown in this figure; as was shown in section 3.3, the values for the slope of the iso-χ lines in figure 3-13 are equal to the optimal storage duration values shown here. Figures B-19, B-20, B-21, and B-22 show similar results for price spikes of other frequencies and heights.

capacities in the model. As the optimal capacity increases, the effect is to decrease the optimal duration of storage as the optimization adjusts to rebalance costs in the denominator. This effect is small, but is also explanatory of the types of noise seen in the data for the real price series with respect to the interplay between changing power capacity and changing energy capacity or storage duration. Also seen in figure 3-14 is a small increase in the slope of the iso-χ lines at very low $C_{\text{storage}}^{\text{energy}}$ similar to what was seen when changing the price spike frequency in figure 3-10. This is actually the same feature, since the frequency used for the duration comparison is 250 spikes per year, putting it between the second and third plot of changing frequency.

Figures 3-15 and 3-16 utilize an artificial price series with varying duration of price spikes within each series. Using time series like those described in figure 2-6, the effect of having a longer price spike every other or every third price spike on the

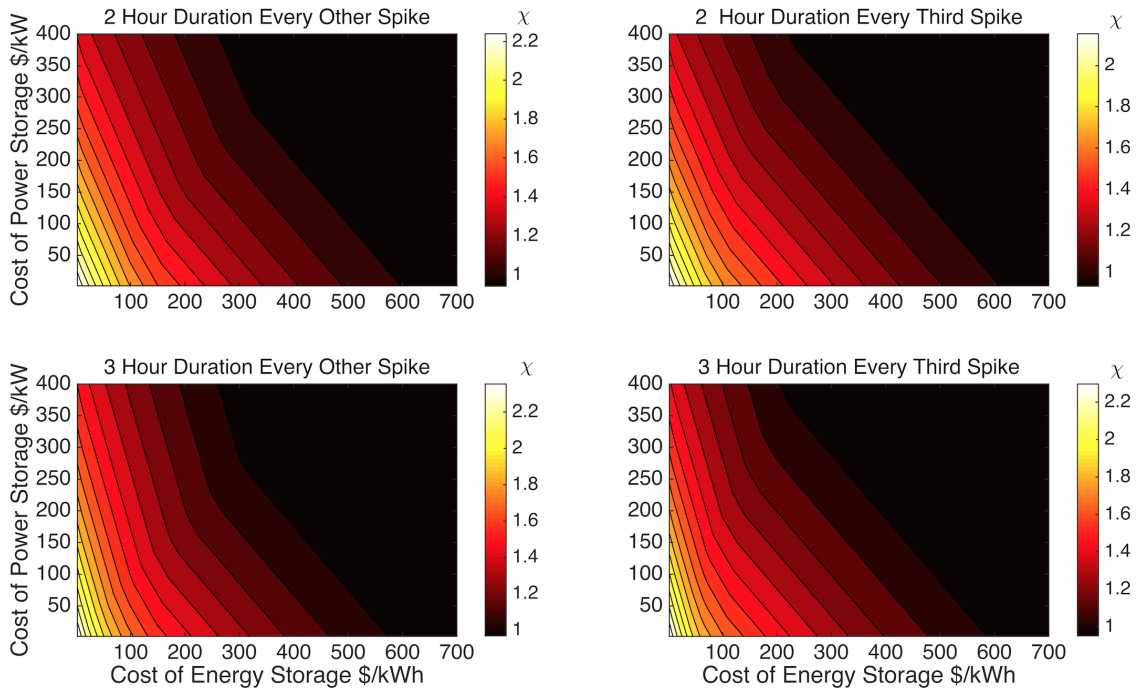

Figure 3-15: Using generation data for solar power in Texas, the effect of the duration of price spikes of constant frequency 250 spikes per year of height \$350 on the benefit/cost ratio χ is shown. Figure 3-16 shows the optimal duration of storage resulting in the χ values shown in this figure, and therefore, as was shown in section 3.3, the values for the slope of the iso-χ lines. Price spikes are of alternatively 1 hour and 2 or 3 hours in duration every other or every third spike. The effect of having different duration price spikes produces the different slopes seen in the iso-χ lines for the real price data series.

values of χ and on optimal storage duration is shown in figures 3-15 and 3-16. In figure 3-15 a clear elbow can be seen either about halfway up each iso-χ line or a third of the way up each iso-χ line respective of the frequency of longer price spikes within the series. Because of the relationship between the slope of the iso-χ line and the optimal storage duration, figure 3-16 provides additional insight into the values of the slope seen in figure 3-15. The optimal duration changes quickly from 1 hour in the region of low power and high energy costs, to 2 hours or 3 hours of storage for the higher power and lower energy costs.

As more variation is introduced into the duration of price spikes within a price series, the optimal duration plots show even more similarity to those for the actual locations studied. Showing the difference between where the transition from less storage

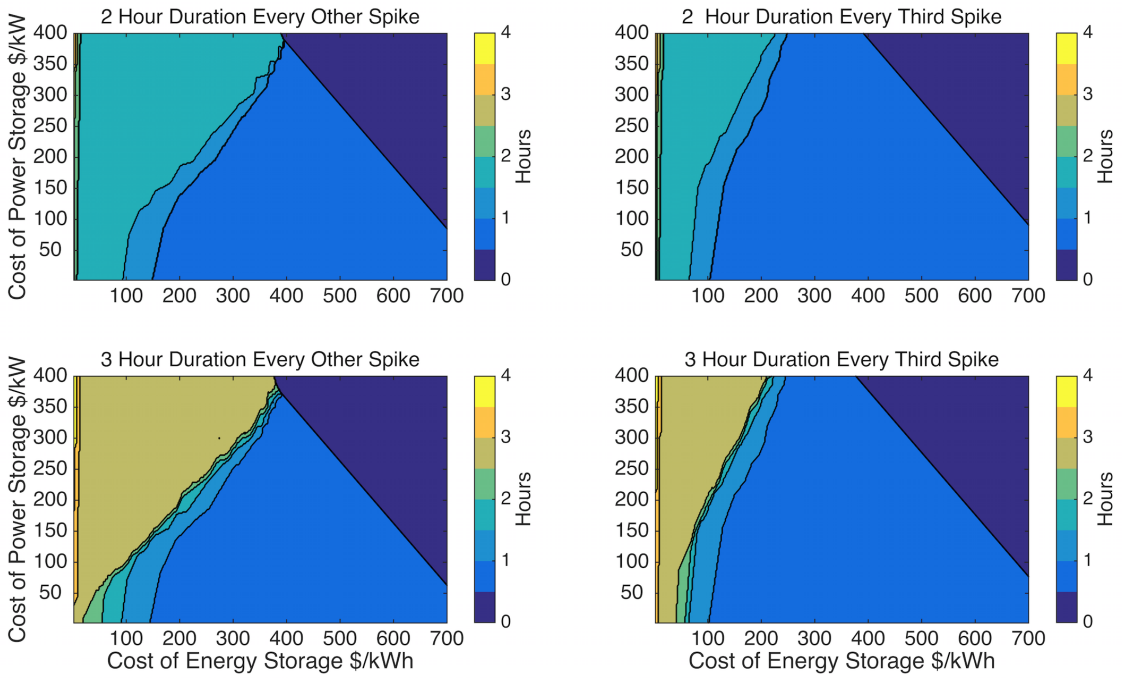

Figure 3-16: Using generation data for solar power in Texas, the effect of the duration of price spikes of constant frequency 250 spikes per year of height \$350 on the optimal duration of storage. Figure 3-15 shows the optimal χ resulting from the optimal storage duration shown in this figure; as was shown in section 3.3, the values for the slope of the iso-χ lines in figure 3-15 are equal to the optimal storage duration values shown here. The duration of storage for these artificial price series begins to resemble the results for the real price series studied, demonstrating the importance of varying durations of price spikes in understanding the tradeoffs between cost intensities of power capacity and energy capacity.

duration to more storage duration occurs on the iso-χ line is important for explaining the difference between Denmark's χ values and slopes and those for locations in the United States seen in section 3.4 and highlighted in figures 3-6 and B-10. Locations with longer duration price spikes will have higher optimal storage duration for a given cost of energy storage and cost of power storage. This indicates that electricity prices in Denmark should exhibit longer duration price spikes than are seen in the U.S. This will be shown to be the case in section 3.7.

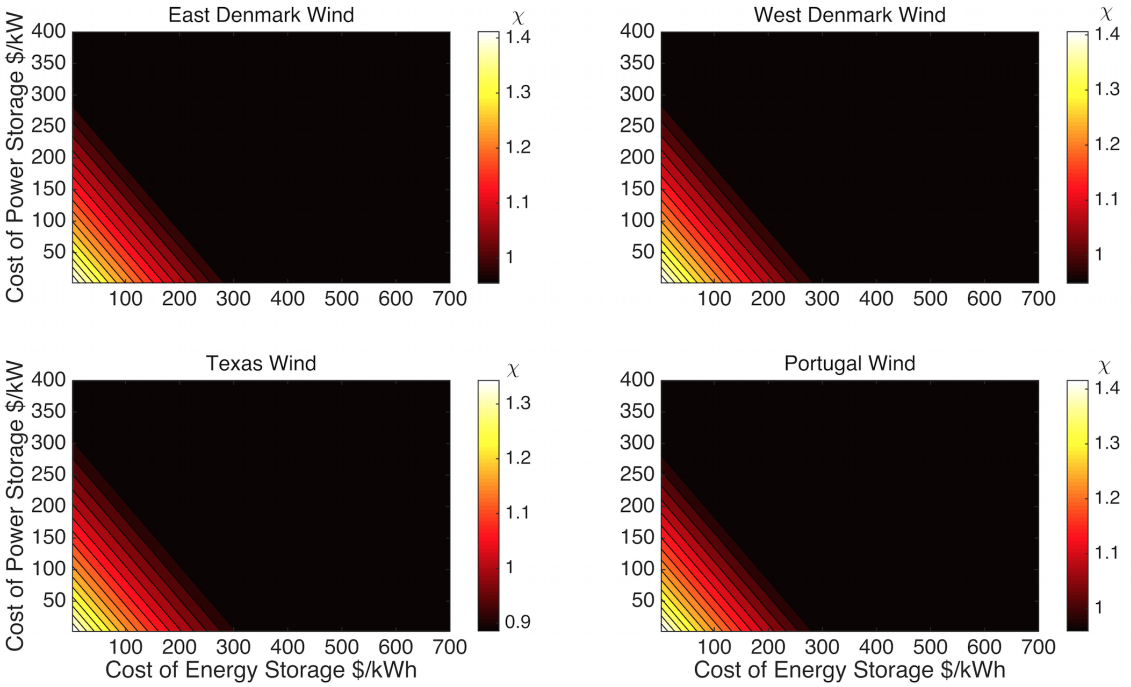

Figure 3-17: χ for generation data for various locations studied is shown in combination with electricity prices with 100 price spikes per year of height \$350 and duration of 1 hour. Generation data has it's greatest impact on the actual values of χ and relatively little impact on the threshold at which storage becomes valuable. Figure B-23 shows similar results for the other locations studied.

3.6.4 Generation data

The results shown above all use solar generation in Texas for the generation data. While this study has focused primarily on the electricity price dynamics as being the drivers for the value added by storage and the relative value of different storage technologies, the generation data is also important for determining the actual χ values. Figure 3-17 shows the χ value for wind generation in Texas, East Denmark, West Denmark, and Portugal. Generation profiles have their greatest impact on χ values, and relatively little effect on the threshold at which storage becomes valuable. Generation data does not provide an explanation for the changing iso-χ slopes seen in figures 3-5 and B-9 which can be verified by observing the optimal storage duration in figure 3-18. Similar results for the other locations studied can be found in figures B-23 and B-24.

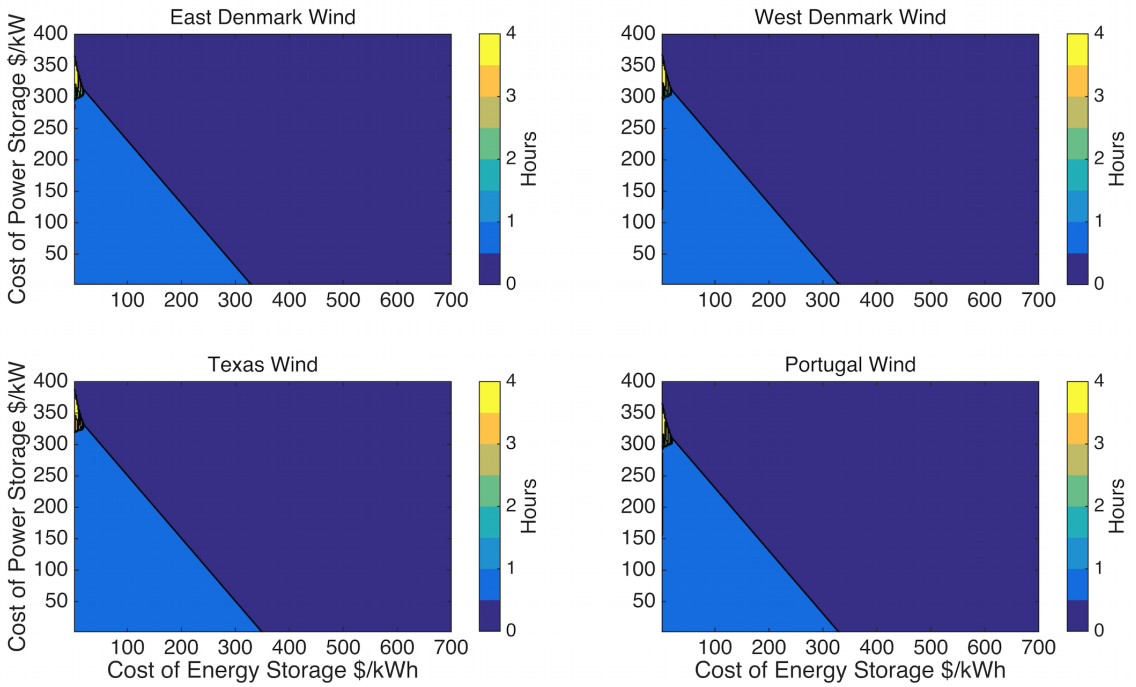

Figure 3-18: Optimal storage duration for generation data for various locations studied is shown in combination with electricity prices with 100 price spikes per year of height $350 and duration of 1 hour. Generation data does not explain the changing iso-χ slopes. Figure B-24 shows similar results for the other locations studied.

3.7 Electricity price dynamics

Having examined the slopes of the iso-χ lines across several locations and the response of χ and the iso-χ lines to artificial price series, this section analyzes empirically observed electricity price series data. Hourly electricity price data for each location studied also exhibit price spikes. However, unlike the artificial price time series used to investigate the impact of the frequency, height, and duration of price spikes on χ, the data used to determine χ for each location is more variable. This last section analyzes the electricity price data for each location for the relative frequency, height, and duration of price spikes. It will be shown that a difference in the duration of price spikes between Denmark and the U.S. is seen which supports the finding that for any given pair of cost intensities the optimal storage in Denmark should be as long or longer than in the U.S.

In a deregulated market, electricity prices are a result of the signals which enable

matching of supply and demand. Prices are correlated with demand, such that times of high demand are generally times of high electricity prices and periods of low demand are periods of low prices, but they are also dependent on generator availability, other service interruptions, and the marginal cost of producing electricity at any given time. Renewables have the effect of reducing electricity prices when the resource is available since their marginal cost of production is effectively zero [5]. Important features of electricity prices are that they are cyclical on both a yearly and a diurnal cycle and they exhibit price spikes of varying frequency, height, and duration. Both of these features will be explained below.

Electricity prices exhibit a diurnal cycle in which they are higher during the day and lower at night. This cycle follows the electricity demand which peaks in the late afternoon and is lowest in the evening. Figure 3-19 shows a fast Fourier transform of the electricity prices in California and West Denmark. Important peaks that can be seen for both locations occur at .0417 cycles per hour and .0833 cycles per hour which correspond to a diurnal cycle and a twice daily cycle. The amplitude for these cycles is higher for West Denmark than it is in California which means there is a stronger cyclical dependence. Similar results are shown in figure B-26 where a stronger cyclical dependence is shown for East Denmark, similar to West Denmark, than for Texas and Massachusetts, which have results comparable to California.

Portuguese electricity prices are regulated and thus show much less cycling than the other five locations presented in figures 3-19 and B-26. For all frequencies shown, the amplitudes for Portugal are lower, and there is significantly less noise in the fast Fourier transform. This demonstrates the extreme end of stability in which the prices are controlled by an external agency. Alternatively, locations with a strong cyclical dependence also present their own form of stability. The highly defined peaks and low noise for both East and West Denmark are an indication that there is lower volatility in the electricity prices in these locations as compared with the locations shown from the United States. Additional indications of greater price stability in Europe will be shown in figures 3-20 and 3-21.

Price spikes are finite duration events in which the price of electricity is abnor-

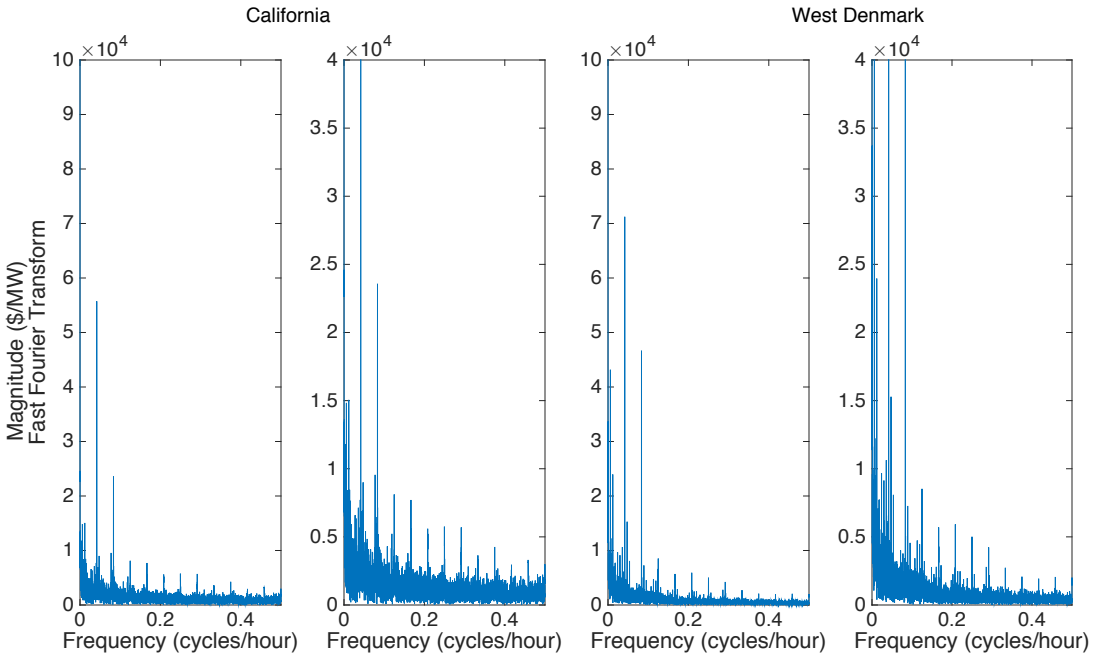

Figure 3-19: Fast Fourier transforms of electricity prices in California and West Denmark show a strong diurnal, at .0417 cycles per hour, and twice daily, at .0833 cycles per hour, pattern. The figure to the right for each location is zoomed in to show more detail for the spikes. The amplitudes for these cycles is higher in West Denmark, suggesting more stable electricity prices. This matches with the lower number of price spikes in West Denmark which is similarly an indication of volatile electricity prices. Fast Fourier transforms for Texas, Massachusetts, East Denmark, and Portugal are shown in figure B-26.

mally high. Two possible definitions of price spikes are used and each shows similar behaviors across the locations studied. The first is to compare prices to the daily mean for the day in which the spike occurred. This removes any seasonal variation in prices by only comparing prices to similar prices for that day. It is also useful for understanding some possible behaviors of energy storage systems which when operating on a diurnal cycle will likely only be concerned with discharging at a price higher than the related, or daily, mean. Figure 3-20 shows the fraction of price spikes of different durations normalized by the total number of price spikes, where price spike is defined as being above the daily mean, in the large plot. The other method of quantifying price spikes is to compare them to the yearly "whisker" price as seen in a box plot. The whisker price is one and a half times the distance between the first

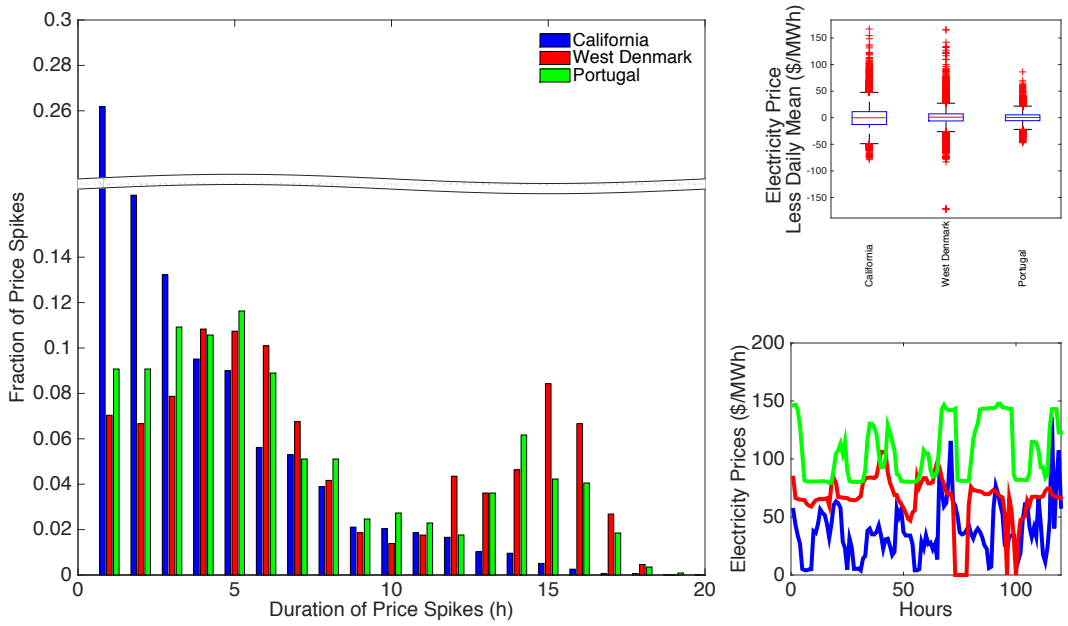

Figure 3-20: Emergent properties of electricity spot market prices for California, West Denmark, and Portugal are shown. In the main plot, the frequency of price spikes of various duration are shown weighted by the total number of price spikes, defined as prices above the daily mean. Note that West Denmark has many more price spikes of duration 14-17 hours. The box plots in the upper left show the range of hourly electricity prices as compared to the daily mean price. The lower left figure shows the actual electricity prices by hour for the first 120 hours of the data set to demonstrate the variability and diurnal cycles of electricity prices. Figure B-25 shows similar results for Texas, Massachusetts, and East Denmark.

and third quartiles added onto the third quartile. The large plot in figure 3-21 shows the normalized fraction of price spike by duration when the price spike is defined as a price above the whisker price.

The large plots in figures 3-20 and 3-21 show the fraction of price spikes, normalized by the total number of price spikes, of different durations for a given location. In figure 3-20 the price spikes are defined relative to the daily mean, while in figure 3-21 the price spikes are defined as being above the yearly whisker price. In Portugal, prices never exceed the yearly whisker price, as this is a regulated market. More important is the comparison between California and West Denmark. For each definition of price spike the same feature is seen in the comparison of duration of price spikes.

West Denmark has a much larger fraction of price spikes that are of 10 to 17 hours of duration as composed to California where the majority of price spikes are of only one to three hours in duration. When price spike is defined as being above the whisker price, half of California's price spikes are of only one hour in duration and 80% are of three hours or less.

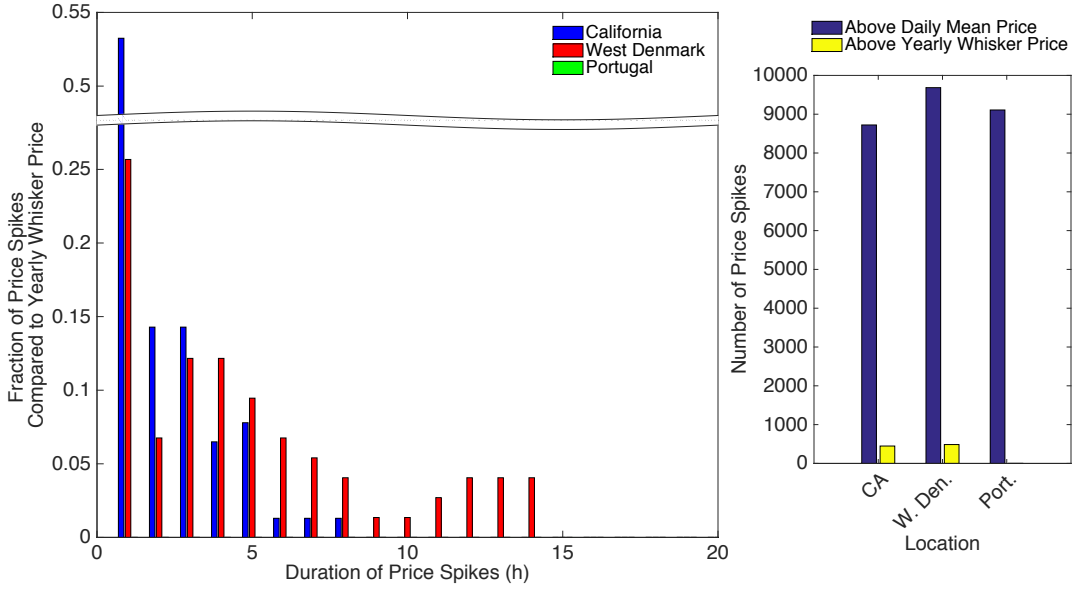

Figure 3-21: Price spikes can also be measured against the whisker price as opposed to the daily mean price, as in figure 3-20. On the left is the fraction of price spikes, defined as prices above the whisker price, normalized by the number of price spikes as a function of duration. As in figure 3-20, West Denmark has a higher proportion of price spikes of longer duration while California has a higher proportion of price spikes of short duration. The figure on the right shows a comparison of the number of hours the price was in a spike for the two different definitions. When defined as price above the whisker price, there are an order of magnitude fewer price spikes. Figure B-27 shows similar results for Texas, Massachusetts, and East Denmark.

Analysis of the price spikes in each location provides information on the relative frequency, height, and duration of price spikes, and how these statistics are similar across locations. The upper right plot in figure 3-20 shows a box plot of prices which have been adjusted to show the spread of prices around the daily mean. This shows the height of price spikes and how they compare across locations. The frequency of

price spikes is highly dependent on how the price spike is defined. The number of price spikes for each definition is shown in the left plot in figure 3-21. As can be seen, when compared to the daily mean, there are significantly more events which qualify as a price spike. This is an important feature, as it indicates the robustness of the features seen when looking at the fraction of price spikes of different durations, the two large plots in figures 3-20 and 3-21.

Price spike analysis can also be used to confirm the features seen in the fast Fourier analysis of the electricity price time series. The lower left of figure fig:MultipanePrice1 shows electricity prices plotted for the first five days of the year; in this plot you can see both the diurnal cycle and evidence of a strong twice daily cycle in West Denmark as was shown in the fast Fourier transforms of figure 3-19. The lower left plot also shows an example of the noise, or variability, in the California prices as compared to the smoother price time-series for West Denmark and Portugal. The box plot in the upper left shows that the variability in height, electricity price, of the price spikes is similar between California and West Denmark, but is much smaller in the regulated Portuguese electricity market.

Similar results can be seen in figures B-25, B-27, and B-28 which show results for Texas, Massachusetts, and East Denmark. The locations in the U.S. exhibit similar electricity price dynamics in the form of weaker diurnal and twice-daily cycles, noisier price time-series, and price spikes that are of shorter duration. East Denmark presents results similar to those of West Denmark in that again, the fraction of price spikes of long duration is much higher there than in any of the U.S. locations. For ease of comparison, figure B-28 is included which shows all six locations studied in one figure.

The longer duration of price spikes seen in figures 3-20 and 3-21 when comparing West Denmark to California, and in figures B-25 and B-27 comparing East Denmark with Massachusetts and Texas are a confirmation of the results expected from the analysis of χ using artificial price series. For any given pair of cost intensities, the optimal duration of storage was as high or higher in Denmark than in the U.S., this means that the slope of the iso-χ lines in Denmark are steeper on average than in the U.S. This is likely a result of the increased duration of price spikes in Denmark,

which make storage with a higher cost of power relative to energy more valuable. This result is confirmed for both definitions of price spike used. Lastly, the regulation of the Portuguese electricity market provides an explanation for the lower χ values and smaller areas of the cost plane where storage is valuable seen in Portugal.

Chapter 4

Discussion

Energy storage is widely recognized as critical for enabling an increasing penetration of renewables in the electricity market. Current and planned investment in energy storage technologies are summarized for both the U.S. and global electricity markets in tables 4.1, 4.2, and 4.3. The data, summarized from the U.S. Department of Energy's Global Energy Storage Database [84], shows the dominance of PHS in both the existing and the planned energy storage markets. Table 4.1 summarizes the currently operating U.S. energy storage facilities as confirmed by the U.S. Department of Energy, while table 4.2 presents the same information for projects that are currently announced, contracted, or under construction. Globally aggregated data is shown in table 4.3.

The future planned investment in energy storage technologies highlights the need for a single metric that enables comparison of technologies across a range of attributes. In this way, the best technology can be chosen for a given system, to provide the most value. The location invariance in the relative value of storage and the cost targets for storage improvement can inform the planners and researchers developing the planned projects in tables 4.2 and 4.3. These results provide guidelines for researchers and private R&D as well informing national research policy and demand-pull market policies for the development and investment in storage, as discussed further in this chapter.

Technology	Confirmed Projects	Rated Power	Energy Capacity
Pumped Hydro Energy Storage	24	15,5000 MW	1237,600 MWh
Compressed Air Energy Storage	3	114 MW	3362 MWh
Thermal Storage	98	433 MW	2300 MWh
Lithium Ion Batteries	66	81 MW	72 MWh
Lead Acid Batteries	19	60 MW	51 MWh
Sodium Batteries (NaS and Others)	14	21 MW	14 MWh
Other Battery Technologies	11	33 MW	10 MWh
Flywheel Energy Storage	4	42.5 MW	10 MWh
Flow Batteries (Zn-Bromine & Vanadium Redox)	6	1 MW	5 MWh

Table 4.1: Energy storage facilities in the United States, ranked by total energy capacity, that are confirmed in current operation as reported by the U.S. Department of Energy [84].

Technology	Confirmed Projects	Rated Power	Energy Capacity
Pumped Hydro Energy Storage	5	3250 MW	17,000 MWh
Compressed Air Energy Storage	2	309 MW	3040 MWh
Thermal and Other Storage	4	316 MW	2300 MWh
Flow Batteries (Zn-Bromine & Vanadium Redox)	9	33 MW	134 MWh
Lithium Ion Batteries	28	40 MW	27 MWh
Other Battery Technologies	6	2 MW	10 MWh
Lead Acid Batteries	2	0.4 MW	0.6 MWh
Flywheel Energy Storage	2	2 MW	0.6 MWh

Table 4.2: Energy storage projects in the U.S., ranked by total planned energy capacity, that are announced, contracted, under construction as reported by the Department of Energy [84].

Technology	Confirmed Projects	Rated Power	Energy Capacity
Pumped Hydro Energy Storage and Electro-Mechanical Storage	28	8900 MW	53,800 MWh
Thermal Storage	11	640 MW	3740 MWh
Other Battery Technologies	31	81 MW	436 MWh
Lithium Ion Batteries	64	90 MW	78 MWh

Table 4.3: Energy storage projects globally, ranked by total planned energy capacity, that are announced, contracted, under construction as reported by the U.S. Department of Energy [84].

4.1 Policy implications

The primary implications resulting from an analysis of the value of storage is the required improvement in the cost intensities of storage to help make renewables competitive. This analysis provides insight into several research policy decisions, at all levels from lab to government funding, that could be made to help advance storage technologies making their combination with renewables valuable, and potentially profitable. The gradients of χ presented in section 3.5 inform a research agenda designed to increase the value of ESS's. The $\bigtriangledown\chi$ results show which aspects of storage, either energy or power, will provide the most improvement for the same reduction in total costs. Lastly, when combined with specific climate change mitigation goals, the values of χ and the respective cost targets can be used to set government subsidies for investment in storage.

Many of the recommendations discussed in this section are based on the results of the thesis research and the usable conclusions to emerge. However, this section also covers suggestions for future input to the model, that could be provided by researchers, policy makers, and firms.

4.1.1 Guidance for researchers

One of the findings of this study which could improve the model results is the range of reported cost estimates for different storage technologies. A study of the value of storage requires accurate initial conditions, or reported cost intensities, in order to be able to say anything definite when comparing one storage technology to another. The range of estimates presented in section 2.2 highlight the difficulty of comparing technologies. The large ellipses in figure 3-4 further exemplify the difficulty in accurately comparing technologies or of saying something concrete about the value of storage in a hybrid storage renewables facility. This is an area of research that could be improved to help modelers in making predictions and comparisons of technologies. Providing cost intensity estimates in real or nominal dollar amounts, and accurately describing the elements included in each intensity would enable fair comparison across the dif-

ferent technologies. This type of research would likely require collaboration between academic institutions and business interests, sharing knowledge generated through research and through experience.

Batteries, specifically sealed batteries, would further benefit from a standardization in reported cost intensities clearly delineating which components are included in the cost of energy storage and which in the cost of power storage. Some references, such as Schoenung and Hassenzahl (2003), clearly specify that only the power conversion system is counted as the cost of power storage [11]. Most studies, however, do not specify what constitutes the elements in the cost of power storage, nor are they clear on whether power conversion systems are considered as a cost intensity of storage or as a balance of plant cost. Not only will this standardize the reported cost intensities, but it will also improve the input technological cost data for the model especially when comparing the relative value of storage technologies. For all technologies, balance of plant costs are an additional capital cost that were not included in this study. These costs also represent an area for research to find specific improvements in overall storage costs in order to improve its value.

The results of this model of a hybrid renewable and storage facility also provide guidance for areas in which researchers can focus their efforts to improve the value of energy storage technologies. For instance, reducing the energy capacity costs of PHS and CAES will provide a larger increase in their value than focusing on similar sized reductions in the power capacity costs. For sealed batteries, the focus on cost reduction should be evenly split between power capacity components and energy capacity components. Researchers who focus on electricity spot-market prices and the systematic features that influence changing prices should research the cause of price spikes, and specifically the underlying causes of longer duration price spikes in order to better understand what the relative value of storage technologies will be in different locations, and how these values may be influenced by grid and market structures.

4.1.2 Private R&D and investment

In addition to working closely with academic researchers to provide better capital cost estimates for storage for model improvement described above, the results of this model highlight the impact businesses can have in making storage and renewables more valuable by reducing the cost of renewables generation. There is a trade-off between the value of storage and the ability of storage to increase the value of renewables as generation costs decrease. At higher generation capital costs, more expensive storage is able to provide value, as evidenced by a larger area in the $C_{\text{storage}}^{\text{energy}}$ and $C_{\text{storage}}^{\text{power}}$ plane. However, at these high generation costs, neither the renewables nor the renewable storage hybrid generation facilities are profitable. However, as the cost of generation for renewables drops to \$1/W the facilities are profitable, but storage costs must be lower for storage to provide value.

The results of this study indicate that investment in storage may be at a "sweet spot" in which storage provides value now, but as generation costs decrease these technologies will stop being valuable if their costs do not fall as well. Investment in storage that provides value, even if the technologies are not profitable, may help lead to cost reductions in storage technologies as learning rates improve. Long term business success and market dominance may be the result of large electricity generation companies investing in storage and storage facilities now, in order to drive down the costs of storage for further future investment.

Cooperating with laboratory researchers and modelers is an important way in which businesses and specifically the independent system operators (ISO) can have a significant impact on improving the quality of electricity modeling. By making more detailed price and demand data available to researchers, better guidance for researchers, private entities, and government policy will result. This project focuses on the impact of storage when operating in arbitrage mode largely as a result of the availability of data only at hourly intervals. Many of the benefits of storage, such as frequency regulation, voltage support, and power quality management, require shifts in storage and operation on the order of seconds or minutes. Accurately modeling

these effects and determining the value of storage for ancillary services requires input price or demand data be provided at intervals of one minute or less. Businesses with access to this data can help support the research community and the development of more accurate models by making this data publicly available. This collaboration across industry and academia can help refine models and thus produce more actionable results.

4.1.3 Public R&D and market creation

The government, through agencies such as the National Science Foundation, the national laboratories, and the Department of Defense research facilities and laboratories, is in the position to set broad national research policy to help further the guidance described in section 4.1.1. This can occur through both government funding of research and also through the kinds of energy storage research being conducted in the national laboratories, particularly at Sandia National Laboratories, where there is a focus on energy storage research. The results of this model can inform government research funding to improve technologies, but also can inform funding that incentivize the kinds of research and collaboration needed to improve the input assumptions of the model described in this study. Government funding and regulations can also be implemented which incentivize businesses and ISO's to provide the kinds of data which will enable more detailed analysis of the value of storage at providing ancillary services. Finally, government research funding can incentivize the types of future research and model development described in section 4.2.

No discussion of the impact of government policy on the penetration of renewables is complete without mentioning the effects of externalities from carbon and the government's role in providing a properly operating free market. Externalities are one of the four main market failures, the others being imperfect information, non-competitive markets, and public goods [107, p. 77-85]. Externalities are a social cost or benefit that is not considered in private decision making. When market failures are present the basic economic assumptions of perfect markets breakdown and efficient outcomes can no longer be assumed. Carbon and other greenhouse gas emissions

are an externality in the electricity markets, as they represent a social cost, in the form of climate change, that is not part of the private calculus in energy usage or the construction of generation facilities. Coal, oil, and natural gas, produce carbon emissions for which they do not pay, artificially lowering their cost of generation compared with technologies which do not produce emissions. Externalities provide one of the foundational principles for why government involvement in markets is important.

Market failures resulting from externalities provide an argument for government intervention in the electricity market through subsidies for desired technologies, such as wind and solar, or for carbon taxes, cap-and-trade, or other mechanisms of internalizing the externality. Government intervention in the market can be generally classified as either demand-pull policies or technology-push policies [108]. Guidance and funding to researchers for the improvement of technologies fall into the technology-push category. While the results of this analysis can provide general guidance for this type of policy, it can provide much more specific input for policies which spur market creation through demand-pull changes in prices and investment incentives.

Government subsidies to spur investment in storage should focus on subsidies and investment credits for both renewables and storage facilities. With wind generation currently at about \$2/W and solar generation at about \$3/W, this analysis shows that most storage technology cost estimates do not find the addition of storage to renewables to be valuable for most technologies at all locations. Additionally, at current prices and operating without storage, renewables are not profitable at any location studied. Spurring the investment in renewables and in storage will require government subsidies of both the renewables generation capital costs and the costs of energy storage and power storage for an ESS. Appropriately setting these subsidies is an area of policy informed by this research. The thresholds of value for storage at different locations show the cost targets that must be achieved by storage. In the short run, to spur investment, storage cost reductions could be achieved through government subsidy to help make up the difference between current costs and cost goals.

Subsidies for storage and renewables based on the cost targets derived from the

value and profitability thresholds that result from this model differ by location. They also differ by technology. Subsidies which remain technologically neutral, and do not "pick winners," will require detailed modeling and accurate knowledge of initial cost intensities. The former is provided by this model, and the latter is one of the important implications of future research highlighted in this analysis.

4.2 Future research

This study focuses on hybrid renewables and storage facilities operating as price-takers in the electricity market. Feedback effects resulting from the variable generation of renewables on electricity prices are ignored, which is reasonable for the case of small renewables penetration but will need to be adjusted as renewables adoption grows. While the model used in this study provides for an efficiency parameter, this value was not changed through the course of the experiments, and only a single roundtrip efficiency value was used. To more accurately model the operations of energy storage systems in order to determine their value, both a charging and discharging efficiency should be included. Similarly, a charging and discharging power capacity should be modeled to better capture technologies such as a double penstock facility. In addition to more detailed efficiencies, self-discharge of the storage facility should be included to accurately capture losses that might occur from trying to save energy over a longer time period. Finally, more analysis is needed on the dependence of these performance intensity metrics on the quantity of power or energy installed.

One example of the importance of future work exploring the effects of feedbacks in the electricity markets is highlighted by the differences in price data between the U.S. locations and Denmark. As discussed in section 2.1, the Danish electricity system is heavily dependent on wind power, with over half of demand being met by wind resources. At these levels, the variability in wind generation is likely to have a strong effect on electricity prices, possibly explaining the longer duration of price spikes in both East and West Denmark. If this is true, then increasing the penetration of renewables is likely to have a positive feedback effect on the value of storage, requiring

longer durations of storage to be installed as more renewables penetrate the market. Additionally, if longer durations of storage are optimal as renewables penetrations increase, the comparison of technologies across iso-χ lines will change as the slopes of the lines transition to higher values.

The inclusion of separable charge and discharge power capacities and efficiencies will help better model the actual cost intensities of storage faced by an investor or entrepreneur. The determination of χ along three cost intensities will certainly complicate the analysis of the models output, but will contribute a deeper understanding of the relative value of different storage technologies. This type of modeling however is dependent on better cost intensity research as described in section 4.1.1. As the field currently stands, no data source provides separable charge and discharge cost intensities for all technologies. Furthermore, the standardization of this practice would require further specification for sealed batteries, where the distinction between power components and energy components is already substantially blurred. Self-discharge is also an important feature to model, as this will clearly distinguish those technologies that are suitable for time-shifting services such as arbitrage, compared to those which might be relegated to only providing short duration ancillary services such as frequency regulation and voltage support.

The variability of an intensity metric as a function of the quantity that it is intensifying is a second-order effect of the features of a technology. In this study, an example might be step changes in the power capacity costs of a CAES facility with increasing sizes of turbine generators. An intensive analysis of the dependence of performance intensity metrics on the quantity of power and energy installed is needed to understand whether these second order effects can be safely ignored. This study models cost intensities and efficiency as independent of the installed capacity. This means that economies of scale are excluded from this analysis, but also the dependence of efficiency on charge and discharge rate. It is likely that all the performance intensity metrics described in section 1.4 are not independent of the installed capacity as modeled in this study. Understanding the dependence of performance intensity metrics on their intensive quality will not only enable more accurate modeling of results, but will

increase understanding of best operating conditions and practices that might likewise change the way in which optimization of storage operation is performed. This is an area of further research that may have important implications for the choice of storage technology.

Appendix A

Supplemental figures to support methodology

The following figures, figures A-1, A-2, and A-3 demonstrate the effects of discharging power capacity limits, efficiency, and self-discharge on the amount of energy in storage and the ability of a hybrid solar and storage facility to meet that demand. The figures are provided to complement the discussion in section 1.4 by demonstrating the effect that each of the performance intensity metrics or system size constraints has on the performance of the hybrid system. Of interest is the effect of the limits on unmet demand and the amount of energy in storage, as well as the relationship between these two quantities.

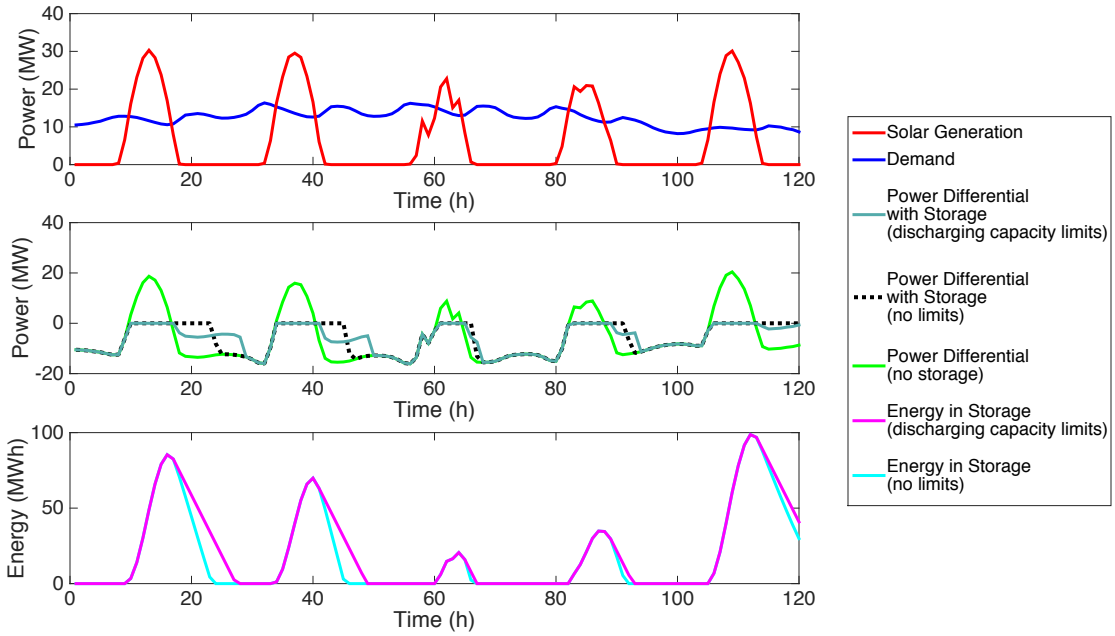

Figure A-1: These figures demonstrate the effect of discharging power capacity on the amount of energy in storage, and the ability of that energy to meet demand. In the top figure, hourly demand and solar generation data are presented for January 1, 2008 through January 5, 2008 for the north central region of ERCOT [98]. The middle figure shows unmet demand, demand minus solar generation, for the case without storage, with storage with no limitations, and with storage with a limitation of 8 MW discharging power capacity. The bottom figure shows the amount of energy in storage for both the limited and non-limited case.

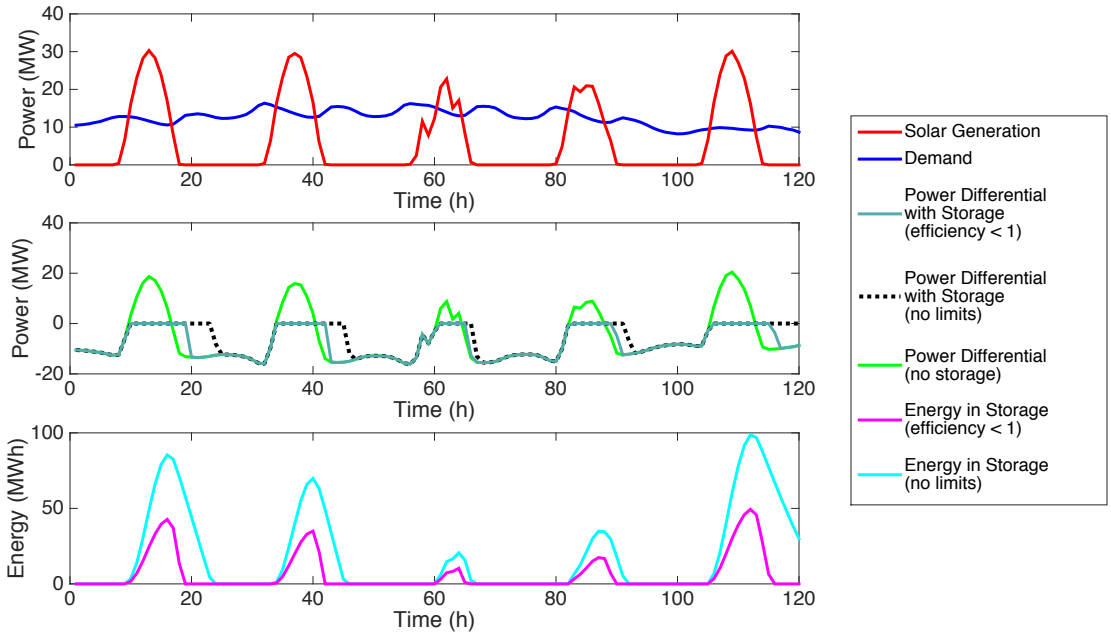

Figure A-2: These figures demonstrate the effect of efficiency on the amount of energy in storage, and the ability of that energy to meet demand. In the top figure, hourly demand and solar generation data are presented for January 1, 2008 through January 5, 2008 for the north central region of ERCOT [98]. The middle figure shows unmet demand, demand minus solar generation, for the case without storage, with storage with no limitations, and with storage with an efficiency of 50%. The bottom figure shows the amount of energy in storage for both the limited and non-limited case.

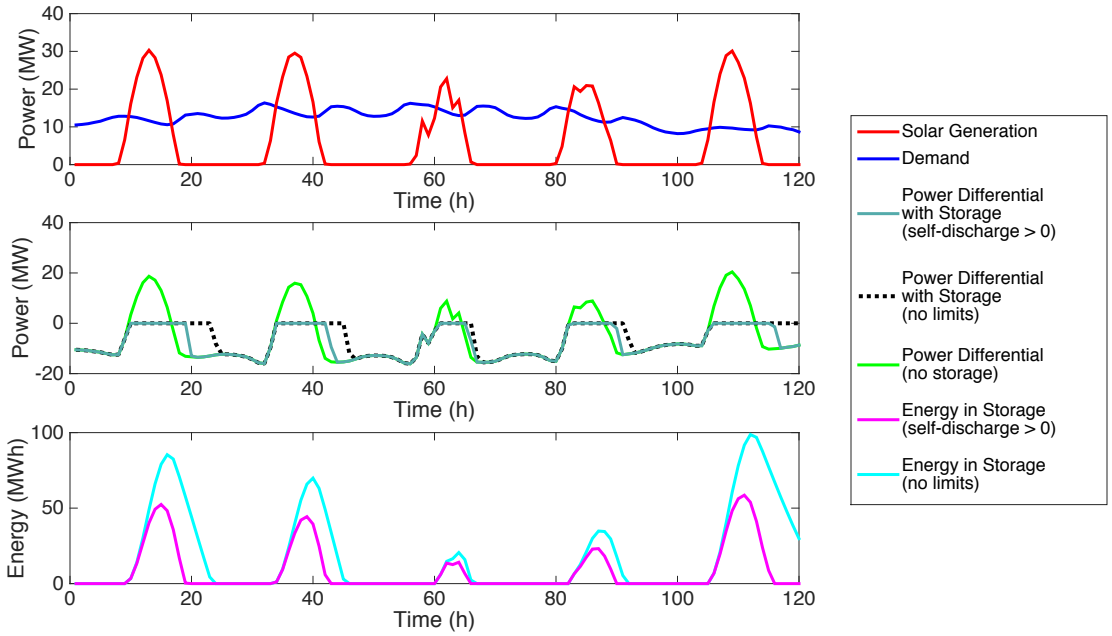

Figure A-3: These figures demonstrate the effect of self-discharge on the amount of energy in storage, and the ability of that energy to meet demand. In the top figure, hourly demand and solar generation data are presented for January 1, 2008 through January 5, 2008 for the north central region of ERCOT [98]. The middle figure shows unmet demand, demand minus solar generation, for the case without storage, with storage with no limitations, and with storage with a self-discharge rate of 20% per hour. The bottom figure shows the amount of energy in storage for both the limited and non-limited case.

Appendix B

Supplemental figures and tables of results

B.1 Technology comparison figures

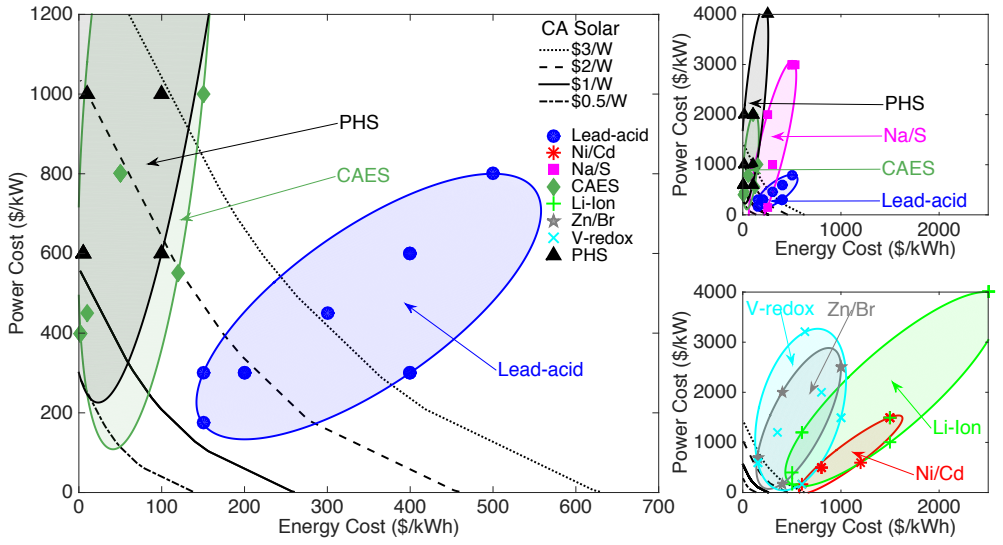

Figure B-1: Cost intensities of a range of energy storage technologies [69, 70, 7, 9, 11, 72] overlaid with lines, for a given generation cost, which show the threshold storage cost intensities at which it becomes valuable to incorporate storage into a California solar farm. The ellipses are plotted for each storage technology to highlight the uncertainty of energy and power costs of storage as discussed in section 2.2 [1].

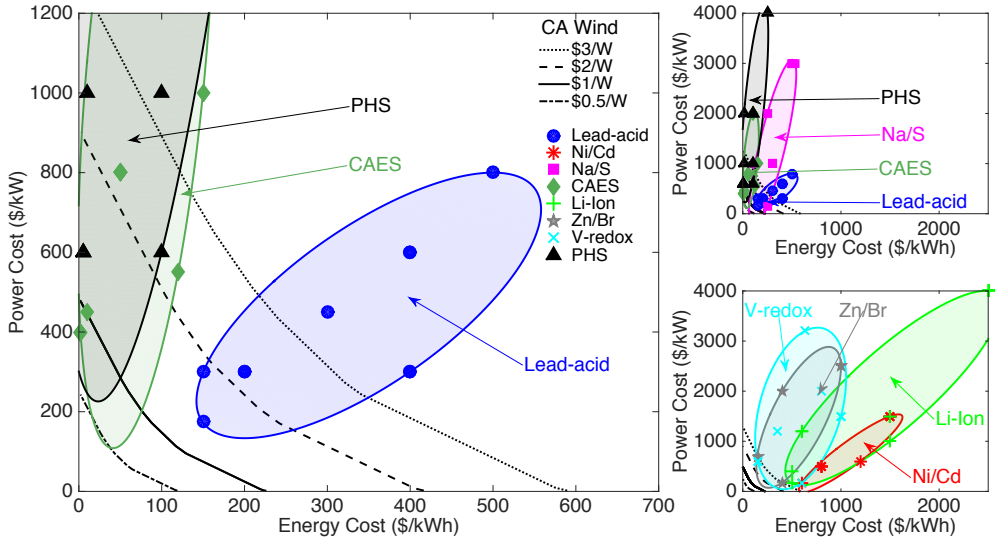

Figure B-2: Cost intensities of a range of energy storage technologies [69, 70, 7, 9, 11, 72] overlaid with lines, for a given generation cost, which show the threshold storage cost intensities at which it becomes valuable to incorporate storage into a California wind farm. The ellipses are plotted for each storage technology to highlight the uncertainty of energy and power costs of storage as discussed in section 2.2 [1].

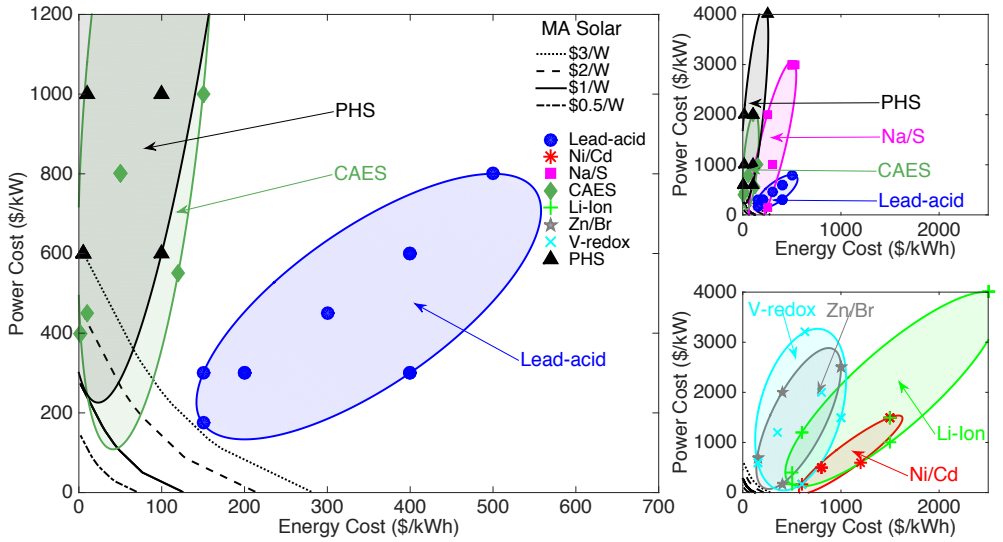

Figure B-3: Cost intensities of a range of energy storage technologies [69, 70, 7, 9, 11, 72] overlaid with lines, for a given generation cost, which show the threshold storage cost intensities at which it becomes valuable to incorporate storage into a Massachusetts solar farm. The ellipses are plotted for each storage technology to highlight the uncertainty of energy and power costs of storage as discussed in section 2.2 [1].

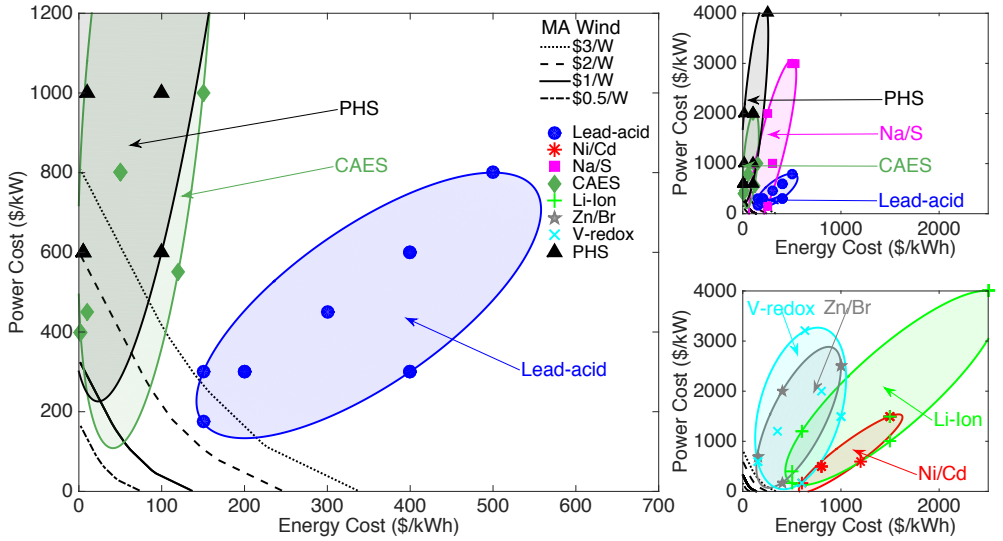

Figure B-4: Cost intensities of a range of energy storage technologies [69, 70, 7, 9, 11, 72] overlaid with lines, for a given generation cost, which show the threshold storage cost intensities at which it becomes valuable to incorporate storage into a Massachusetts wind farm. The ellipses are plotted for each storage technology to highlight the uncertainty of energy and power costs of storage as discussed in section 2.2 [1].

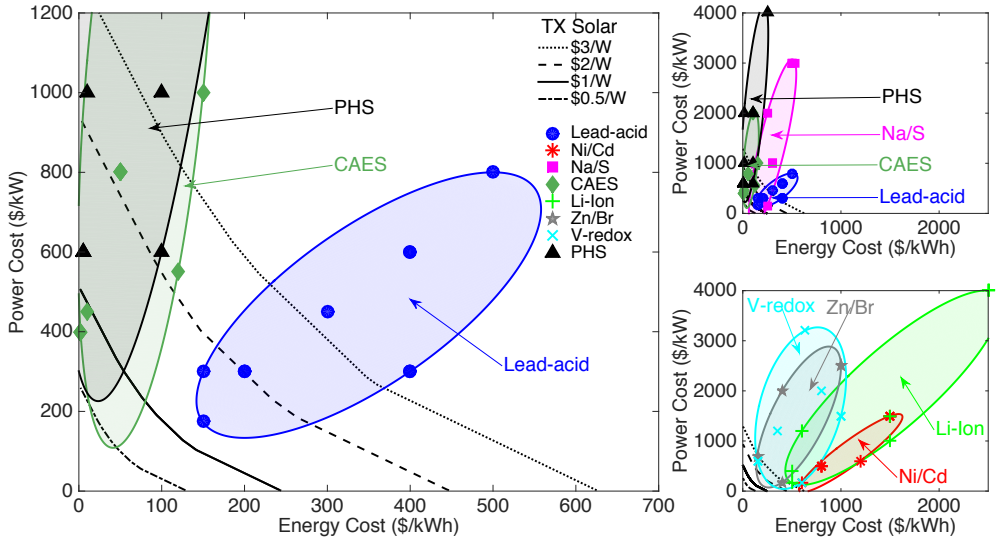

Figure B-5: Cost intensities of a range of energy storage technologies [69, 70, 7, 9, 11, 72] overlaid with lines, for a given generation cost, which show the threshold storage cost intensities at which it becomes valuable to incorporate storage into a Texas solar farm. The ellipses are plotted for each storage technology to highlight the uncertainty of energy and power costs of storage as discussed in section 2.2 [1].

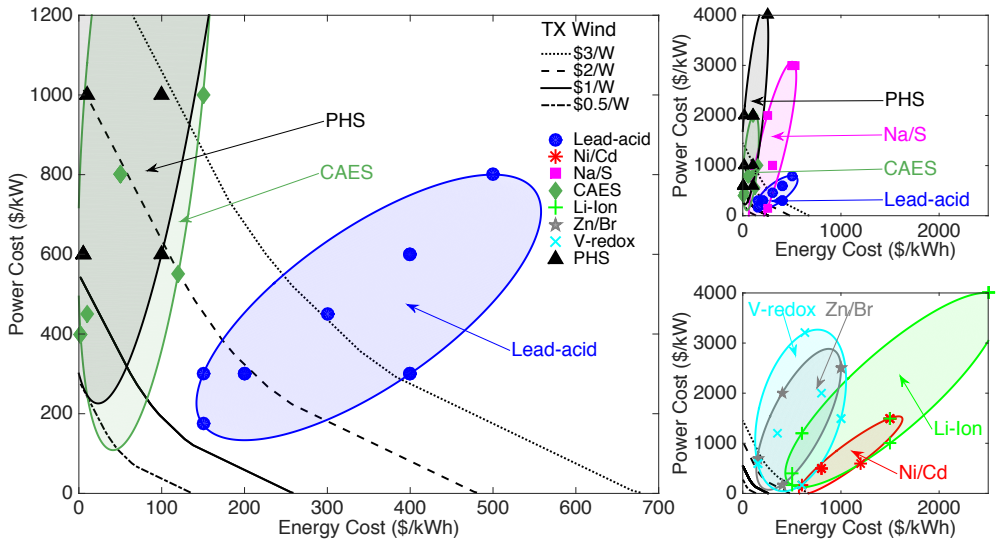

Figure B-6: Cost intensities of a range of energy storage technologies [69, 70, 7, 9, 11, 72] overlaid with lines, for a given generation cost, which show the threshold storage cost intensities at which it becomes valuable to incorporate storage into a Texas wind farm. The ellipses are plotted for each storage technology to highlight the uncertainty of energy and power costs of storage as discussed in section 2.2 [1].

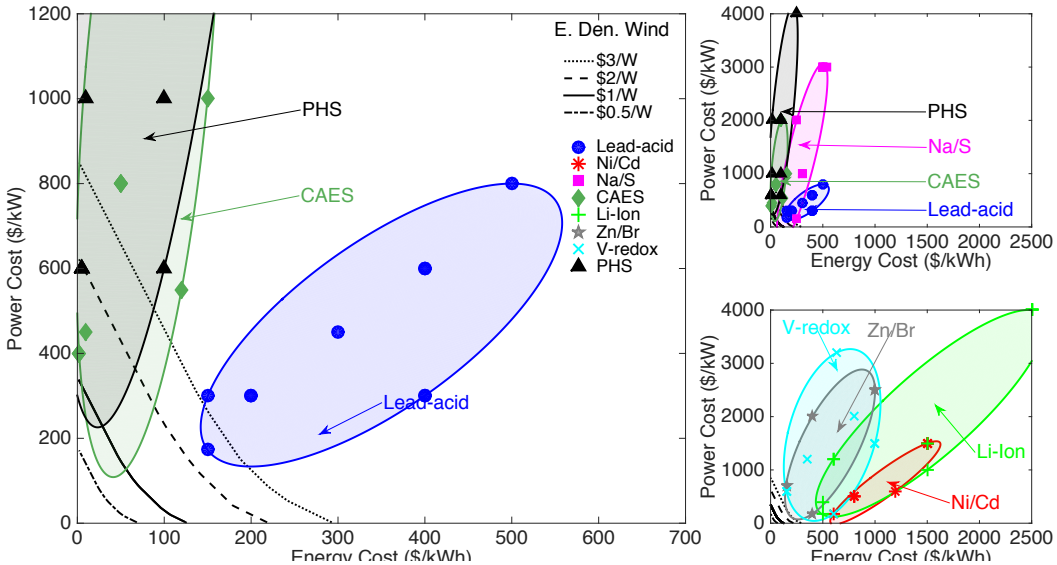

Figure B-7: Cost intensities of a range of energy storage technologies [69, 70, 7, 9, 11, 72] overlaid with lines, for a given generation cost, which show the threshold storage cost intensities at which it becomes valuable to incorporate storage into an East Denmark wind farm. The ellipses are plotted for each storage technology to highlight the uncertainty of energy and power costs of storage as discussed in section 2.2 [1].

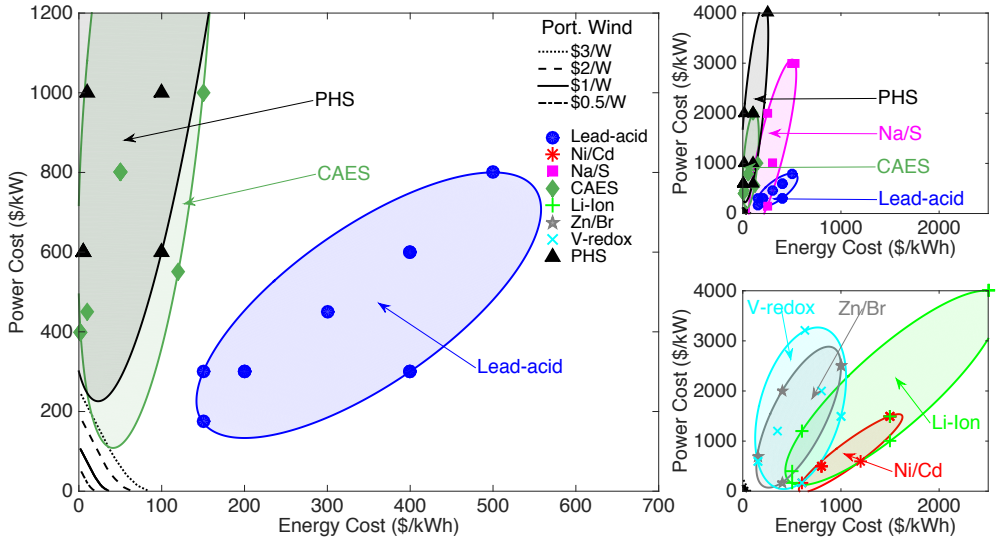

Figure B-8: Cost intensities of a range of energy storage technologies [69, 70, 7, 9, 11, 72] overlaid with lines, for a given generation cost, which show the threshold storage cost intensities at which it becomes valuable to incorporate storage into a Portugal wind farm. The ellipses are plotted for each storage technology to highlight the uncertainty of energy and power costs of storage as discussed in section 2.2 [1].

B.2 Iso-χ lines figures and tables

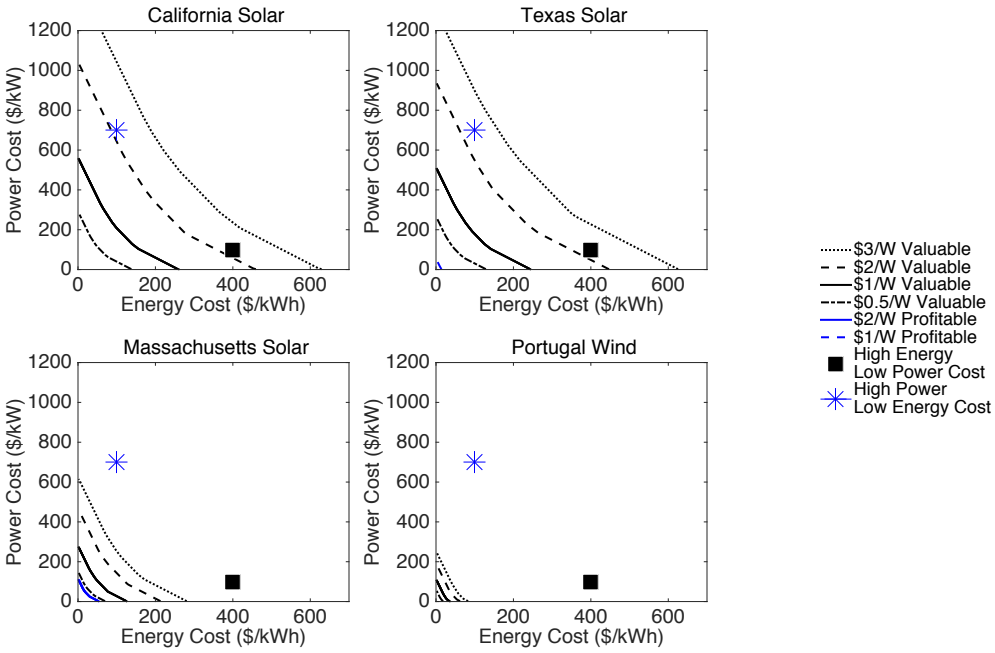

Figure B-9: As in figure 3-5, thresholds of value for storage with renewables are shown for different generation capital cost intensities for wind in Portugal and solar in the United States. The blue lines show profitability thresholds, $\chi = 1$. For wind in Portugal, generation capital cost intensities of \$2/W and less are always profitable. However, it should be noted that for storage with wind to be valuable in Portugal, storage power and energy cost intensities must be significantly lower than in all other locations studied.

Location	Technology	Required Improvement to Meet Generation Cost	Energy Cost Reduction	Power Cost Reduction	Energy Cost Reduction Percent	Power Cost Reduction Percent
California	Solar	\$1/W	\$140/kWh	\$98/kW	35%	98%
California	Wind	\$1/W	\$175/kWh	\$98/kW	44%	98%
Massachusetts	Solar	\$3/W	\$119/kWh	\$98/kW	30%	98%
Massachusetts	Wind	\$2/W	\$155/kWh	\$98/kW	39%	98%
Texas	Solar	\$1/W	\$157/kWh	\$98/kW	39%	98%
Texas	Wind	\$1/W	\$142/kWh	\$98/kW	36%	98%
E. Denmark	Wind	\$3/W	\$107/kWh	\$98/kW	27%	98%
W. Denmark	Wind	\$2/W	\$152/kWh	\$98/kW	38%	98%
Portugal	Wind	\$3/W	\$317/kWh	\$98/kW	79%	98%

Table B.1: Required cost improvements for a high energy (\$400/kWh) and low power cost (\$100/kW) technology to reach the nearest generation threshold when this threshold is a corner solution at a power cost of \$2/kW. Also shown are the corner solutions to reach the next lower generation cost for locations with solutions shown in table 3.1.

Location	Technology	Required Improvement to Meet Generation Cost	Energy Cost Reduction	Power Cost Reduction	Energy Cost Reduction Percent	Power Cost Reduction Percent
California	Solar	\$1/W	\$98/kWh	\$145/kW	98%	21%
California	Wind	\$1/W	\$98/kWh	\$222/kW	98%	32%
Massachusetts	Solar	\$3/W	\$98/kWh	\$85/kW	98%	12%
Massachusetts	Wind	\$2/W	\$98/kWh	\$107/kW	98%	15%
Texas	Solar	\$1/W	\$98/kWh	\$195/kW	98%	28%
Texas	Wind	\$1/W	\$98/kWh	\$158/kW	98%	23%
E. Denmark	Wind	\$2/W	\$98/kWh	\$78/kW	98%	11%
W. Denmark	Wind	\$1/W	\$98/kWh	\$329/kW	98%	47%
Portugal	Wind	\$3/W	\$98/kWh	\$454/kW	98%	65%

Table B.2: Required cost improvements for a low energy (\$100/kWh) and high power cost (\$700/kW) technology to reach the nearest generation threshold when this threshold is a corner solution at an energy cost of \$2/kWh. Also shown are the corner solutions to reach the next lower generation cost for locations with solutions shown in table 3.2.

Location	Technology	Required Improvement to Meet Generation Cost	Energy Cost Reduction	Power Cost Reduction	Energy Cost Reduction Percent	Power Cost Reduction Percent
California	Wind	\$2/W	\$337/kWh	\$98/kW	84%	98%
Massachusetts	Solar	\$1/W	\$347/kWh	\$98/kW	87%	98%
Massachusetts	Wind	\$2/W	\$382/kWh	\$98/kW	95%	98%
Texas	Solar	\$2/W	\$386/kWh	\$98/kW	96%	98%
Texas	Wind	\$2/W	\$289/kWh	\$98/kW	72%	98%
E. Denmark	Wind	\$2/W	\$388/kWh	\$98/kW	97%	98%
W. Denmark	Wind	\$2/W	\$397/kWh	\$98/kW	38%	98%

Table B.3: Required cost improvements for a high energy (\$400/kWh) and low power cost (\$100/kW) technology to reach the profitability threshold when one exists for a given generation cost. Note that as in table B.1 this threshold is a corner solution at a power cost of \$2/kW.

Location	Technology	Required Improvement to Meet Generation Cost	Energy Cost Reduction	Power Cost Reduction	Energy Cost Reduction Percent	Power Cost Reduction Percent
California	Wind	\$2/W	\$98/kWh	\$544/kW	98%	78%
Massachusetts	Solar	\$1/W	\$98/kWh	\$592/kW	98%	85%
Massachusetts	Wind	\$2/W	\$98/kWh	\$645/kW	98%	92%
Texas	Solar	\$2/W	\$98/kWh	\$653/kW	98%	93%
Texas	Wind	\$2/W	\$98/kWh	\$495/kW	98%	71%
E. Denmark	Wind	\$2/W	\$98/kWh	\$660/kW	98%	94%
W. Denmark	Wind	\$2/W	\$98/kWh	\$696/kW	98%	99%

Table B.4: Required cost improvements for a low energy (\$100/kWh) and high power cost (\$700/kW) technology to reach the profitability threshold when one exists for a given generation cost. Note that as in table B.2 this threshold is a corner solution at an energy cost of \$2/kWh.

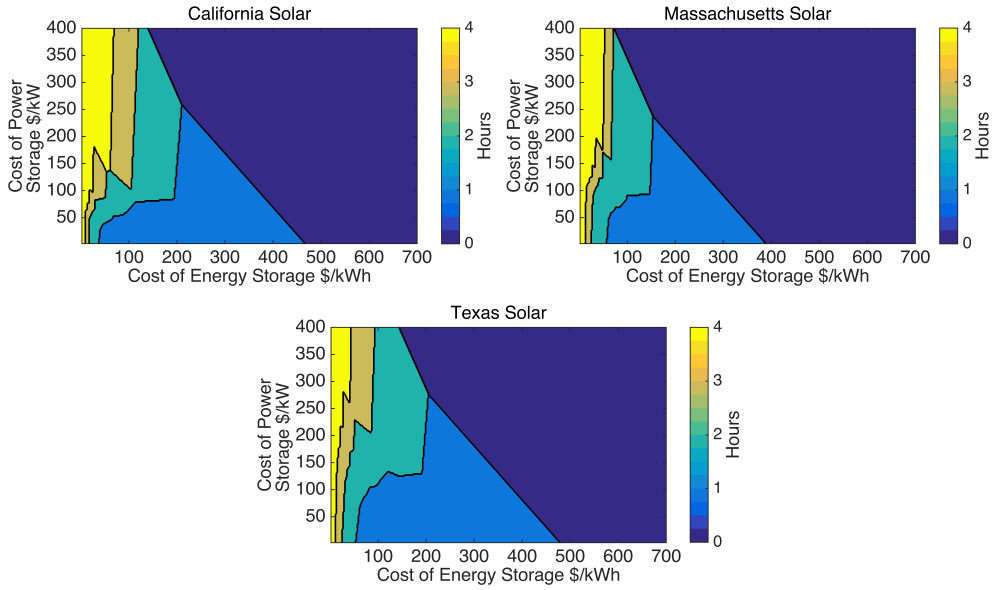

Figure B-10: Hours of storage duration for solar power are shown for California, Massachusetts, and Texas. Results show that hours of optimal storage duration follow the same general cost intensities as seen for the same locations with wind power, seen in figure 3-6. This compares to results for West and East Denmark where optimal storage duration is as high or higher for any given cost of energy storage and cost of power storage.

B.3 Gradients of χ

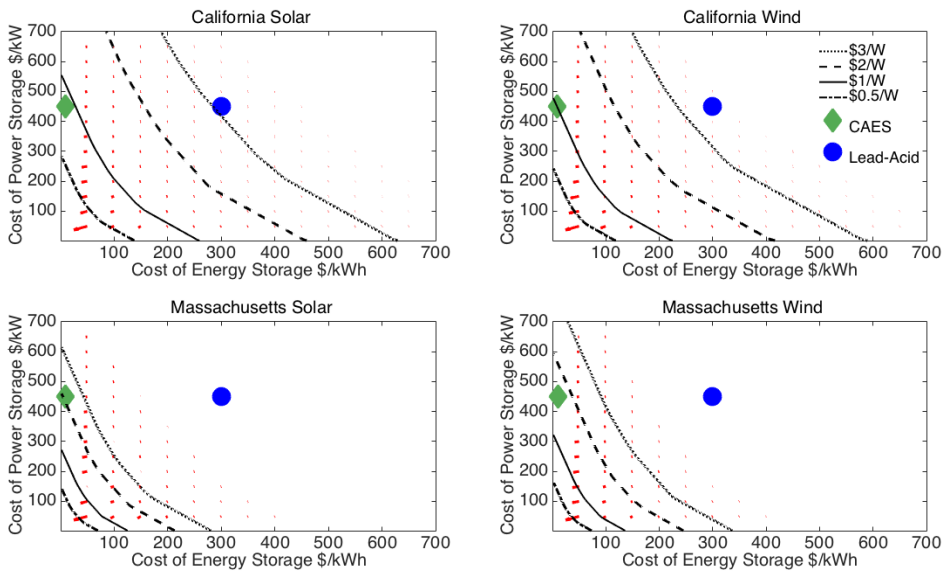

Figure B-11: Gradients for both wind and solar for California and Massachusetts. $\bigtriangledown\chi$ shows the direction of greatest improvement in χ. It is largely invariant across generation technologies and locations. It is greater for lower costs because the same absolute improvement in cost of energy storage or cost of power storage is a relatively greater improvement in cost for lower cost technologies. For reference, the cost estimates as provided by [72] are shown for CAES and lead-acid batteries.

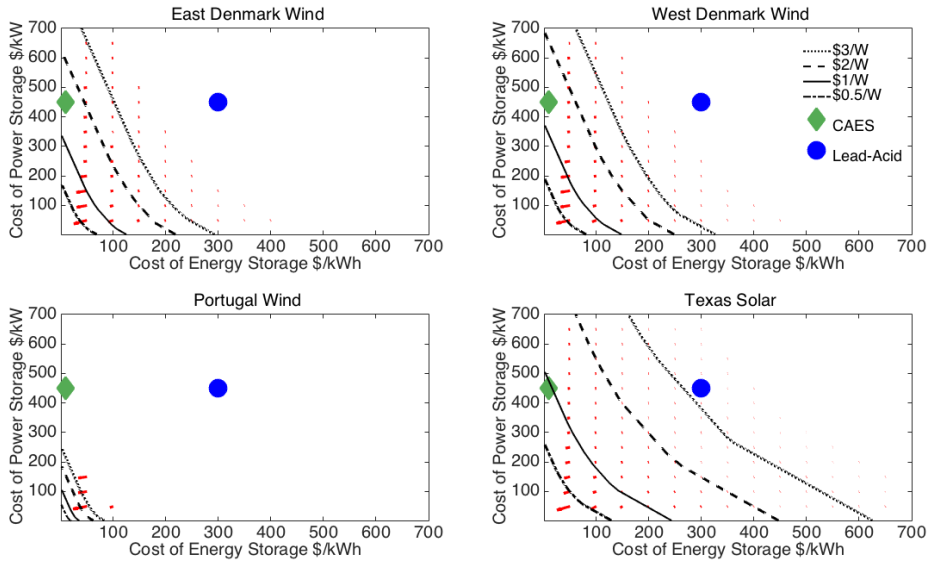

Figure B-12: Gradients for both wind and solar for Denmark, Portugal, and solar power in Texas. $\bigtriangledown\chi$ shows the direction of greatest improvement in χ. It is largely invariant across generation technologies and locations. It is greater for lower costs because the same absolute improvement in cost of energy storage or cost of power storage is a relatively greater improvement in cost for lower cost technologies. For reference, the cost estimates as provided by [72] are shown for CAES and lead-acid batteries.

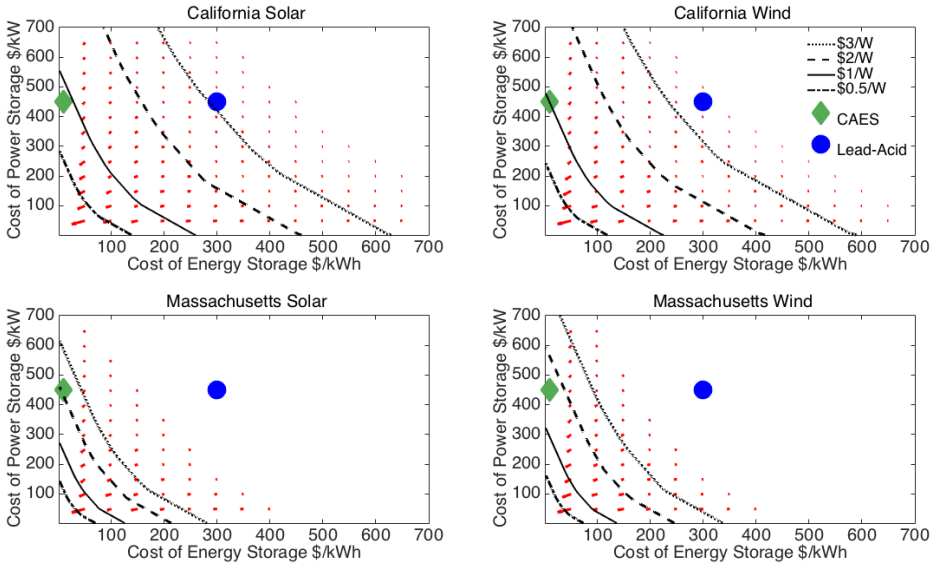

Figure B-13: Gradients for both wind and solar for California and Massachusetts. $\bigtriangledown\chi$ shows the direction of greatest improvement in χ given a 10% decrease in cost of energy storage or cost of power storage. Proportional changes in cost show a generally consistent relative improvement in χ as compared with figure B-11. For reference, the cost estimates as provided by [72] are shown for CAES and lead-acid batteries.

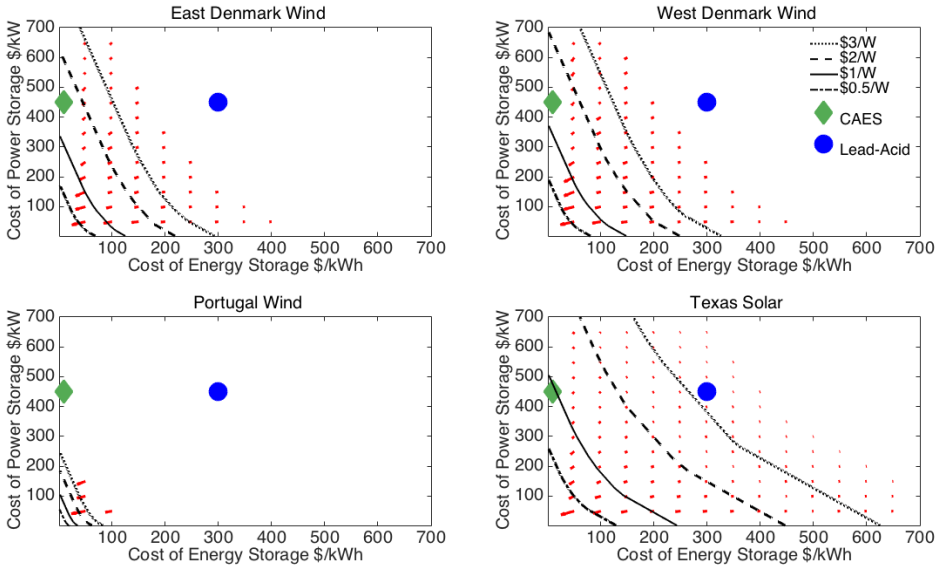

Figure B-14: Gradients for both wind and solar for Denmark, Portugal, and solar power in Texas. $\bigtriangledown\chi$ shows the direction of greatest improvement in χ given a 10% decrease in cost of energy storage or cost of power storage. Proportional changes in cost show a generally consistent relative improvement in χ as compared with figure B-12. For reference, the cost estimates as provided by [72] are shown for CAES and lead-acid batteries.

B.4 Artificial price series figures

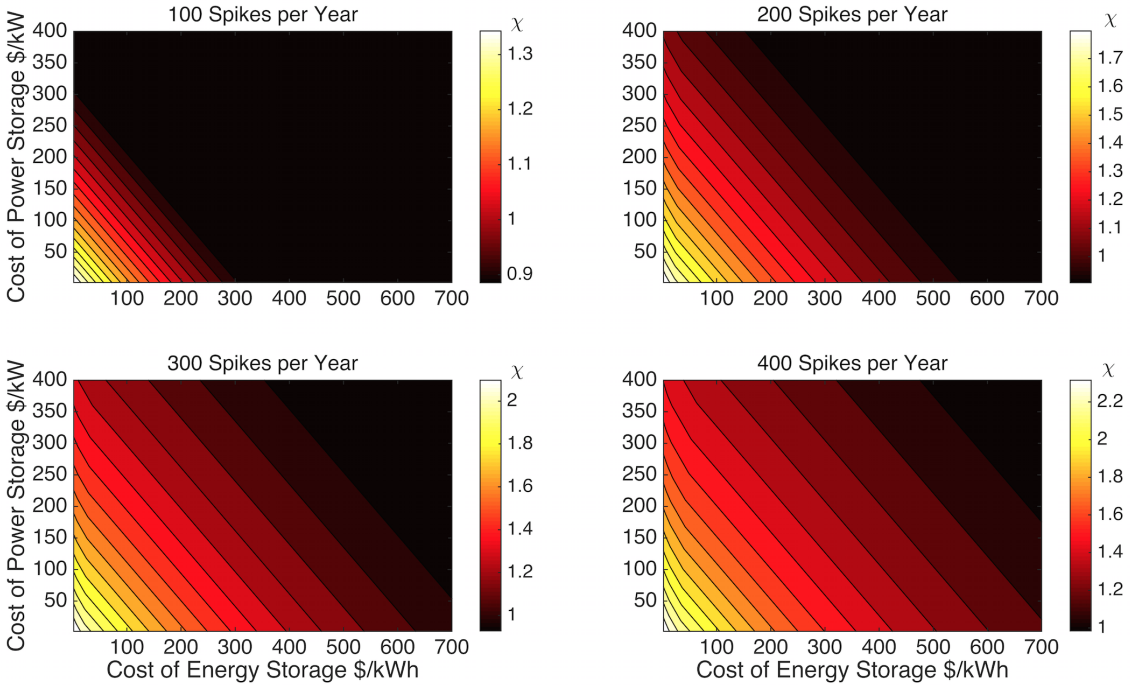

Figure B-15: Using generation data for solar power in Texas, the effect of the frequency of price spikes of constant height \$350 and duration 1 hour on the benefit/cost ratio χ is shown. Figure B-16 shows the optimal duration of storage resulting in the χ values shown in this figure, and therefore, as was shown in section 3.3, the values for the slope of the iso-χ lines.

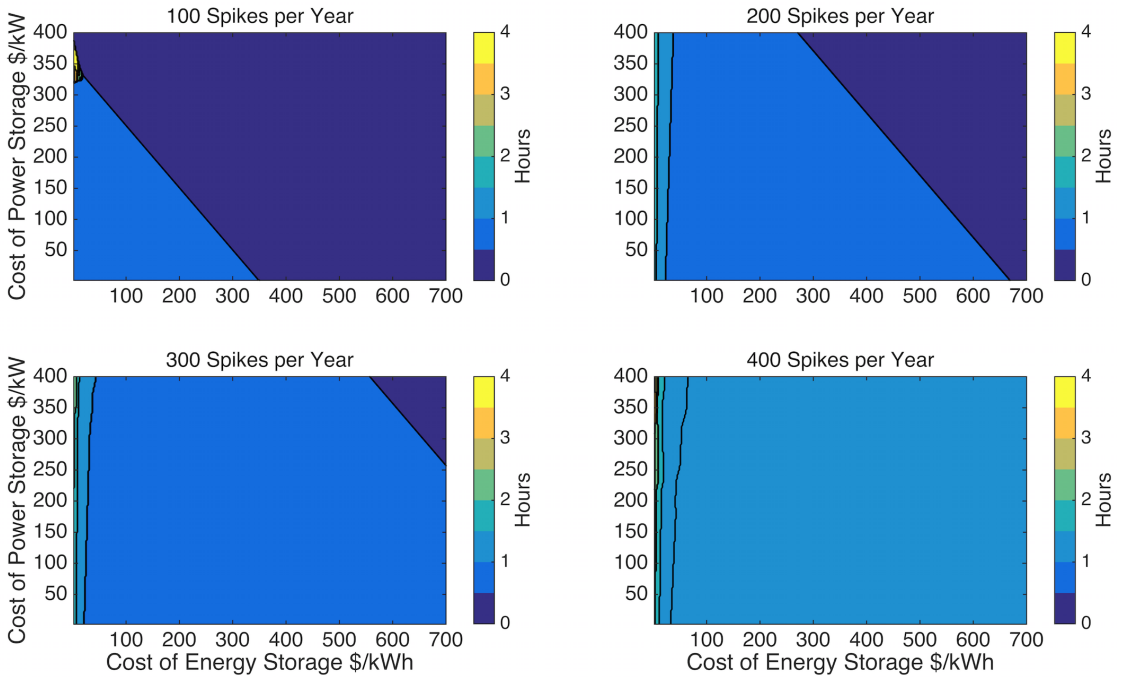

Figure B-16: Using generation data for solar power in Texas, the effect of the frequency of price spikes of constant height \$350 and duration 1 hour on the optimal duration of storage is shown. Figure B-15 shows the optimal χ resulting from the optimal storage duration shown in this figure; as was shown in section 3.3, the values for the slope of the iso-χ lines in figure B-15 are equal to the duration values shown here.

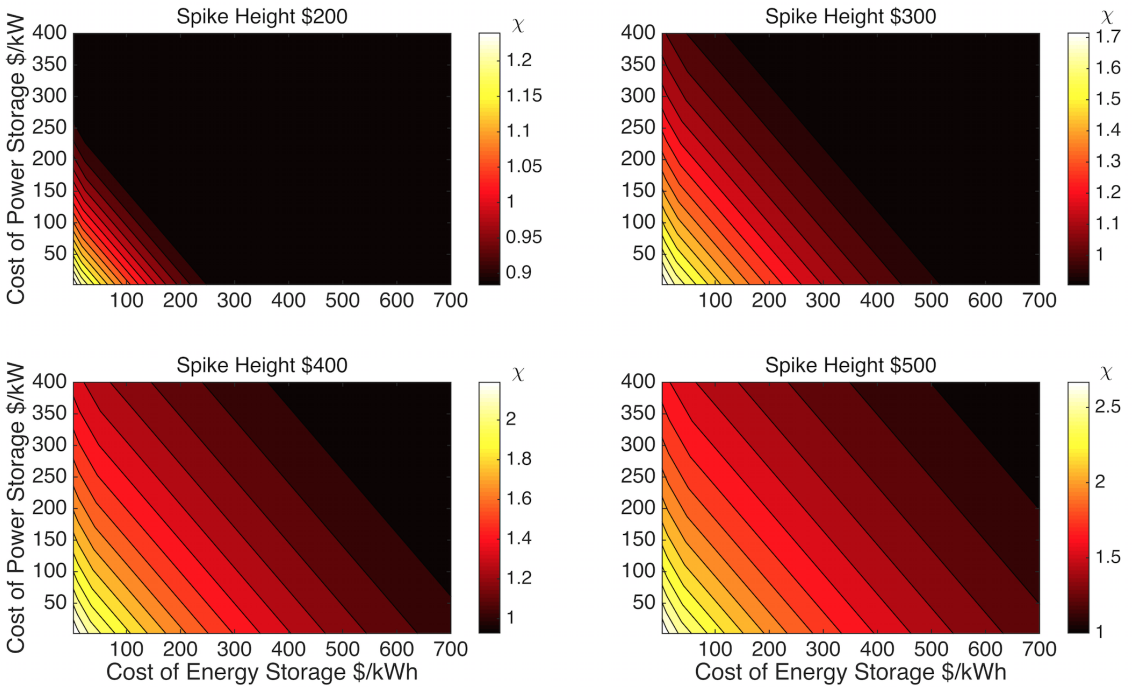

Figure B-17: Using generation data for solar power in Texas, the effect of the height of price spikes of constant frequency 250 spikes per year of duration 1 hour on the benefit/cost ratio χ is shown. Figure B-18 shows the optimal duration of storage resulting in the χ values shown in this figure, and therefore, as was shown in section 3.3, the values for the slope of the iso-χ lines.

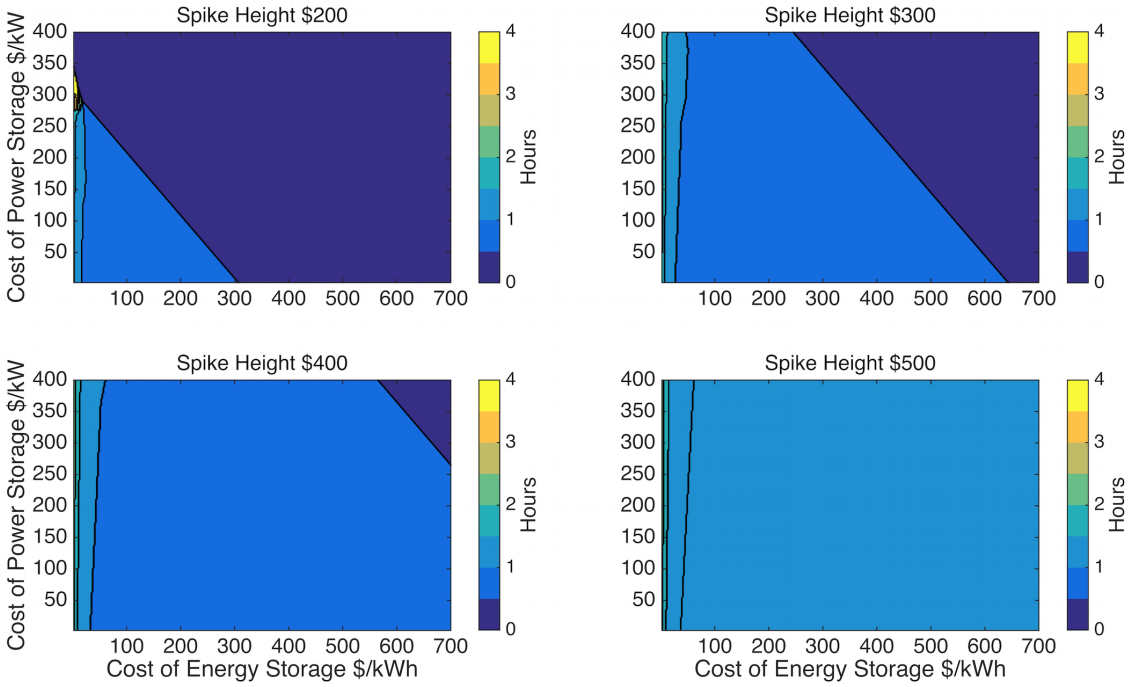

Figure B-18: Using generation data for solar power in Texas, the effect of the height of price spikes of constant frequency 250 spikes per year of duration 1 hour on the optimal duration of storage. Figure B-17 shows the optimal χ resulting from the optimal storage duration shown in this figure; as was shown in section 3.3, the values for the slope of the iso-χ lines in figure B-17 are equal to the duration values shown here.

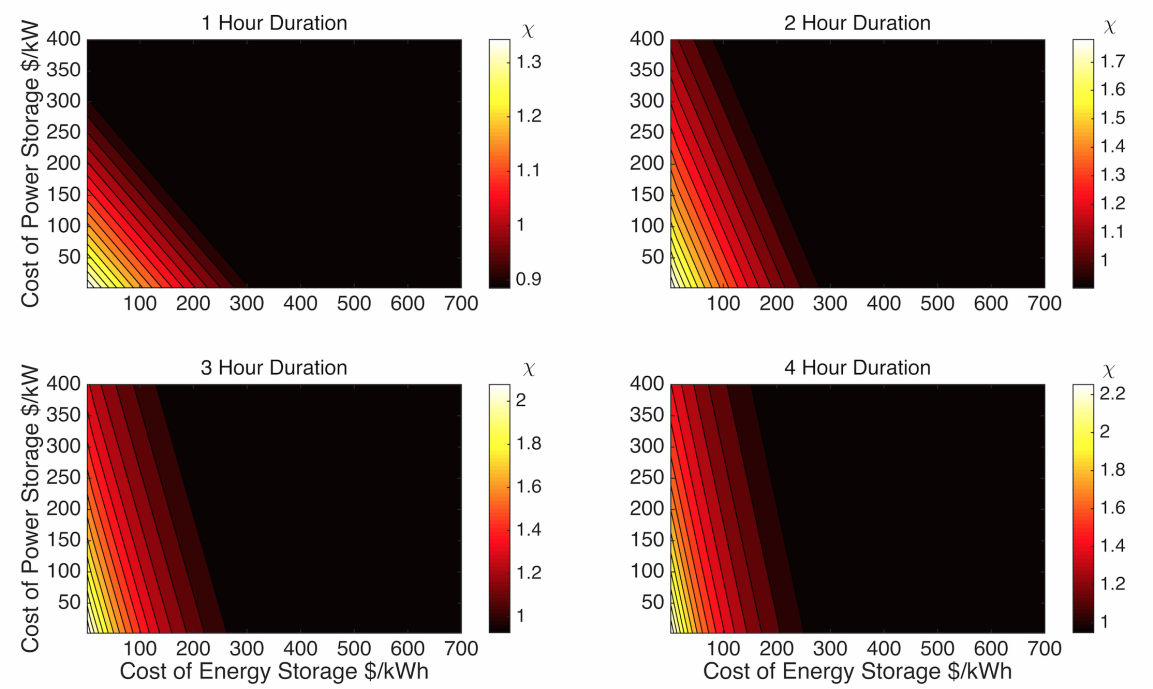

Figure B-19: Using generation data for solar power in Texas, the effect of the duration of price spikes of constant frequency 100 spikes per year of height $350 on the benefit/cost ratio χ is shown. Figure B-20 shows the optimal duration of storage resulting in the χ values shown in this figure, and therefore, as was shown in section 3.3, the values for the slope of the iso-χ lines. Figures 3-13, 3-14, B-21, and B-22 show similar results for price spikes of other frequencies and heights.

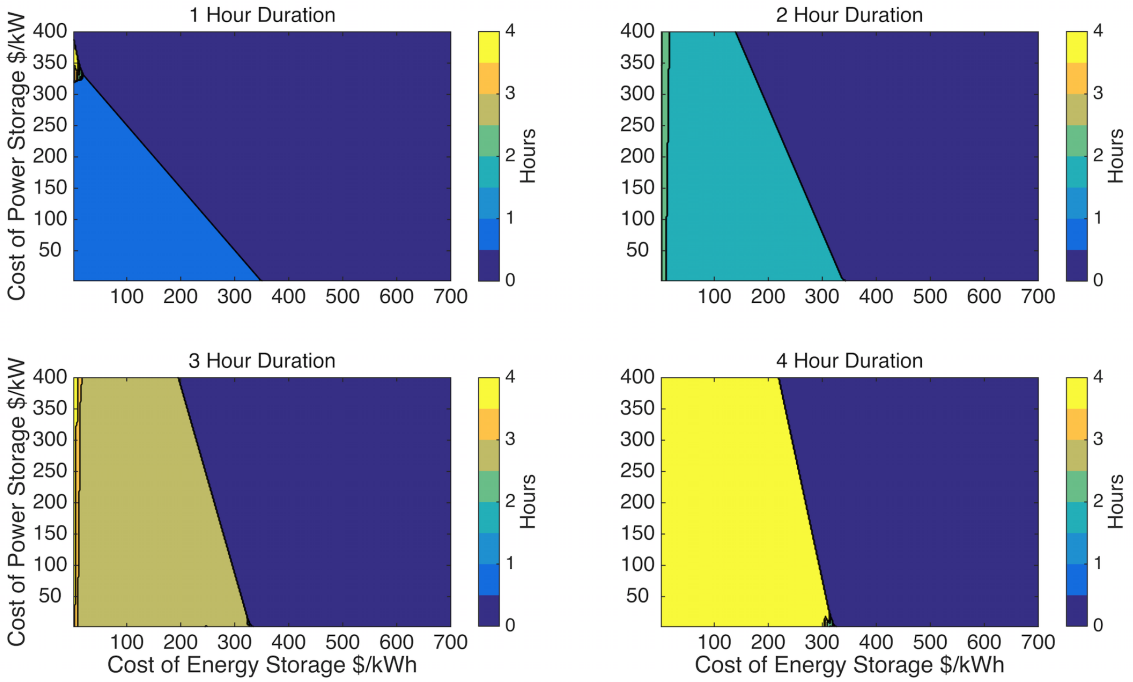

Figure B-20: Using generation data for solar power in Texas, the effect of the duration of price spikes of constant frequency 100 spikes per year of height \$350 on the optimal duration of storage. Figure B-19 shows the optimal χ resulting from the optimal storage duration shown in this figure; as was shown in section 3.3, the values for the slope of the iso-χ lines in figure B-19 are equal to the optimal storage duration values shown here. Figures 3-13, 3-14, B-21, and B-22 show similar results for price spikes of other frequencies and heights.

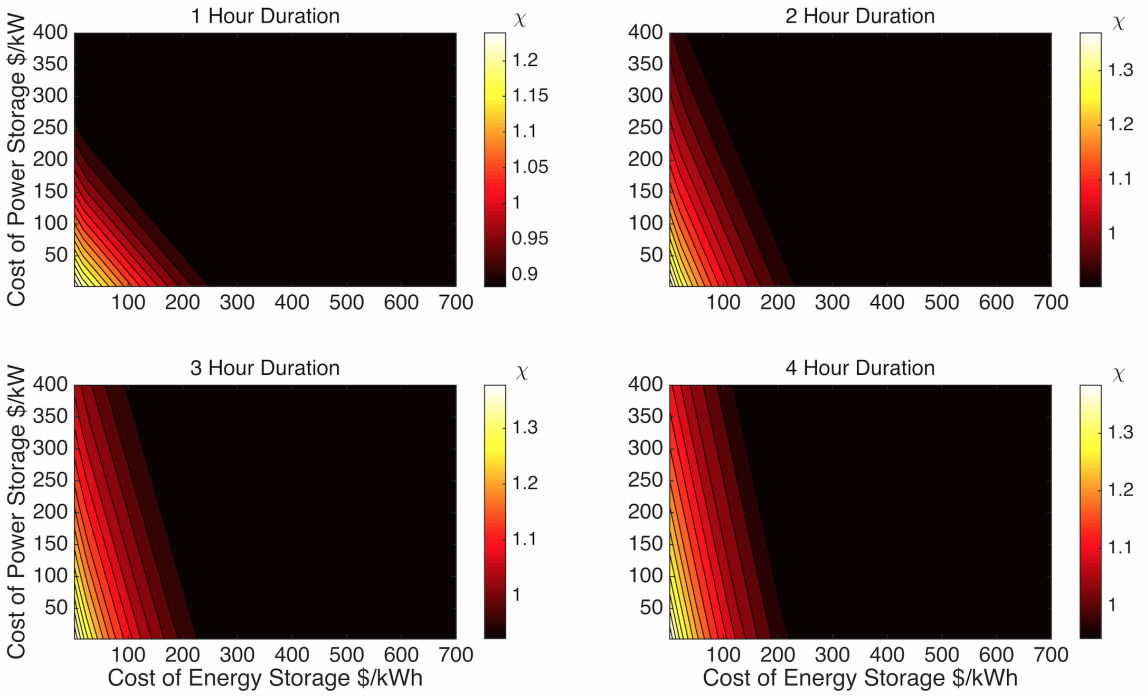

Figure B-21: Using generation data for solar power in Texas, the effect of the duration of price spikes of constant frequency 250 spikes per year of height \$200 on the benefit/cost ratio χ is shown. Figure B-22 shows the optimal duration of storage resulting in the χ values shown in this figure, and therefore, as was shown in section 3.3, the values for the slope of the iso-χ lines.

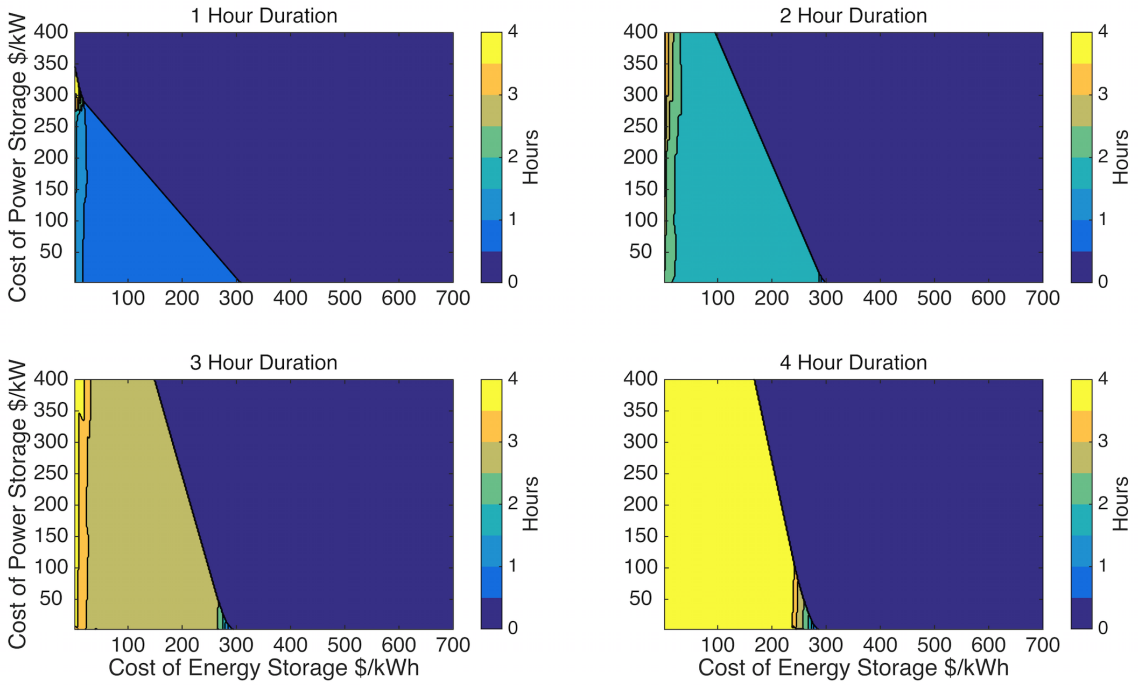

Figure B-22: Using generation data for solar power in Texas, the effect of the duration of price spikes of constant frequency 250 spikes per year of height $200 on the optimal duration of storage. Figure B-21 shows the optimal χ resulting from the optimal storage duration shown in this figure; as was shown in section 3.3, the values for the slope of the iso-χ lines in figure B-21 are equal to the optimal storage duration values shown here.

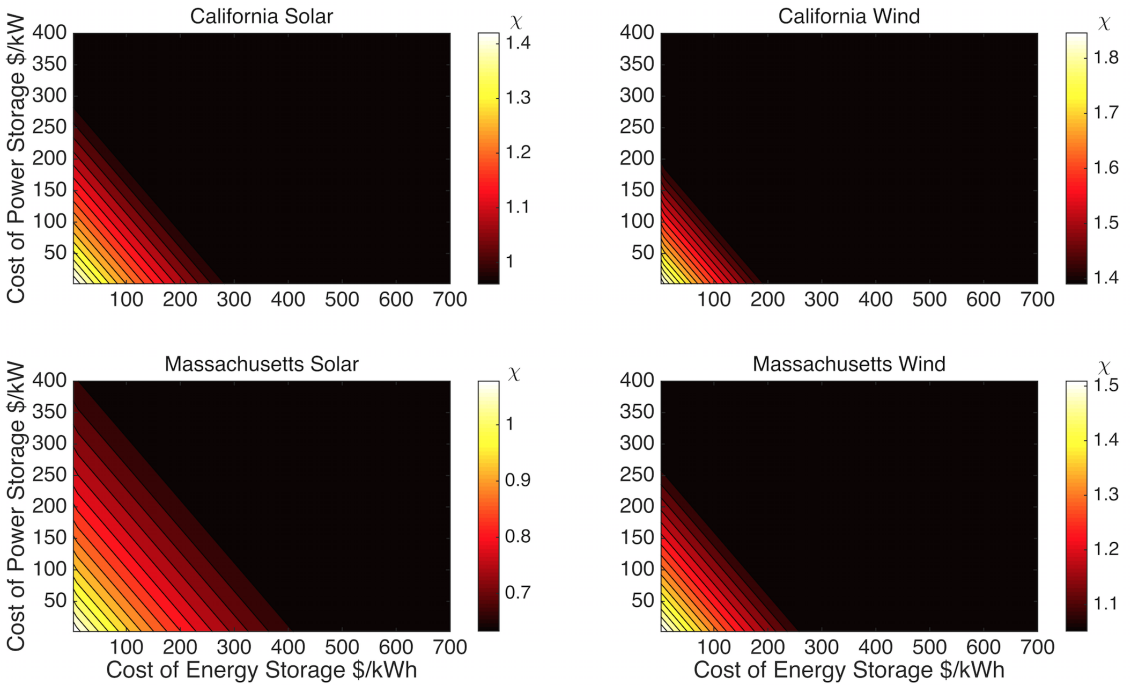

Figure B-23: χ values for generation data for various locations studied is shown in combination with electricity prices with 100 price spikes per year of height \$350 and duration of 1 hour. Generation data has it's greatest impact on the actual values of χ and relatively little impact on the threshold at which storage becomes valuable. Figure 3-17 shows similar results for the other locations studied.

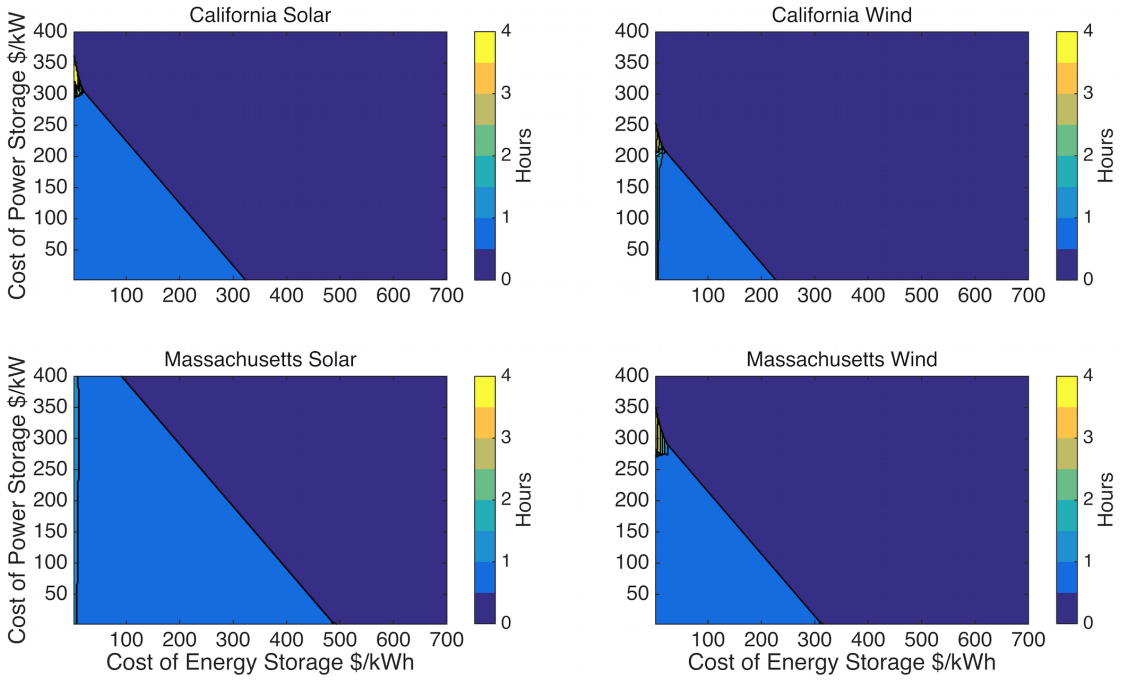

Figure B-24: Optimal storage duration for generation data for various locations studied is shown in combination with electricity prices with 100 price spikes per year of height \$350 and duration of 1 hour. Generation data does not explain the changing iso-χ slopes. Figure 3-18 shows similar results for the other locations studied.

B.5 Electricity price dynamics

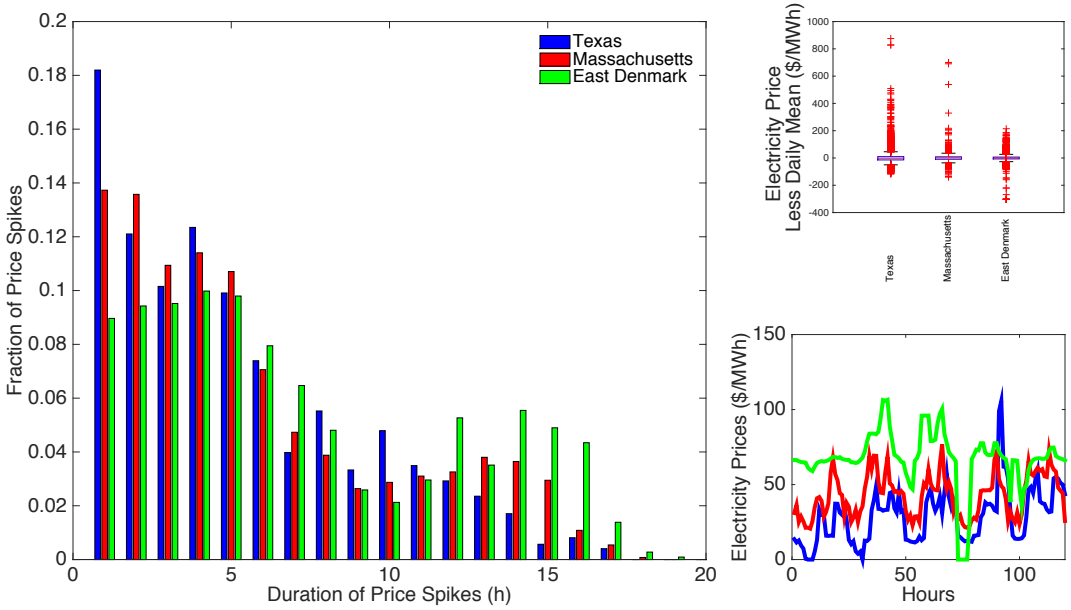

Figure B-25: Emergent properties of electricity spot market prices for Texas, Massachusetts, and East Denmark are shown complementing figure 3-20. In the main plot, the frequency of price spikes of various duration are shown weighted by the total number of price spikes, defined as prices above the daily mean. The box plots in the upper left show the range of hourly electricity prices as compared to the daily mean price. The lower left figure shows the actual electricity prices by hour for the first 120 hours of the data set to demonstrate the variability and diurnal cycles of electricity prices.

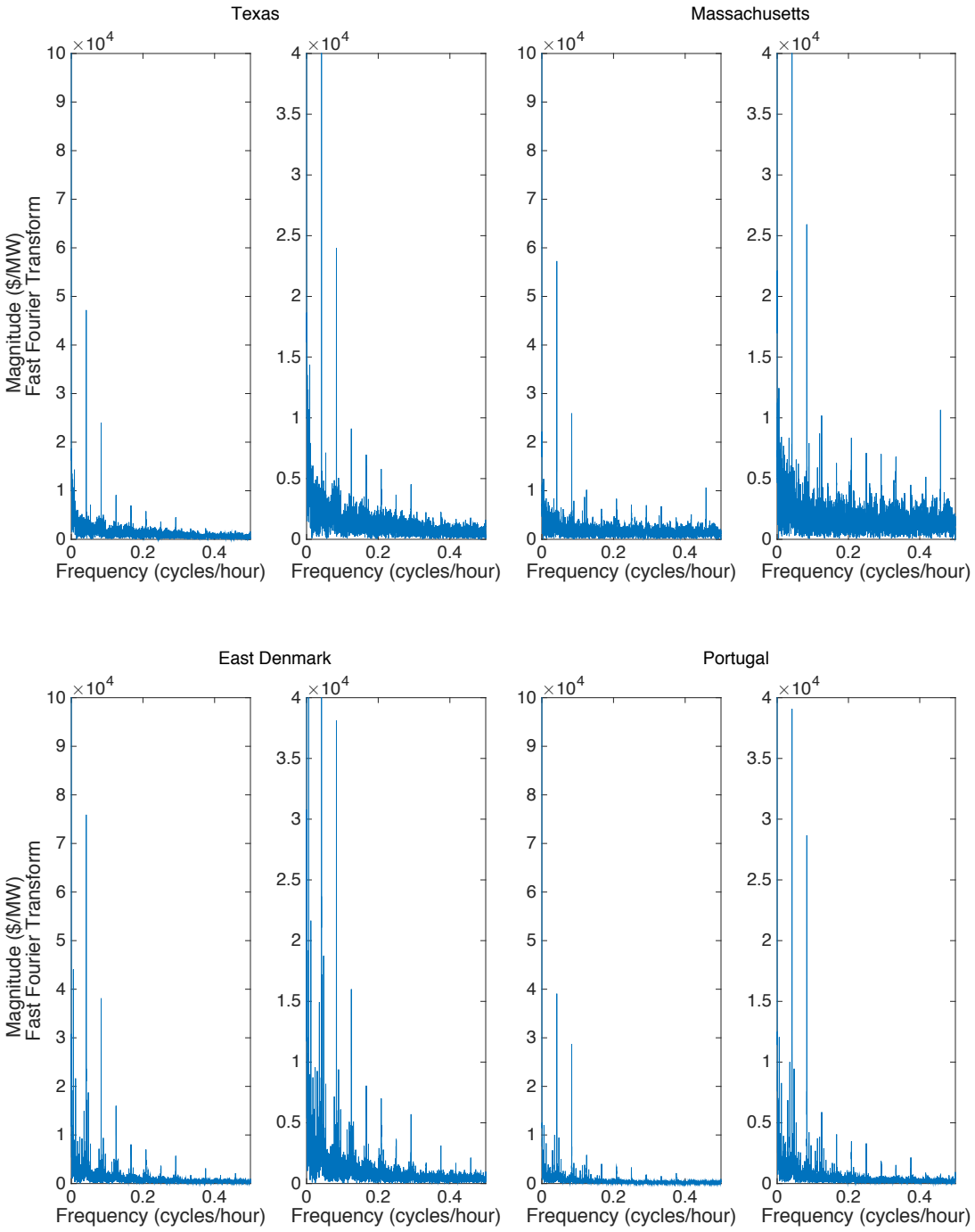

Figure B-26: Fast Fourier transforms of electricity prices in Texas, Massachusetts, East Denmark, and Portugal to complement figure 3-19. As in figure 3-19, the peaks at .0417 cycles per hour and .0833 cycles per hour correspond to daily and twice daily patterns in the prices. East Danish prices are similarly more stable than U.S. prices. Portugal's Fourier transform shows the effect of regulation on electricity prices.

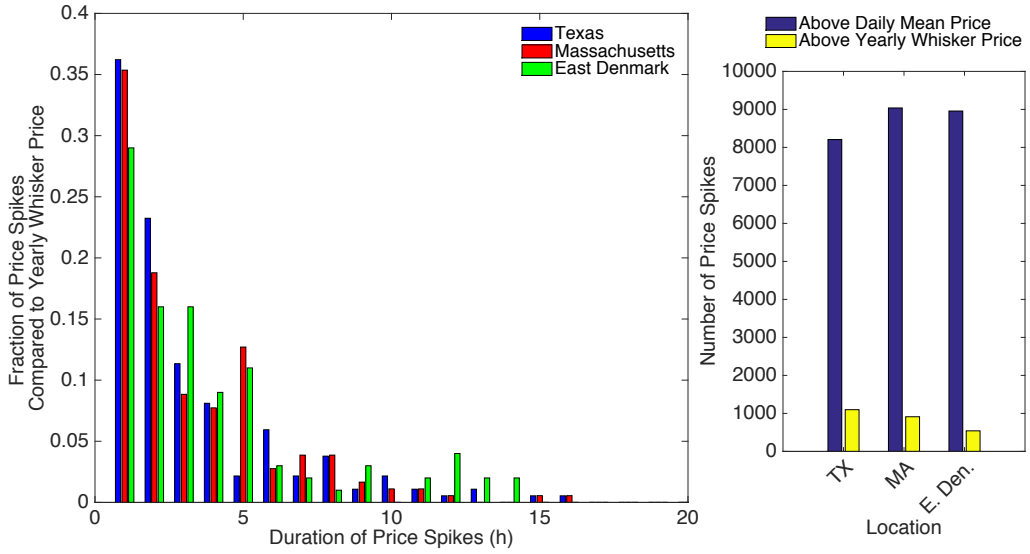

Figure B-27: Price spikes can also be measured against the whisker price as opposed to the daily mean price, complementing figures B-25 and 3-21. On the left is the fraction of price spikes, defined as prices above the whisker price, normalized by the number of price spikes as a function of duration. The figure on the right shows a comparison of the number of hours the price was in a spike for the two different definitions. When defined as price above the whisker price, there are an order of magnitude fewer price spikes.

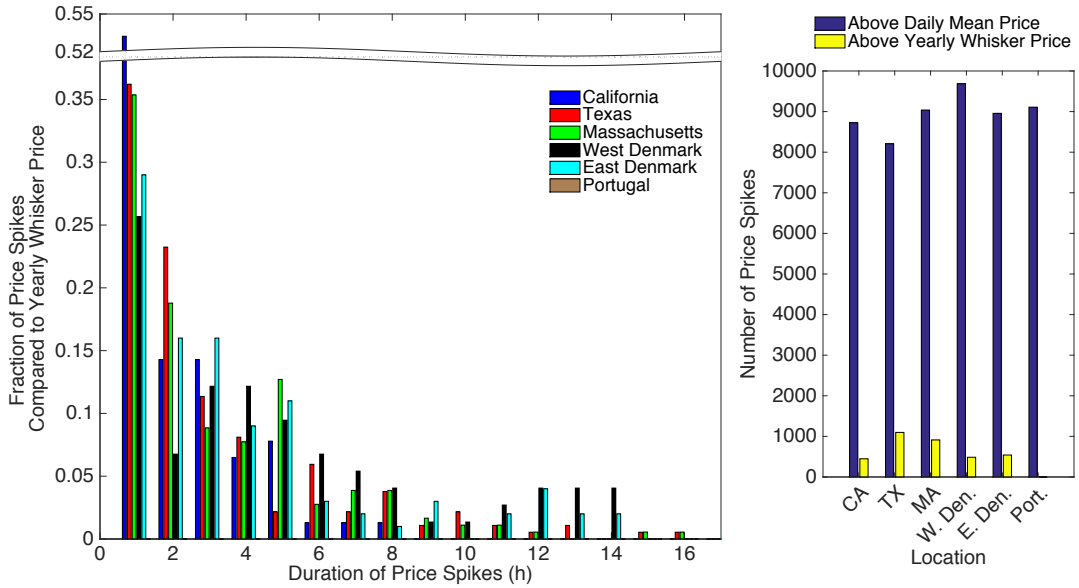

Figure B-28: For ease of comparison, the data presented in figures 3-21 and B-27 are shown to allow comparison of electricity price dynamics across all locations studied.

Bibliography

[1] William Braff, Joshua M. Mueller, and Jessika E. Trancik. Value of storage technologies for wind and solar energy. *In Review*, 2015.

[2] Joshua Mueller and Jessika Trancik. Determinants of storage cost targets for renewable energy arbitrage. *In Preparation*, 2015.

[3] Jessika E Trancik and Daniel Cross-Call. Energy technologies evaluated against climate targets using a cost and carbon trade-off curve. *Environmental science & technology*, 47(12):6673–80, June 2013.

[4] Peter J. Hall. Energy storage: The route to liberation from the fossil fuel economy? *Energy Policy*, 36(12):4363–4367, December 2008.

[5] Charles Forsberg. Hybrid systems to address seasonal mismatches between electricity production and demand in nuclear renewable electrical grids. *Energy Policy*, 62:333–341, 2013.

[6] Ramteen Sioshansi, Riccardo Fagiani, and Vincenzo Marano. Cost and emissions impacts of plug-in hybrid vehicles on the Ohio power system. *Energy Policy*, 38(11):6703–6712, 2010.

[7] Annette Evans, Vladimir Strezov, and Tim J. Evans. Assessment of utility energy storage options for increased renewable energy penetration. *Renewable and Sustainable Energy Reviews*, 16(6):4141–4147, 2012.

[8] John Baker. New technology and possible advances in energy storage. *Energy Policy*, 36(12):4368–4373, December 2008.

[9] T. Kousksou, P. Bruel, A. Jamil, T. El Rhafiki, and Y. Zeraouli. Energy storage: Applications and challenges. *Solar Energy Materials and Solar Cells*, 120:59–80, 2014.

[10] Francisco Díaz-González, Andreas Sumper, Oriol Gomis-Bellmunt, and Roberto Villafáfila-Robles. A review of energy storage technologies for wind power applications. *Renewable and Sustainable Energy Reviews*, 16(4):2154–2171, May 2012.

[11] Susan M Schoenung and William V Hassenzahl. Long- vs . Short-Term Energy Storage Technologies Analysis A Life-Cycle Cost Study A Study for the DOE Energy Storage Systems Program. *Power Quality*, SAND2011-2(April), 2003.

[12] Eoin McLean and Derek Kearney. An Evaluation of Seawater Pumped Hydro Storage for Regulating the Export of Renewable Energy to the National Grid. *Energy Procedia*, 46:152–160, 2014.

[13] Chi-Jen Yang and Robert B. Jackson. Opportunities and barriers to pumped-hydro energy storage in the United States. *Renewable and Sustainable Energy Reviews*, 15(1):839–844, January 2011.

[14] J.P. Deane, B.P. Ó Gallachóir, and E.J. McKeogh. Techno-economic review of existing and new pumped hydro energy storage plant. *Renewable and Sustainable Energy Reviews*, 14(4):1293–1302, May 2010.

[15] Helder Lopes Ferreira, Raquel Garde, Gianluca Fulli, Wil Kling, and Joao Pecas Lopes. Characterisation of electrical energy storage technologies. *Energy*, 53:288–298, 2013.

[16] Derk J Swider. Compressed Air Energy Storage in an Electricity System with Significant Wind Power Generation. *IEEE Transactions on Energy Conversion*, 22(1):95–102, 2007.

[17] Hossein Safaei, David W. Keith, and Ronald J. Hugo. Compressed air energy storage (CAES) with compressors distributed at heat loads to enable waste heat utilization. *Applied Energy*, 103:165–179, March 2013.

[18] Kermit Allen. CAES: The Underground Portion. *IEEE Transactions on Power Apparatus and Systems*, 104(4):809–812, 1985.

[19] Ben Mehta. CAES Geology. *EPRI Journal*, 17(7):38–41, 1992.

[20] Drew Robb. The CAES for wind. *Renewable Energy Focus*, 12(1):18–19, January 2011.

[21] Fritz Crotogino, KU Mohmeyer, and Roland Scharf. Huntorf CAES: More than 20 years of successful operation, 2001.

[22] Curtis M. Oldenburg and Lehua Pan. Porous Media Compressed-Air Energy Storage (PM-CAES): Theory and Simulation of the Coupled Wellbore-Reservoir System. *Transport in Porous Media*, 97:201–221, January 2013.

[23] Giuseppe Grazzini and Adriano Milazzo. Thermodynamic analysis of CAES/TES systems for renewable energy plants. *Renewable Energy*, 33:1998–2006, 2008.

[24] H Ibrahim, A Ilinca, and J Perron. Energy storage systems - Characteristics and comparisons. *Renewable and Sustainable Energy Reviews*, 12(5):1221–1250, 2008.

[25] R. Hebner, J. Beno, and A. Walls. Flywheel batteries come around again. *IEEE Spectrum*, 39(4):46–51, April 2002.

[26] Bjorn Bolund, Hans Bernhoff, and Mats Leijon. Flywheel energy and power storage systems. *Renewable and Sustainable Energy Reviews*, 11:235–258, 2007.

[27] Haichang Liu and Jihai Jiang. Flywheel energy storage - An upswing technology for energy sustainability. *Energy and Buildings*, 39:599–604, 2007.

[28] Paulo F Ribeiro, Senior Member, Brian K Johnson, Mariesa L Crow, Aysen Arsoy, and Yilu Liu. Energy Storage Systems for Advanced Power Applications. *Proceedings of the IEEE*, 89(12):1744–1756, 2001.

[29] William F. Pickard, Amy Q. Shen, and Nicholas J. Hansing. Parking the power: Strategies and physical limitations for bulk energy storage in supply-demand matching on a grid whose input power is provided by intermittent sources. *Renewable and Sustainable Energy Reviews*, 13(8):1934–1945, 2009.

[30] J. Kondoh, I. Ishii, H. Yamaguchi, A. Murata, K. Otani, K. Sakuta, N. Higuchi, S. Sekine, and M. Kamimoto. Electrical energy storage systems for energy networks. *Energy Conversion and Management*, 41(17):1863–1874, 2000.

[31] Marc Beaudin, Hamidreza Zareipour, Anthony Schellenberglabe, and William Rosehart. Energy storage for mitigating the variability of renewable electricity sources: An updated review. *Energy for Sustainable Development*, 14(4):302–314, 2010.

[32] The Storage of Electricity. *Science (New York, N.Y.)*, 13(312):53–56, 1889.

[33] Sam Koohi-Kamali, V.V. Tyagi, N.a. Rahim, N.L. Panwar, and H. Mokhlis. Emergence of energy storage technologies as the solution for reliable operation of smart power systems: A review. *Renewable and Sustainable Energy Reviews*, 25:135–165, September 2013.

[34] Richard Perez. Lead-Acid Battery State of Charge vs. Voltage. *Home Power*, 36:66–70, 1993.

[35] K.C. Divya and Jacob Ostergaard. Battery energy storage technology for power systems - An overview. *Electric Power Systems Research*, 79(4):511–520, 2009.

[36] Carl Johan Rydh. Environmental assessment of vanadium redox and lead-acid batteries for stationary energy storage. *Journal of Power Sources*, 80(1-2):21–29, July 1999.

[37] J.W. Stevens and G.P. Corey. A study of lead-acid battery efficiency near top-of-charge and the impact on PV system design. *Conference Record of the Twenty Fifth IEEE Photovoltaic Specialists Conference*, pages 1485–1488, 1996.

[38] James F. Manwell and Jon G. McGowan. Lead acid battery storage model for hybrid energy systems. *Solar Energy*, 50(5):399–405, May 1993.

[39] Bunyamin Tamyurek, David K. Nichols, and Osman Demirci. The NAS Battery: A Multi-Function Energy Storage System. In *Power Engineering Society General Meeting, IEEE*, volume 4, pages 1991–1996, 2003.

[40] Ryoichi Okuyama and Eiichi Nomura. Relationship between the total energy efficiency of a sodium-sulfur battery system and the heat dissipation of the battery case. *Journal of Power Sources*, 77(2):164–169, February 1999.

[41] K. Iba, R. Ideta, and K. Suzuki. Analysis and Operational Records of NaS Battery. In *Proceedings of the 41st International Universities Power Engineering Conference*, pages 491–495, 2006.

[42] Makoto Kamibayashi, David K. Nichols, and Taku Oshima. Development update of the NAS battery. In *IEEE/PES Transmission and Distribution Conference and Exhibition*, volume 3, pages 1664–1668. Ieee, 2002.

[43] M Armand and J-M Tarascon. Building better batteries. *Nature*, 451:652–7, March 2008.

[44] C. Nair Nirmal-Kumar and Niraj Garimella. Battery energy storage systems: Assessment for small-scale renewable energy integration. *Energy and Buildings*, 42(11):2124–2130, November 2010.

[45] A G Ritchie. Recent developments and future prospects for lithium rechargeable batteries. *Journal of Power Sources*, 96:6–9, 2001.

[46] Bruno Scrosati, Jusef Hassoun, and Yang-Kook Sun. Lithium-ion batteries. A look into the future. *Energy & Environmental Science*, 4(9):3287–3295, 2011.

[47] Satishkumar B. Chikkannanavar, Dawn M. Bernardi, and Lingyun Liu. A review of blended cathode materials for use in Li-ion batteries. *Journal of Power Sources*, 248:91–100, February 2014.

[48] Steven G. Chalk and James F. Miller. Key challenges and recent progress in batteries, fuel cells, and hydrogen storage for clean energy systems. *Journal of Power Sources*, 159(1):73–80, September 2006.

[49] Bruno Scrosati and Jürgen Garche. Lithium batteries : Status , prospects and future. *Journal of Power Sources*, 195:2419–2430, 2010.

[50] Carl Johan Rydh and Magnus Karlstrom. Life cycle inventory of recycling portable nickel - cadmium batteries. *Resources, Conservation, and Recycling*, 34:289–309, 2002.

[51] Peter J Hall and Euan J Bain. Energy-storage technologies and electricity generation. *Energy Policy*, 36:4352–4355, 2008.

[52] C. Ponce de Leon, A. Frias-Ferrer, J. Gonzalez-Garcia, D. A. Szanto, and F. C. Walsh. Redox flow cells for energy conversion. *Journal of Power Sources*, 160:716–732, 2006.

[53] Robert M. Darling, Kevin G. Gallagher, Jeffrey a. Kowalski, Seungbum Ha, and Fikile R. Brushett. Pathways to low-cost electrochemical energy storage: a comparison of aqueous and nonaqueous flow batteries. *Energy Environ. Sci.*, 7(11):3459–3477, 2014.

[54] E H Sanders, K A Mcgrady, G E Wnek, C A Edmondson, J M Mueller, J J Fontanella, S Suarez, and S G Greenbaum. Characterization of electrosprayed Nafion films. *Journal of Power Sources*, 129:55–61, 2004.

[55] Joshua M Mueller. Complex Impedance Studies of Electrosprayed and Extruded Nafion Membranes. Technical Report 324, 2004.

[56] Sarada Kuravi, Jamie Trahan, D. Yogi Goswami, Muhammad M. Rahman, and Elias K. Stefanakos. Thermal energy storage technologies and systems for concentrating solar power plants. *Progress in Energy and Combustion Science*, 39(4):285–319, August 2013.

[57] Belén Zalba, José M Marin, Luisa F. Cabeza, and Harald Mehling. Review on thermal energy storage with phase change: materials, heat transfer analysis and applications. *Applied Thermal Engineering*, 23(3):251–283, February 2003.

[58] AA Akhil, Georgianne Huff, and AB Currier. DOE/EPRI 2013 electricity storage handbook in collaboration with NRECA. Technical Report July, 2013.

[59] Eric Hittinger, J.F. Whitacre, and Jay Apt. What properties of grid energy storage are most valuable? *Journal of Power Sources*, 206:436–449, May 2012.

[60] R. L. Fares and J.P. Meyers. Economic Operational Planning of Grid-connected Battery Energy Storage. *ECS Transactions*, 45(26):1–16, 2013.

[61] Richard de Neufville and Stefan Scholtes. *Flexibility in Engineering Design*. MIT Press, 2011.

[62] J Doyne Farmer and Jessika Trancik. Dynamics of technological development in the energy sector. *The London Accord*, pages 1–24, 2007.

[63] Heebyung Koh and Christopher L. Magee. A functional approach for studying technological progress: Extension to energy technology. *Technological Forecasting and Social Change*, 75(6):735–758, July 2008.

[64] Eric Cutter, Ben Haley, Jeremy Hargreaves, and Jim Williams. Utility scale energy storage and the need for flexible capacity metrics. *Applied Energy*, 124:274–282, July 2014.

[65] California ISO Demand Response and Energy Efficiency Roadmap: Maximizing Preferred Resources. Technical Report December, 2013.

[66] Brian L. Ellis and Linda F. Nazar. Sodium and sodium-ion energy storage batteries. *Current Opinion in Solid State and Materials Science*, 16(4):168–177, 2012.

[67] NGK Insulators, LTD. http://www.ngk.co.jp, 2015.

[68] Morgan R Edwards and Jessika E Trancik. Climate impacts of energy technologies depend on emissions timing. *Nature Climate Change*, 4:347–352, 2014.

[69] Haisheng Chen, Thang Ngoc Cong, Wei Yang, Chunqing Tan, Yongliang Li, and Yulong Ding. Progress in electrical energy storage system: A critical review. *Progress in Natural Science*, 19(3):291–312, 2009.

[70] Anya Castillo and Dennice F. Gayme. Grid-scale energy storage applications in renewable energy integration: A survey. *Energy Conversion and Management*, 87:885–894, 2014.

[71] Robert Socolow, Craig Arnold, Greg Davies, Thomas Kreutz, Warren Powell, Michael Schwartz, and Daniel Steingart. Grid-Scale Electricity Storage Implications for Renewable Energy, 2014.

[72] Sandhya Sundararagavan and Erin Baker. Evaluating energy storage technologies for wind power integration. *Solar Energy*, 86(9):2707–2717, 2012.

[73] Andres Yaksic and John E. Tilton. Using the cumulative availabiity curve to assess the threat of mineral depletion: The case of lithium. *Resources Policy*, 34:185–194, 2009.

[74] Liliana E. Benitez, Pablo C. Benitez, and G. Cornelis van Kooten. The economics of wind power with energy storage. *Energy Economics*, 30(4):1973–1989, July 2008.

[75] D. Connolly, H. Lund, B.V. Mathiesen, E. Pican, and M. Leahy. The technical and economic implications of integrating fluctuating renewable energy using energy storage. *Renewable Energy*, 43:47–60, July 2012.

[76] Paul Denholm, Gerald L Kulcinski, and Tracey Holloway. Emissions and energy efficiency assessment of baseload wind energy systems. *Environmental science & technology*, 39(6):1903–1911, 2005.

[77] Jeffery B. Greenblatt, Samir Succar, David C. Denkenberger, Robert H. Williams, and Robert H. Socolow. Baseload wind energy: modeling the competition between gas turbines and compressed air energy storage for supplemental generation. *Energy Policy*, 35(3):1474–1492, 2007.

[78] Dunbar P. Birnie. Optimal battery sizing for storm-resilient photovoltaic power island systems. *Solar Energy*, 109:165–173, November 2014.

[79] Jason Leadbetter and Lukas Swan. Battery storage system for residential electricity peak demand shaving. *Energy and Buildings*, 55:685–692, December 2012.

[80] Abdelhamid Kaabeche and Rachid Ibtiouen. Techno-economic optimization of hybrid photovoltaic/wind/diesel/battery generation in a stand-alone power system. *Solar Energy*, 103:171–182, May 2014.

[81] J.K. Kaldellis and D. Zafirakis. Optimum energy storage techniques for the improvement of renewable energy sources-based electricity generation economic efficiency. *Energy*, 32(12):2295–2305, December 2007.

[82] Eric Hittinger, J. F. Whitacre, and Jay Apt. Compensating for wind variability using co-located natural gas generation and energy storage. *Energy Systems*, 1:417–439, August 2010.

[83] Ramteen Sioshansi. Increasing the value of wind with energy storage. *Energy Journal*, 32(2):1–29, 2011.

[84] Department of Energy Global Energy Storage Database. http://www.energystorageexchange.org, 2014.

[85] J.T. Alt, M.D. Anderson, and RG Jungst. Assessment of untility side cost saving from battery energy storage. *IEEE Transactions on Power Systems*, 12(3):1112–1120, 1997.

[86] Alexandre Oudalov, Daniel Chartouni, and Christian Ohler. Optimizing a battery energy storage system for primary frequency control. *IEEE Transactions on Power Systems*, 22(3):1259–1266, 2007.

[87] D. Connolly, H. Lund, P. Finn, B.V. Mathiesen, and M. Leahy. Practical operation strategies for pumped hydroelectric energy storage (PHES) utilising electricity price arbitrage. *Energy Policy*, 39(7):4189–4196, July 2011.

[88] M.G. Ippolito, M.L. Di Silvestre, E. Riva Sanseverino, G. Zizzo, and G. Graditi. Multi-objective optimized management of electrical energy storage systems in an islanded network with renewable energy sources under different design scenarios. *Energy*, 64:648–662, January 2014.

[89] Edgardo D. Castronuovo and João a Peças Lopes. Optimal operation and hydro storage sizing of a wind-hydro power plant. *International Journal of Electrical Power and Energy Systems*, 26:771–778, 2004.

[90] O.A. Jaramillo, M.A. Borja, and J.M. Huacuz. Using hydropower to complement wind energy: A hybrid system to provide firm power. *Renewable Energy*, 29(11):1887–1909, 2004.

[91] James Mason, Vasilis Fthenakis, Ken Zweibel, Tom Hansen, and Thomas Nikolakakis. Coupling PV and CAES Power Plants to Transform Intermittent PV Electricity into a Dispatchable Electricity Source. *Progress in Photovoltaics: Research and Applications*, 16:649–668, 2008.

[92] Yi Feng, Lei Jun Shao, Bang Ling Zhang, Meng Jie Wu, Yu Pei Shao, Qiang Qiang Liao, Guo Ding Zhou, and Bo Sun. Technical and Economic Analysis on Grid-Connected Wind Farm Based on Hybrid Energy Storage System for Active Distribution Network. *Applied Mechanics and Materials*, 672-674:274–279, October 2014.

[93] J K Kaldellis, D Zafirakis, and K Kavadias. Techno-economic comparison of energy storage systems for island autonomous electrical networks. *Renewable and Sustainable Energy Reviews*, 13:378–392, 2009.

[94] Ramteen Sioshansi, Paul Denholm, and Thomas Jenkin. A comparative analysis of the value of pure and hybrid electricity storage. *Energy Economics*, 33(1):56–66, January 2011.

[95] Rahul Walawalkar, Jay Apt, and Rick Mancini. Economics of electric energy storage for energy arbitrage and regulation in New York. *Energy Policy*, 35(4):2558–2568, 2007.

[96] XE Currency Converter. http://www.xe.com, 2014.

[97] Henrik Lund and Georges Salgi. The role of compressed air energy storage (CAES) in future sustainable energy systems. *Energy Conversion and Management*, 50(5):1172–1179, May 2009.

[98] Energy Reliability Council of Texas Website. http://www.ercot.com, 2013.

[99] California ISO Website. http://www.caiso.com, 2013.

[100] ISO New England Website. http://www.iso-ne.com, 2013.

[101] National Solar Radiation Database. http://rredc.nrel.gov/solar/old_data/nsrdb/1991-2010/, 2013.

[102] Vestas Website. http://www.vestas.com, 2013.

[103] Danish Climate and Energy Ministry. http://www.energinet.dk, 2014.

[104] H. Holttinen. Optimal electricity market for wind power. *Energy Policy*, 33(16):2052–2063, November 2005.

[105] Henrik Lund. Large-scale integration of wind power into different energy systems. *Energy*, 30(13):2402–2412, October 2005.

[106] The Iberian Energy Derivatives Exchange. http://www.omip.pt, 2014.

[107] Joseph E. Stieglitz. *Economics of the Public Sector Third Edition*. W. W. Norton & Company, 2000.

[108] Gregory F. Nemet. Demand-pull, technology-push, and government-led incentives for non-incremental technical change. *Research Policy*, 38(5):700–709, 2009.